INFORMATION TO USERS

This manuscript has been reproduced from the microfilm master. UMI films the text directly from the original or copy submitted. Thus, some thesis and dissertation copies are in typewriter face, while others may be from any type of computer printer.

The quality of this reproduction is dependent upon the quality of the copy submitted. Broken or indistinct print, colored or poor quality illustrations and photographs, print bleedthrough, substandard margins, and improper alignment can adversely affect reproduction.

In the unlikely event that the author did not send UMI a complete manuscript and there are missing pages, these will be noted. Also, if unauthorized copyright material had to be removed, a note will indicate the deletion.

Oversize materials (e.g., maps, drawings, charts) are reproduced by sectioning the original, beginning at the upper left-hand corner and continuing from left to right in equal sections with small overlaps.

UMI®

University of Alberta

DIFFUSION OF AMMONIUM THROUGH GLACIAL CLAY SOILS

by

Won Jae Chang (C)

A thesis submitted to the Faculty of Graduate Studies and Research in partial fulfillment
of the requirement for the degree of Master of Science

in

Geoenvironmental Engineering

Department of Civil and Environmental Engineering

Edmonton, Alberta
Spring 2005

Canada

DEDICATION

This thesis is dedicated to my families
They provided me with the greate opportunity to study abroad
They encouranged all my enthusiasm and hope on a cleaner Earth
And
They believed in me
Whithout you
This thesis would never have been completed
Thank you

ABSTRACT

The primary objective of this study is to investigate the diffusion of ammonium through glacial clay soils with attention to the geochemical conditions beneath EMS facilities. An anaerobic radial diffusion cell method was employed to experimentally simulate the in situ geochemical conditions under EMS facilities. The resulting distribution coefficient for ammonium ranged from 0.3 to 0.4 L/kg. Significant ammonium exchange reactions led to a 137% average increase in hardness in the reservoirs due to the extraction of exchangeable calcium and magnesium. Geochemical mix model using PHREEQC, adequately simulated the linear ammonium adsorption at the low dissolved ammonium concentrations. The reactive model is able to provide both radial diffusion transport, including reactions, and the change in pore fluid chemistry. The three-dimensional radial diffusion modeling provided an ammonium effective diffusion coefficient of $2.29 \times 10^{-10} \, m^2/sec$ for glacial clays collected in Ponoka, Alberta.

ACKNOWLEDGEMENTS

Table of Contents

LIST OF TABLES

LIST OF FIGURES

CHAPTER 1.0   INTRODUCTION

During the previous two decades, the livestock industry of Alberta has experienced
tremendous growth and has encountered significant challenges involving environmental
regulations and public health, such as greenhouse gas emissions and mad-cow disease
(Alberta Agriculture, Food and Rural Development, 2003, Willoughby et al., 2003). In
addition, the production, storage, and management of liquid manure generated by
intensive livestock operations have also become issues of public concern due to the
substantial volumes of waste and potential for its adverse impact on adjacent
hydrogeologic regimes.

Earthen manure storage (EMS) is a common means of storing liquid manure in Alberta,
Canada. Currently, Alberta continues to have the largest cattle and calf herd (5.68
million head) in Canada. Alberta also has 32 percent of the western Canadian pig
population of 6.3 million head (Agri-Food Statistics Update, 2004). As a by-product of
these intensive livestock operations, cattle manure generated annually is estimated to
increase to 6.4 million tones between 2008 and 2012 (Okine and Basarab, 2003).

The Agricultural Operation Practices Act (AOPA) strictly regulates the installation of
engineered liner systems at the bottom and sides of EMS structures; nevertheless,
preliminary site investigations by professional engineers indicate 32 to 87% of EMS in

1

areas of low to high intensity livestock operation in Alberta have exceeded maximum acceptable levels for N-NO$_3$ and N-NO$_2$ (CAESA Water Quality Study, 1998, 2004). Furthermore, about 36% of the liquid manure storage facilities installed in Alberta for dairy cattle, beef cattle, and hogs have no engineered liner or barrier system.

Nitrate contamination resulting from the oxidation of ammonium through aerobic zones, is one of the major contaminators of groundwater resources. It is known that an elevated nitrate level in water resources causes blue baby syndrome in infants, oxygen transport problems for elderly people, eutrophication of lakes and rivers, and nitrate poisoning in cattle (Comly, 1945; Pauwels et al., 2001; Stoltenow and Lardy, 1998). Hence, Canadian Council Ministers of the Environment (CCME) have prescribed maximum concentration levels for nitrogen nitrate and nitrogen nitrite on the order of 10 mg/L in drinking water.

A large portion of the Canadian Prairies are covered by glacial clays and clay till soils. These glacial soils are fractured such that the dominant process for the transport of fluids is advection along fractures. For the transport of contaminants, the process becomes advective transport along the fracture with diffusive transport of solute from the facture into the soil matrix (Donahue, 1999; Freeze and Cherry, 1979). As a result of theses process the diffusion mechanism needs to be evaluated in order to accurately account for loss of nitrogen to the soil matrix (See Figure 1.1).

Most liquid cattle and hog manure consists of substantial amounts of ammonium. Liquid manure is commonly composed of about 70 to 80% ammonium and 10 to 20% potassium and sodium in mole fractions (Fonstad, 2004). Therefore, in this study,

2

ammonium (NH_4^+) is regarded as the origin of potential nitrate contamination. In addition, anaerobic conditions beneath EMS enable nitrogen compounds to maintain their reduced form (NH_4^+) in nitrogen cycle.

Through experimental simulation of ammonium diffusion through glacial clay soils under anaerobic conditions, this research project provides the geochemical parameters appropriate for the design and decommissioning strategy of EMS and development of a groundwater risk assessment.

Specific objectives of this study are to achieve the following:

1. Apply an anaerobic radial diffusion cell method to simulate diffusion of ammonium.
2. Measure changes in pore fluid chemistry during the interaction of liquid manure and soils.
3. Characterize adsorption of ammonium generated by cation exchange reactions.
4. Develop a reactive transport model accounting for diffusion and competitive exchange reactions.
5. Determine effective diffusion coefficients, selectivity coefficients, and distribution coefficients for ammonium in manure.
6. Predict net ammonium adsorption capacity for glacial soils using a reactive transport model

3

REFERENCES

Agri-Food Statistics Update, Issue No. 70 - February 18, 2004. January 1, 2004 Livestock Inventory Estimates - Alberta/Canada

Alberta Agriculture, Food and Rural Development, November, 2002. Effects of Manure on Soil and Groundwater Quality.

Alberta Agriculture, Food and Rural Development, June, 2004. 2004 Reference Guide Agricultural Operation Practices Act (AOPA).

Alberta Agriculture, Food and Rural Development, 1998. Monitoring nitrogen in Alberta's farmland waters.

Alberta Agriculture, Food and Rural Development, March, 2004. Assessing Alberta's water quality (CAESA Study).

Comly, H. H., 1945. Cyanosis in infants caused by nitrates in well water. Journal of the American Medical Association 129:112-116.

Donahue, R.B., Barbour, S.L., Headley, J.V., 1999. Diffusion and adsorption of benzene in Regina clay. Canadian Geotechnical Journal, 36, 430-442.

Fonstad, T.A., 2004. Transport and fate of nitrogen from earthen manure storage effluent seepage. Ph.D. thesis, University of Saskatchewan.

Freeze, R.A., Cherry, J.A., 1979. Groundwater. Prentice-Hall, Inc., Englewood Cliffs, New Jersey, USA.

Okine, E.K., Basarab J.A., 2003. Livestock feed efficiency as it relates to nutrient balancing: improved nutrient utilization reduces nutrient loss in manure. Manure management 2003 conference, Progress and Opportunities, Lethbridge, Alberta.

Pauwels, H., Lachassagne, P., Bordenave, P., Foucher, J.C., Martelat, A., 2001. Temporal variability of nitrate concentration in a schist aquifer and transfer to surface waters. Journal of Applied Geochemistry, 16, 583-596.

Stoltenow, C., Lardy, G., 1998. Nitrate poisoning of livestock. North Dakota State University Extension Service Publication, Vol. 839.

Willoughby, A.R., Biggar, K.W., Sego, D.C., 2003. Freeze separation to treat hog manure, Manure management 2003 conference, Progress and Opportunities, June, 2003, Lethbridge, AB.

4

CHAPTER 2.0   LITERATURE REVIEW

2.1 AMMONIUM AS A SOURCE CONTAMINANT BENEATH EMS

EMS characterization studies to date have focused on evaluating the quantity and rate of

manure loss from EMS sites through the investigation of effluent plume (Fonstad, 2004).

Such studies have analyzed soil samples collected from beneath EMS, installed

monitoring wells adjacent to EMS, or used remote sensing survey equipment (Fonstad,

2004). Of particular interest, ammonium is identified as a dominant species in various

liquid manures and has been recognized as both a major adsorbate beneath EMS, and a

source for potential nitrate contamination (Heaton et al., 1983; Hendry et al., 1984;

Oenema et al., 1998; Power and Schepers, 1989; Spalding and Exner, 1993; Williams et

al., 1998). This section reviews how ammonium beneath EMS has been identified and

evaluated in the past and develops a conceptual model for typical EMS subsurface

environments in Alberta.

Kreitler and Jones (1975) studied the cause of nitrate contamination in groundwater after

several cattle died of anoxia due to drinking water containing nitrate at concentrations of

the order of 250 mg/L as indicated by the 230 groundwater samples taken in Runnels

Country, west-central Texas (cf. a maximum acceptable nitrate (NO_3^-) concentration is

45 mg/L). Nitrogen isotope analysis was conducted by measuring natural variations of

5

the stable nitrogen isotopes with a mass spectrometer. The stable isotopes of nitrogen are N^{14} and N^{15}, of which N^{14} dominates and makes up about 99% of all atmospheric nitrogen. The study revealed that the high nitrate levels were derived from the decomposition of animal wastes and the oxidation of natural soil nitrogen.

Devitt et al. (1976) found that agricultural activities have contributed substantially to the excess nitrate levels found in surface and groundwater. Through the analysis of soil solutions collected from six intensive agricultural areas in southern California, it was also determined that $N-NO_3^-$ movement was significantly affected by soil characteristics. In coarse-textured soil there is low denitrification potential and nitrate movement is dependent on water flow. In layers with high clay fractions, however, nitrate leaching is restricted and anaerobic conditions favour the promotion of denitrification.

In the 1970s, numerous researchers reported a sealing effect, or clogging, at the interface of liquid wastes and the soils used to construct the storages facilities. The combination of these effects caused a reduction in hydraulic conductivity through the bottom of waste storage facilities (Change, 1974; Davis et al., 1973; DeTar, 1979; Hills, 1976; Lo, 1977). Sealing is the initial physical entrapment of waste particles in the soil pores; it may be disrupted by hydrostatic pressure fluctuations in the water table during the wetting and drying of embankment soil and by microbial activity in the soil beneath the seal (Chang et al., 1974; Nordstedt and Baldwin, 1973).

Ciravolo et al. (1979) observed the seepage entering groundwater from anaerobic swine waste lagoons located in the Atlantic Coastal Plain region. Groundwater from several

6

wells in the area surrounding the lagoons was sampled and analyzed for the density of fecal coliforms and concentrations of Cl, Cu, Mn, NH_4-N, NO_3-N, PO_4-P, and Zn. It was concluded groundwater contamination was attributable to seepage from the lagoon, which resulted from a rupture in the sealing.

EMS during pumped out- *Aerobic conditions*
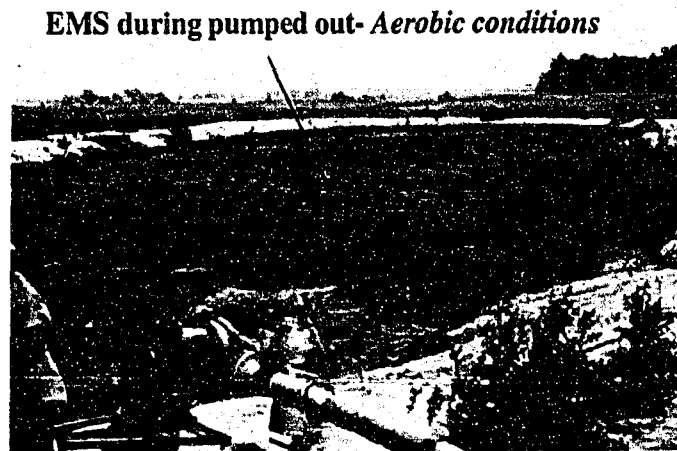
Figure 2.1 Typical earthen manure storage facility
(Modified from Fleming et al., 1999)

Hendry et al. (1984) investigated the source and distribution of elevated nitrate levels in Alberta areas. Groundwater samples were collected from piezometers and water wells within a 30 km^2 area of the Interior Great Plains Region of southern Alberta. The samples were used to carry out laboratory experiments for geochemical studies (NO_3^--N and NH_4^+-N), environmental isotope studies (tritium), and microbial analyses (nitrifiers). The experiments showed that high nitrate nitrogen concentrations, in excess of more than 100 mg/L, occurred in the weathered till regions below the water table. Hendry et al. concluded the elevated nitrate concentrations resulted from the oxidation of ammonium

7

present within the weathered tills.

Wassenaar (1995) evaluated the origin of nitrate in the Abbotsford Aquifer, located in British Columbia, Canada. Using isotope analysis for ^{15}N and ^{18}O in NO_3^-, it was determined that approximately 80% of the area studied exceeded the maximum acceptable level for nitrate, which was 40 mg/L. The analysis revealed that nitrate in the aquifer originated predominately from poultry manure and ammonium fertilizer. It was predicted that the high nitrate concentration would likely persist for decades since the residence time of groundwater in the aquifer was of the order of decades and there were no sustainable bacterial denitrification.

Fonstad and Maule (1996) examined seepage loss from liquid hog manure storage sites constructed over clay till, sandy till, layered lacustrine, and layered alluvial deposits in Saskatchewan. Soil samples were collected from different depths, ranging from 1.8 m to 10 m below the base of the storage structures. Soluble ions (ammonium, chloride, potassium, etc.) were extracted from the saturated pastes of the collected samples. The analysis indicated that ammonium and potassium was transported differently through the various soil types. Effluent transport in clayey soils was limited to depths of 2 to 4 m, while elevated ammonium and potassium were detected in sandy till, lacustrine and alluvial deposit to depths of 5 to 10 m. In addition, it was reported that nitrate nitrogen levels were negligible below all of the storage sites. Fonstad and Maule concluded that ammonium was the dominant species and nitrification did not occur beneath EMS (e.g. Figure 2.2).

8

Ham and DeSutter (1999) estimated seepage loss from earthen animal waste lagoons in Kansas in the U.S. Seepage losses were calculated from the measurements of evaporation and changes in lagoon depth during the addition or removal of waste (water balance method). Seepage losses resulted in the movement of ammonium nitrogen into the subsoil (3280 to 113960 kg per site). It was postulated that large fractions of ammonium would be adsorbed and remain in close proximity to the lagoon in anaerobic regions (Figure 2.2). As a result of this adsorption, Ham and DeSutter pointed out that substantial amounts of ammonium could potentially be converted to nitrate when a lagoon was emptied and dried for long periods.
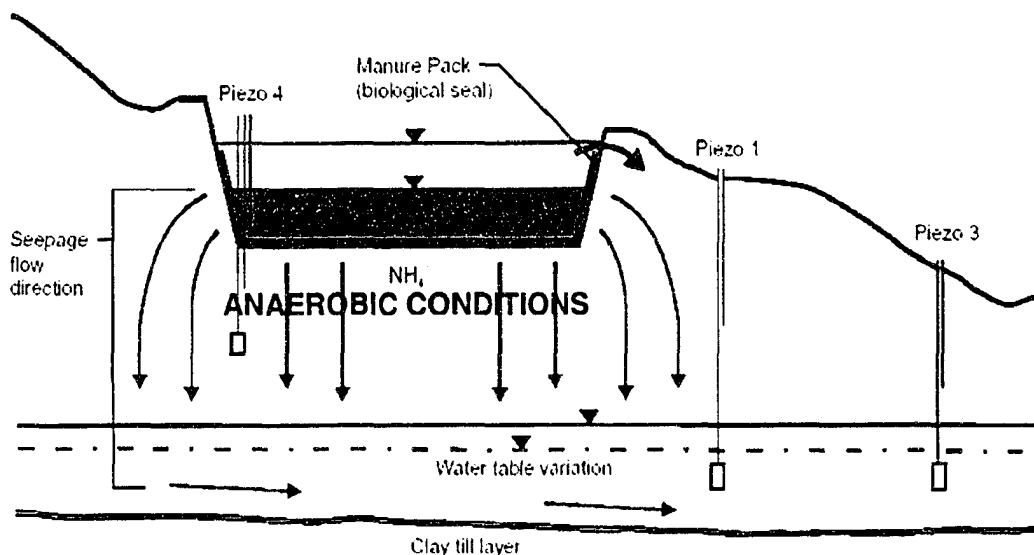
Figure 2.2 NH_4^+ as a source for potential groundwater contamination-*modified*
(Modified from: Alberta Agriculture, Food and Rural Development 2001)

9

Hudak (2000) evaluated regional patterns of nitrate manifested in Texas groundwater by compiling and mapping water chemistry data from 7793 wells. About 74% the groundwater consumed in the state comes from west Texas, due to its relative abundance of groundwater. However, the analysis revealed that 50% of the readings in north central and west central Texas exceeded the maximum acceptable level for nitrate, or 44.27 mg/L. The author pointed out that intensive agricultural practices that employed or produced fertilizers, manure, and soil organic nitrogen were probable sources of nitrate throughout west Texas.

Pauwels et al. (2001) indicated that nitrate contamination within aquifers was influenced by temporal hydrogeological events and by agricultural activities in the Schist aquifer located in Rennes, Western France. Annual changes in nitrate concentrations were reported in aquifer and stream water as derivative of agricultural activities at the surface. Over the short term, rainfall events were a major factor that influenced the change of nitrate concentrations. Seasonally, nitrate was attenuated by heterotrophic denitrification. In spite of the high rates of denitrification in the experimental areas, temporal variation in nitrate concentrations appeared only at depths below the water table because water moved rapidly along the fissures and factures of the Schist aquifer.

Alberta Agriculture, Food and Rural Development (2001) conducted a detailed site investigation of five old, unlined EMS facilities, typical of those found in central Alberta. This was done to assess potential risks to groundwater. It was indicated that ammonium was attenuated near the perimeter and base of the earthen manure storage facilities in most soils. Attenuated ammonium beneath the floors and at the sides of the storage sites

10

may become a problem if these facilities are abandoned and aerobic conditions are allowed to develop within these soils.

Fukada et al. (2004) investigated nitrate contamination in urban aquifers using a dual-isotope approach. The data for an analysis of ^{15}N-NO_3^- and O-NO_3^- was collected from multi-level piezometers in the Sherwood sandstone aquifer beneath Nottingham in the U.K. It appeared the existing nitrate concentrations, ranging from 31.7 to 66.7 mg/L, resulted from the nitrification of sewage-derived inputs. In contrast, denitrification was identified by plotting the distributions of dissolved nitrogen isotopes (NO_3^-, ^{15}N-NO_3^- and O-NO_3^-). However, analysis conducted to confirm denitrification was inconclusive because of potential mixing reactions between sewage and other sources of nitrate.

Widory et al. (2004) mentioned that in spite of increasing efforts at national and European (ES Directive 91/976/EEC) levels to reduce nitrate input from intensive agriculture operations, nitrate is still one of the major contaminants of groundwater resources. The results of an isotopic multi-trace study ($\delta^{15}N, \delta^{11}B, ^{87}Sr/^{86}Sr$) in two small catchments of the Arguenon watershed in Brittany, France, demonstrated that the spreading of hog manure and sewage effluent from a point source significantly impacted high nitrate contamination in the study areas.

The Environmental Manual for Hog Producers in Alberta (2004) states that "seepage from improperly constructed or maintained manure storage structures and the associated risk of groundwater contamination is a serious concern in some areas, particularly where the subsoil underlying the storage consists of sand, gravel or fractured bedrock that allows movement of contaminants through the soil profile to shallow groundwater."

11

2.2 GEOCHEMICAL ENVIRONMENT BENEATH EMS

According to the literature, liquid manure from both hogs and cattle was identified as a major contributing source of high nitrate levels in groundwater and surface water. In order to simulate the interaction between liquid manure and local soil, it is necessary to characterize the geochemical environment beneath manure storage structures; this must be done to determine the geochemical reactions that may occur between the manure, pore fluid, and the local geological properties. Characterization of the EMS subsurface will play a key role in simulating manure-soil systems in both the experimental and numerical study.

2.2.1 Anaerobic conditions beneath EMS

The EMS subsurface comprises an oxygen-limited environment that plays a key role in the establishment of the reducing conditions for nitrogen compounds.

Fonstad and Maule (1996) and Ham and DeSutter (1999) pointed out that the anaerobic conditions beneath EMS sites produce reducing conditions for nitrogen compounds. Therefore, ammonium (NH_4^+) is generally a dominant species as a consequence of the nitrogen cycle, as shown in Figure 2.3.

The Minnesota Pollution Control Agency (2001) conducted groundwater monitoring to observe the anaerobic conditions beneath EMS facilities on a field scale. The study was conducted from 1994 to 2000 at several feedlots in Minnesota that have EMS. The

maximum concentrations of ammonia, Kjeldahl nitrogen, phosphorous, potassium, and

organic carbon were measured down gradient from the manure storage basins

constructed with a cohesive soil liner. The analysis revealed that plumes extended for

distances of 250 to more than 400 feet, and reducing conditions were observed below

and down-gradient from the EMS basins.
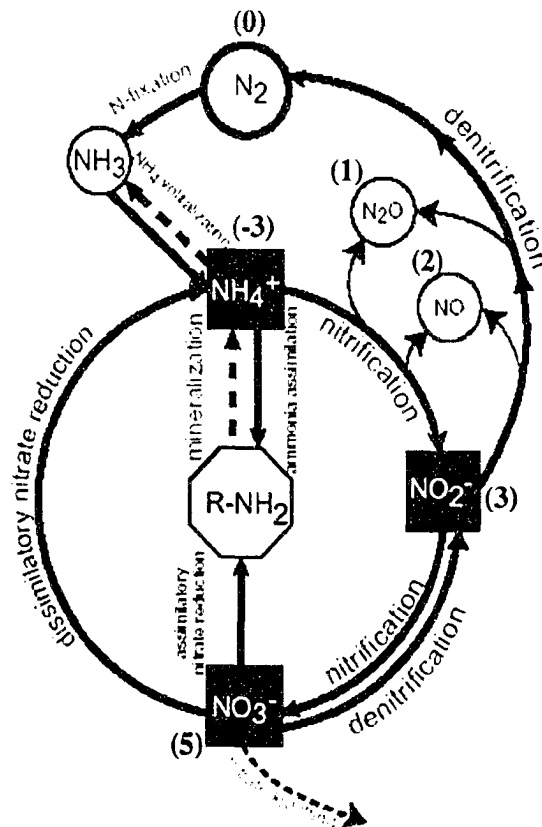
Figure 2.3 Nitrogen cycle
(Modified from Wallenstein, 1999)

In Iowa, U.S., in order to assess how groundwater quality is affected by manure storage

facilities groundwater around EMS facilities has been monitored monthly since 1993

13

(Libra et al., 1998). The local surficial deposits in north-central and east-central Iowa are mainly glacial till. The manure storage structures were constructed in supraglacial till that has low bulk density and highly variable textures. Twelve monitoring wells were installed around two basins in both upgradient and downgradient directions. Nitrate-N, ammonia-N, organic-N, total organic carbon, sulfate, and fecal coliform bacteria were measured in the groundwater samples. The analysis showed that the decline in nitrate-N and sulfate concentrations was a result of denitrification and sulfate reduction, respectively. Both of these reactions require the development of anaerobic conditions beneath EMS.

Goody et al. (2002) also found that denitrification occurred beneath two unlined cattle manure storage sites on the Chalk aquifer of southern England. As shown in Figure 2.4, soil samples from directly beneath the two unlined EMS were obtained by drilling an inclined borehole. The inclined hole allowed for the installation of gas samplers, made from plastic waste pipe, at 3.5, 5.5, 7.5, 10.5, 14.3, and 17.7 m below the EMS. To ensure the gas was in equilibrium, samples were taken about 12 months after installation. Core samples adjacent to the EMS were also collected from a vertical borehole. Analysis indicated sulfate reduction occurred below the EMS and was confirmed by a decrease in the sulfate concentration from 150 to 50 mg/L and by an enhanced ratio of $\delta^{34}S - SO_4$ and $\delta^{18}O - SO_4$ (Figure 2.5-(A)). Furthermore, limited nitrate concentrations enhanced the reducing conditions beneath the EMS. Data for N_2/Ar and $\delta^{15}N - N_2$ was obtained by gas chromatography and mass spectrometry analysis and showed that denitrification was occurring 14 m below the EMS.

14
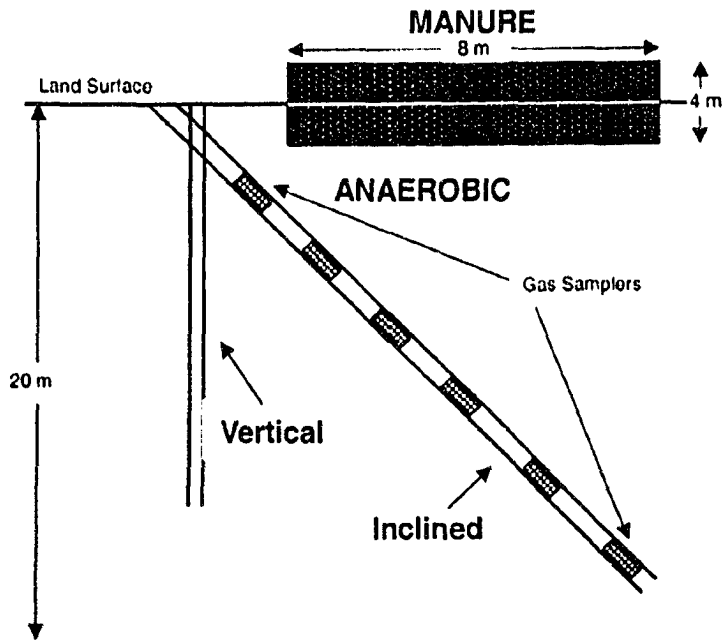
Figure 2.4 Schematic of the inclined and vertical boreholes drilled for soil and gas samplers beneath the unlined EMS on the Chalk aquifer, U.K.
(Modified from Goody et al., 2002)
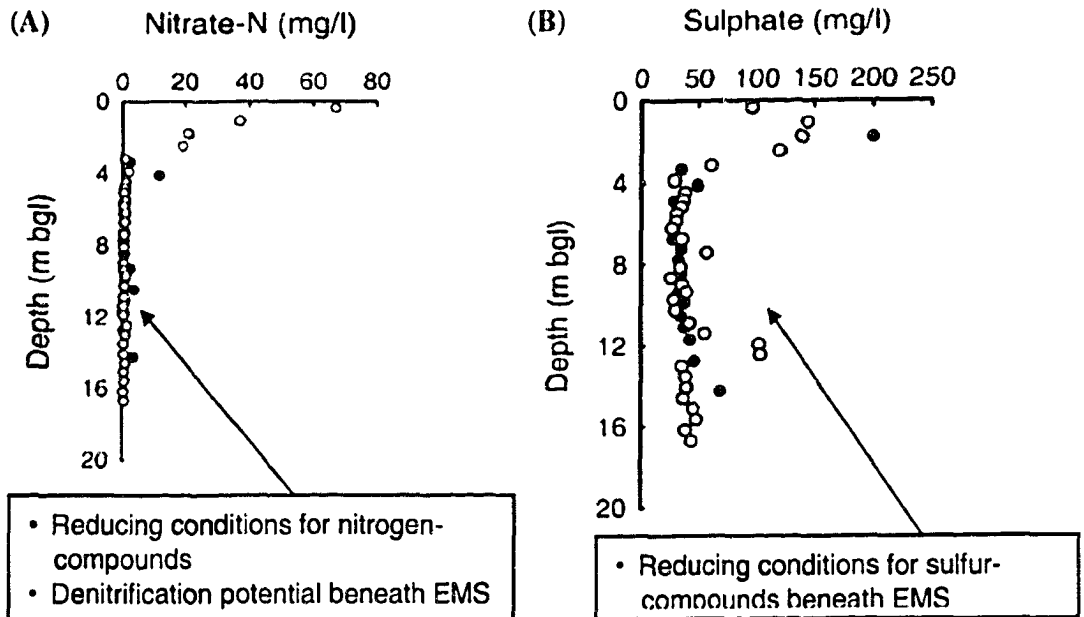
Figure 2.5. (A) Measured nitrate concentrations beneath EMS and (B) measured sulfate concentrations beneath EMS on the Chalk aquifer, U.K.
(Modified from Goody et al., 2002)

15

2.2.2 Adsorption by cation exchange

Ammonium (NH_4^+) with its positive charge preferentially is adsorbed to clay minerals due to exchange reactions. As a result of the exchange reactions, cations originally presented on the clays such as calcium and magnesium are displaced into the pore fluid.

From the Iowa example mentioned previously, the wells, which were installed below EMS, indicated that a considerable build-up of nitrogen occurred below the basin via cation exchange processes on the clayey materials used to construct the facilities. It was estimated that roughly 5,300 pounds of nitrogen would be retained in the glacial deposits beneath the 1/2-acre basin each year. It was anticipated that adsorption by cation exchange would continue until the capacity of the glacial materials beneath EMS was exceeded. The processes of ammonium adsorption by cation exchange result in chemical redistribution of cations in the pore fluid (Semmens et al., 1977) and are described by the following reactions.

$$NH_4^+ + HX \Rightarrow NH_4X + H^+; K = \frac{[NH_4X][H^+]}{[NH_4^+][HX]}$$ Eq.[1]

$$[X]M^+ + NH_4^+ + HCO_3^- \Rightarrow [X]NH_4^+ + MHCO_3$$ Eq.[2]

$$[X]M^{2+} + NH_4^+ + 2HCO_3^- \Rightarrow [X]NH_4^+ + M(HCO_3)_2$$ Eq.[3]
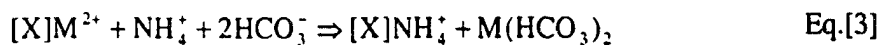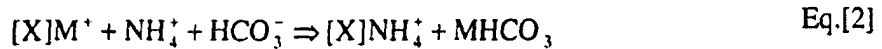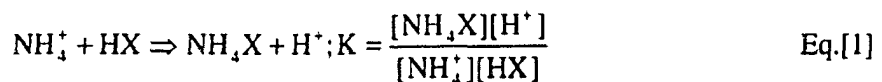
where X^- refers to exchange sites with monovalent (Jenne, 1995). M^+ and M^{2+} denote cations participating in monovalent and divalent exchange reactions. The redistribution of cations generated by exchange reactions may directly impact changes in pH because of the hydrogen and ammonium exchanges denoted by Eq. [1] and bicarbonate

16

complexation with major cations in Eq. [2] and [3], respectively. Adsorption by exchange reactions is dependent on the exchange characteristics of the soil mineralogy (Balci, 2004), and are a major geochemical reaction in the subsurface EMS environment affecting pore fluid chemistry beneath and around EMS.

Fonstad and Maule (2001) investigated a seepage plume from an EMS constructed in a layered lacustrine sand, silt, and clay deposit in Saskatchewan, Canada. In addition, laboratory column tests were performed with soil samples from the site. During the test, hog manure effluent was subjected to the soil in the columns for two years. The results showed a chromatographic series, which revealed evidence of ion exchange and indicated that potassium and ammonium displaced sodium, magnesium, and calcium on the exchange sites. It caused an increase in hardness at the front of the plume.

2.2.3 Diffusion controlled adsorption

Diffusion should be considered when characterizing the subsurface EMS facilities, since it is major contaminant transport mechanism through the fractured glacial clay and till deposits that are present in Alberta. When ammonium reacts with local geological materials beneath EMS in diffusion dominant areas, diffusion and adsorption promote the long-term regeneration of aqueous phase ions that exist in the soil materials (Freeze and Cherry, 1979; Donahue, 1994; Parker et al.).

Alberta Agriculture Food and Rural Development (2001) conducted several field investigations in Alberta to study older EMS sites built around 1985 and that had no

17

engineered liner system. One field investigation focused on a site with a storage facility measuring 46 m long, 44 m wide, and 4m deep, located over a 10-meter layer of silty sand overlaying glacial clay till. The investigation revealed that some seepage and contaminant transport were present within the upper sandy soil layer which had these adversely affected the shallow groundwater quality. However, most of the contaminant transport that took place in the studied areas was governed by unsaturated flow and the diffusion phenomena.

Diffusion controls transport of ions that participate in the ammonium adsorption process, accompanied by cation exchange reactions through clay particles. Kithome et al. (1998) explicitly described the diffusion-controlled adsorption mechanism as follows:

1. Diffusion of ions through the pore fluid up to the clay mineral particle;

2. Ion diffusion through the clay particles;

3. Exchange reactions take place between the diffused ions and cations on the exchange sites in the interior of the clay minerals;

4. Re-diffusion of the displaced cations occurs from the interior of the clay minerals;

5. Diffusion of the displaced ions through the bulk solutions moves away from the clay minerals.

The internal diffusion of ammonium also results in nitrogen fixation within the interlayer of clays. Fonstad (2004) states that ammonium with an ionic size similar to that of potassium readily penetrates the interlayer fraction of clays, causing collapse of the layer

18

in the clays. Subsequently, nitrogen fixation takes place within the collapsed layers and makes it extraordinarily difficult for ammonium nitrogen to be removed by exchange reactions.

2.2.4 Competition

Liquid manure is similar to existing in-situ pore fluid chemistry in that it is a mixture of ammonium, potassium, calcium, magnesium, etc.; therefore, the cations in both the liquid manure and the pore fluid compete with each other to occupy exchange sites.

Buss et al. (2003) also noted the effects of competition for exchange sites by other cations in solution. It is possible for this competition to significantly impact the value of the distribution coefficient, K_d, as noted in the Chalk and Mercia Mudstone example. In the case of the Chalk site, the K_d value determined by artificial ammonium reagent (10 mg NH_4-N/L; pH 8) was 1.43 mL/g; whereas, the K_d from the leachate was 0.03 mL/g. For the Mercia Mudstone experiment, the estimated K_d values were 7.78 mL/g and 5.24 mL/g for artificial ammonium solution and leachate, respectively.

Lumbanraja and Evangelou (1990) showed that co-existing ammonium in solutions suppressed potassium adsorption on a vermiculitic soil surface. However, ammonium adsorption was enhanced by the presence of potassium. It was speculated that the similar sizes of potassium and ammonium produced the competition to occupy the sorption sites. In addition, James and Harward (1964) and Mortland (1968) stated that the ability of ammonium to diffuse through the expanded interlayer of the clay surfaces was enhanced by the competition for the sorption sites.

19

2.3 NUMERICAL STUDIES FOR REACTIVE RADIAL DIFFUSION MODEL

A modified radial diffusion cell experiment modeling soil-manure interactions was implemented to simulate the geochemical environment beneath EMS, including (1) anaerobic conditions; (2) adsorption by cation exchange; (3) diffusion controlled adsorption; and (4) cation competition. To simulate both radial diffusive transport and the change in pore fluid chemistry, it is necessary to develop a coupled reactive model. The reactive simulation should account for the subsurface environment of EMS and will include conditions (1) through (4) to obtain geochemical and hydrogeological parameters needed to predict long-term diffusion associated with ammonium adsorption. The following section describes previous radial diffusion models developed to study soil-manure interactions as well as examples of coupled reactive transport models.

2.3.1 Previous models for radial diffusion

Several radial diffusion models were independently developed to simulate transient diffusive transport and geochemical reactions. Novakowski and Van der Kamp (1996) derived a semi-analytical radial diffusion model based on the Bessel functions and effectively simulated transient radial diffusive transport. The models were used to determine effective porosities and effective diffusion coefficients for the porous media by fitting the modeling results with experimental data. Van Stempvoort and Garth (2003) also developed a geochemical model that was based on radial diffusion through a cell.

20

r_c r_R — Central reservoir

L

— Porous media
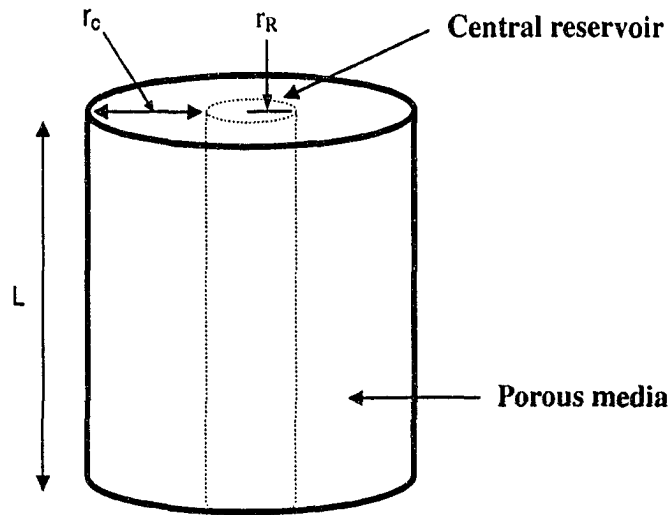
Figure 2.6 Schematic diagram of a radial diffusion cell

The model employed PHREEQC (Parkurst and Appelo, 1999) to predict the major

cation and anion concentrations, aqueous speciation, calcite/atmospheric CO_2

equilibrium, and sulfur/carbon redox reactions.

Figure 2.6 demonstrates the radial geometry of the diffusion cell used to obtain the semi-

analytical solutions of Novakowski and Van der Kamp's model (1996). It was assumed

that the porous media was homogeneous and completely water saturated. Therefore,

there is no diffusion through the base or the top of the reservoir. The governing equation

was based on Crank's cylindrical semi-infinite diffusion equation (1975) and was used to

account for radial diffusion through the porous media as follows:

$$\frac{\partial C}{\partial t} = \frac{D^*\partial^2 C}{R\partial r^2} + \frac{D^*\partial C}{Rr\partial r} - \frac{\lambda}{R}C \qquad r_R \leq r \leq r_c \qquad \text{Eq.[4]}$$

21

In the equation above, C denotes the resident concentration and r refers to the radial distance from the center of the reservoir. Therefore, a change in concentration is a function of the radial distance from the reservoir and the diffusion time allowed. D^*, R, and λ are constants, representing the effective diffusion coefficient, retardation factor, and decay constant, respectively. The effective diffusion coefficient is equivalent to ωD_0, where D_0 is the free-water diffusion coefficient of a given solute, and w accounts for the pore geometry (i.e., tortuosity). Using Laplace transformation and the limiting forms of the Bessel functions, Novakowski and Van der Kamp (1996) developed the semi-analytical radial solution as shown below:

$$C_{DR}(\infty) = \frac{2\beta_1}{(r_{DC}^2 + 2\beta_1 - 1)} \qquad \text{Eq.[5]}$$

Where $C_{DR}(\infty)$ is the concentration at equilibrium. Rearranging for β_1 gives:

$$\beta_1 = \frac{C_{DR}(\infty)[r_{DC}^2 - 1]}{2[1 - C_{DR}(\infty)]} \qquad \text{Eq.[6]}$$

Where β_1 is the dimensionless mixing coefficient for the reservoir and is equal to $\dfrac{V_R}{R\theta_c\gamma_R r_R}$. r_{DC} denotes the dimensionless radius of core sample. V_R is the volume of the reservoir [L^3], γ_R is the cross-sectional area through which diffusion occurs [L^2], and r_R is the radius of reservoir [L].

Figure 2.7 presents the unreactive radial diffusion experiment simulated by Novakowski and Van der Kamp's semi-analytical solution (1996). The best fit to the experimental

22

results was obtained using an effective coefficient of $1.7 \times 10^{-10} \text{ m}^2/\text{s}$ (Figure 2.7).
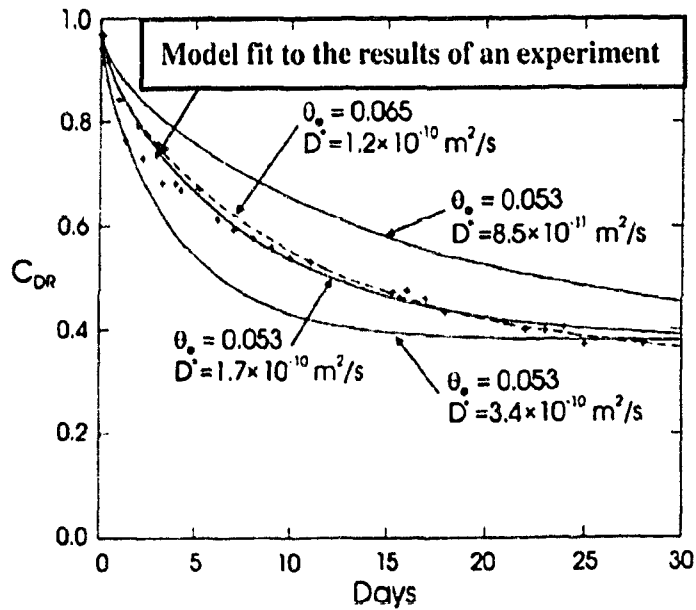
Figure 2.7 The radial diffusion model and effective diffusion coefficient simulated by the semi-analytical solution
(Modified from Novakowski, K.S., Van der Kamp, G, 1996)

On the other hand, the geochemical model used to investigate the change in the geochemistry of the porous media (i.e., the aquitard sample) was designed as a series of reactive steps, including mixing solution, reaction, and exchange equilibration. The radial diffusion cells containing the aquitard samples were successively subjected to deionized water and/or a salt solution during dilution-diffusion steps. The equilibration process generated by radial diffusion between the reservoir and the porous media requires from 45 to 75 days. (The time to reach equilibrium predominately depends on the properties of the soil in the cells).

23

After reaching diffusive equilibrium, the reservoir solutions were sampled using a syringe to obtain major cation and anion concentrations. In this method, the effective pore fluid volume refers to the pore volume in the porous media and the water added into the central reservoir. The effective volume of pore fluid used in the PHREEQC model was determined by calculating the mass balance during each addition episode. It was assumed that the chemical events, including mixing, reaction, and equilibration, took place at a steady rate during the run time. Thus, the exchange coefficient provided in the PHREEQC database (PHREEQC.DAT) was used without modification. Due to the possibility of CO_2 degassing during sampling, measuring, and adding, the aqueous CO_2 was equilibrated in the model to the same pressure found in the atmosphere CO_2 (log $P_{CO2} = -3.51$). Calcite and exchange equilibration were added to the reaction terms. Accordingly, the simulated concentrations for major cation and anions were in agreement with the measured concentrations collected from the diffusion experiment. It was indicated by the model that sulfate reduction was taking place simultaneously; therefore, oxidation of pyrite and organic carbon were employed in the simulation. It was observed that the simulated exchangeable cations modeled by using the radial diffusion cell method were generally lower when compared to those generated by conventional methods, such as the ammonium acetate test.

2.3.2 Coupled reactive transport models

Previous simulations that used a radial diffusion experiment were done for unreactive contaminants. For this research, it is necessary to develop a reactive radial diffusion model which can simulate exchange reactions. This section presents a review of existing

24

researches that utilized models for diffusion, mixing, and ion exchange for various transport problems.

Jungnickel et al. (2002) conducted coupled multi-ion reactive transport modeling using the numerical model CMIRT, which is based on a finite element method. The author pointed out that the standard diffusion theory based on Fick's first law provided inaccurate design parameters, particularly with respect to diffusion coefficients for geoenvironmental practices. This is because the standard diffusion equation does not consider the movement of ions in response to an electric field. Therefore, a fully coupled transport equation, derived from the Nernst-Planck equation, was adapted as the governing equation to describe macroscale ion transport through an isotropic clay soil in the presence of electrochemical forces. It was indicated that the CMIPT prediction gave more realistic results for multi-ion transport systems. In the case of unreactive transport, the diffusion coefficient could be accurately estimated. However, the model inadequately simulated the reactive transport problem that accompanies the exchange reactions that account for both the adsorption of diffused ions on clay surface and the displacement of ions originally present in the surface. It was concluded that total pore fluid composition and reactive transport terms should be taken into consideration in the multi-ion diffusion problem.

Boris et al. (2004) performed reactive transport modeling to investigate changes in leachate composition downstream of the Banisveld landfill, located in the Netherlands. The PHREEQC one-dimensional reactive transport model was employed to simulate field observation including the degradation of DOC coupled with the reduction of iron

25

oxide, cation exchange, proton buffering, and kinetic precipitation of siderite and calcite. In particular, ammonium and potassium were significantly retarded due to cation exchange with the clay minerals. Therefore, the desorption process of exchangeable Ca, Fe(II), and proton occurred and released to the leachate, increasing the pH of the leachate.

Carlyle (2004) attempted to predict long-term changes in major cation concentrations in a Triassic Sandstone aquifer in northwest England as it was invaded by estuary water . Cation exchange capacity and selectivity coefficients for Ca^{2+}, Mg^{2+}, Na^+, and K^+ were determined by standard laboratory methods. The exchange parameters obtained from the laboratory experiment were used in a one-dimensional reactive transport model in PHREEQM. The predictions were compared with 40 years of field well data. The predicted concentration trends based on Gaines-Thomas exchange, with calcite in equilibrium, were in agreement with measured patterns. However, the divalent ions were considerably overestimated, while the sulfate concentrations and alkalinity were underestimated.

Gaucher et al. (2004) investigated diffusion of an alkaline plume moving from a concrete structure into bentonite used for sealing access galleries for radioactive waste repositories. The model was systemized as an OPC (Ordinary Portland Cement) barrier, an MX bentonite clay barrier, and the corresponding equilibrated pore fluid. The clay barrier was modeled as a semi-infinite medium with a single diffusion coefficient of 10^{-11} m^2/s. A one-dimensional transport provided in the PHREEQC geochemical code was used for the long-term transient diffusion problem. It was assumed that the system was

26

at thermodynamic equilibrium and that the concrete pore fluid concentrations were constant. A specific database was created for the aqueous complexes, mineral-phase solubilities, and ion exchange parameters for Na^+, K^+, Ca^{2+}, Mg^{2+}, and H^+ in the pore fluid of the MX80 bentonite. The simulation revealed that mineralogical transformation from the host clayey rock to the concrete began with ion exchange reactions that changed Na-nontmorillonite into a more potassic and calcic phase. The sensitivity of the calculations to exchange reactions and the diffusion coefficients was evaluated. The sensitivity analysis enabled the authors to develop a phenomenological law indicating that the extent of the mineral transformation is proportional to the square root of the diffusion time and the diffusion coefficient. The simulation provided the efficiency of pH buffering by demonstrating the efficiency of the mineralogical assemblage that controlled the CO_2 partial pressure.

2.4. KEY FINDINGS

The key findings from the literature review are as follows:

- Geochemical conditions for the EMS subsurface can include

    (1) Anaerobic conditions beneath EMS

    (2) Significant cation exchange reactions resulting in adsorption

    (3) Diffusion-controlled adsorption

    (4) Cation competition for exchange sites

- A diffusion experiment to obtain advanced parameters should reflect the geochemical requirements, (1) to (4).

- A radial diffusion cell experiment should be modified to account for the anaerobic conditions listed in (2) to (4) of the EMS characterization.

- Physical, chemical, and mineralogical characterizing of the soil plays an important role in ammonium diffusion problems.

- A reactive transport model is required in addition to the radial diffusion cell method to account for reactive species.

- The reactive modeling should also consider the geochemical conditions beneath EMS listed in conditions (1) to (4).

- The reactive modeling accounts for both radial diffusion and the change in pore fluid chemistry by employing diffusion transport, mixing solutions, and exchange reactions.

28

REFERENCES

Alberta Agriculture, Food and Rural Development, 2002. Beneficial Management Practices: Environmental Manual for Hog Producers in Alberta.

Alberta Agriculture, Food and Rural Development, July. 2001. Earthen Manure Storage Seepage, A study of five typical sites, AGDEX, July. 2001. AGRI-FACTS.

Balci, S., 2004. Nature of ammonium ion adsorption by sepiolite: analysis of equilibrium data with several isotherms. Water Research, 38, 1129–1138.

Buss, S.R., Herbert, A.W., Morgan, P., Thornton, S.F., 2003. Review of ammonium attenuation in soil and groundwater, National Groundwater and Contaminated Land Centre, Environmental Agency, Almondsbury, Bristol, U.K.

Carlyle, H.F., Tellam, J.H., Parker, K.E., 2004. The use of laboratory-determined ion exchange parameters in the predictive modelling of field-scale major cation migration in groundwater over a 40-year period. Journal of Contaminant Hydrology, 68, 55–81.

Chang, A.C., Olmstead, W.R., Johanson, J.B., Yamashita, G., 1974. The sealing mechanism of wastewater ponds. Journal of Water Pollution Control Federation, 46(7), 1715–1721.

Ciravolo, T.G., Martens, D.C., Hallock, D.L., Collins Jr., E.R., Kornegay, E.T., Tomas, H.R., 1979. Pollutant movement to shallow groundwater tables from anaerobic swine waste lagoons, Journal of Environmental Quality, 8(1), 126–130.

Crank, J. 1975. The mathematics of diffusion, 2nd ed. Clarendon Press. Oxford.

Davis, S., Fairbank, W., Weisheit, H., 1973. Dairy waste ponds effectively self-sealing. Transactions of the ASAE, 16, 69–71.

DeTar, W.R., 1979. Infiltration of liquid dairy manure into soil. Transactions of the American Society of Agricultural Engineers, 22, 520–558.

Devitt D., Letey, J., Lund, L.J., and Blair, J.W., 1976. Nitrate-nitrogen movement through soil as affected by soil profile characteristics. Journal of Environmental Quality, 5(3), 283–288.

Donahue, R.B., Barbour, S.L., Headley, J.V., 1999. Diffusion and adsorption of benzene in Regina clay. Canadian Geotechnical Journal, 36, 430–442.

Fleming, R., Johnston, J., Fraser, H., 1999. Leaking of liquid manure storage—Literature

review, July, 1999, Ridgetown College-University of Guelph, Ridgetown, Ontario.

Fonstad, T.A., 2004. Transport and fate of nitrogen from earthen manure storage effluent seepage. Ph.D. thesis, University of Saskatchewan.

Fonstad, T.A., Maule, C.P., 1996. Solute migration beneath earthen hog manure storages in Saskatchewan. ASAE International Meeting, Pheonix, Arizona. July, 1996. Paper presentation, Pub.No.: CSAE paper No. 962049.

Fonstad, T.A., Maule, C.P., Barbour, S.L., Donahue, R., Ingram, L., Meier, D., 2001. Fluid movement and chemical transport from animal wastes storages. Preferential Flow, Water Movement and Chemical Transport in the Environment, Proceedings of the 2nd International Symposium, January 2001, Honolulu, Hawaii, USA. ASAE Pub # 701P0006.

Freeze, R.A., Cherry, J.A., 1979. Groundwater. Prentice-Hall, Inc., Englewood Cliffs, New Jersey, USA.

Fukada, T., Hiscock, K.M., Dennis, P.F., 2004. A dual-isotope approach to the nitrogen hydrochemistry of an urban aquifer. Journal of Applied Geochemistry, 19, 709–719.

Gaucher, E.C., Blanc, P.B., Matray, J.M., Michau, N., 2004. Modeling diffusion of an alkaline plume in a clay barrier. Journal of Applied Geochemistry, 19, 1505–1515.

Gooddy, D.C., Clay, J.W., Bottrell, S.H., 2002. Redox-driven changes in porewater chemistry in the unsaturated zone of the chalk aquifer beneath unlined cattle slurry lagoons. Journal of Applied Geochemistry, 17, 903–921.

Ham, J. M., DeSutter, T. M., 1999. Seepage losses and nitrogen export from swine-waste lagoons: a water balance study. Journal of Environmental Quality, 28, 1090–1099.

Heaton, T.H.E., Talma, A.S., Vogel, J.C., 1983. Origin and history of nitrate in confined groundwater in the western Kalahari. Journal of Hydrology, 62, 243–262.

Hendry, M.J., McCready, R.GL., Gould, W.D., 1984. Distribution, source and evolution of nitrate a glacial till of southern Alberta, Canada. Journal of Hydrology, 70, 177–198.

Hills, D.J., 1976. Infiltration characteristics from anaerobic lagoons. Journal of the Water Pollution Control Federation, 48,695–709.

Hudak, P.F., 2000. Regional trends in nitrate content of Texas groundwater. Journal of Hydrology, 228, 37–47.

James, D.W., Harward, M.G., 1964. Competition of NH_3 and H_2O for adsorption sites on

30

clay minerals. Soil Science Society of America Journal Proceeding, 28, 636–640.

Jenne, E.A., 1995. Metal adsorption onto and desorption from sediments. I . Rates. In Metal speciation and contamination of aquatic sediments, ed H.E. Allen. Ann Arbor, MI: Ann Arbor Press.

Jungnickel C., Smith, D., Fityus, S., 2002. Coupled multi-ion electrodiffusion analysis for clays soils. Canadian Geotechnical Journal, 41, 287–298.

Kithome, M., Paul, J.W., Lavkulich, L.M., Bomke, A.A., 1998. Kinetics of ammonium adsorption and desorption by the natural zeolite clinoptilolite. Soil Science Soceity of America Journal, 62, 622–629.

Kreitler, C.W., Jones, D.C., 1975. Natural soil nitrate: The cause of the nitrate contamination of groundwater in Runnels Country, Texas. Ground Water, 13(1), 53–61.

Libra, R.D., Quade, D.J., Seigley, L.S., 1998. Groundwater monitoring at earthen manure-storage structures in Iowa. Sixth National Nonpoint-Source Monitoring Workshop, September 21, 1998. Cedar Rapids, IA, p. 5–14.

Lo, K.V., 1977. A study of the infiltration characteristics of dairy waste storage lagoons. CSAS Paper No. 77–208, CSAE Annual Meeting, August, 1977.

Lumbanraja, J., Evangelou, V.P., 1990. Binary and ternary exchange behavior of potassium and ammonium at low exchangeable fractional loads in three Kentucky subsoils. Soil Science Society of America Journal, 157(5), 269–277.

Minnesota Pollution Control Agency (MPCA), April, 2004. Effects of liquid manure storage systems on groundwater quality—Summary Report.

Mortland, M.M., 1968. Protonation of compounds at clay minerals surfaces. Transactions 9th International Congress Soil Science I : 691–699.

Nordstedt, R.A., Baldwin, L.B., 1973. Lagoon disposal of dairy wastes in Florida. American Society of Agricultural Engineering, Special Publication, SP-01-73. ASAE, St. Joseph, Michigan.

Novakowski, K.S., Van der Kamp, G., 1996. The radial diffusion method 2. A Semianalytical model for the determination of effective diffusion coefficients, porosity, and adsorption. Water Resources Research, 32(6), 1823–1830.

Oenema, O., Boers, P.C.M., Willems, W.J., 1998. Leaching of nitrate from agriculture to groundwater. The effect of policies and measure in the Netherlands. Environmental Pollution 102, 471–487.

31

Parker, B.C., Gillham, R.W., Cherry, J.A., 1994. Diffusive disappearance of immoscoble-phase organic liquids in fractured geology media. Canadian Geotechnical Journal, 32, 805–820.

Parkhurst D.L., Appelo, C.A.J, 1999. User guide to PHREEQC—A computer program for speciation, reaction-path, 1D-transport and inverse geochemical calculations. U.S. Geological Survey Water Resource Inv.

Pauwels, H., Lachassagne, P., Bordenave, P., Foucher, J.C., Martelat, A., 2001. Temporal variability of nitrate concentration in a schist aquifer and transfer to surface waters. Journal of Applied Geochemistry, 16, 583–596.

Power, J.F. and J.S. Schepers,1989. Nitrate contamination of groundwater in North America. Agriculture, Ecosystems & Environment, 26, 165–187.

Semmens, M.J., Wang, J.T., Booth, A.C., 1997. Biological regeneration of ammonium-saturated clinoptilolite II. Mechanism of regeneration and influence of salt concentration. Environmental Science and Technology, 11(3), 260–265.

Spalding, R.F., Exner, M.E., 1993. Occurrence of nitrate in groundwater—a review. Journal of Environmental Quality, 22, 392–402.

Van Breukelen, B.M., Griffioen, J., Roling, W.F.M., van Verseveld, H.W., 2004. Reactive transport modelling of biogeochemical processes and carbon isotope geochemistry inside a landfill leachate plume. Journal of Contaminant Hydrology, 70, 249–269.

Van Stempvoort, D.R., Van der Kamp, G, 2003. Modeling the hydrogeochemistry of aquitard using minimally disturbed samples in radial diffusion cells. Journal of Applied Geochemistry, 18, 551–565.

Wallenstein, M.D., 1999. Nitrogen saturation, http://www.duke.edu/~mdw7/nitrogen/ncycle.html

Wassenaar, L., 1995. Evaluation of the origin and fate of nitrate in the Abbotsford aquifer using the isotopes of ^{15}N and ^{18}O in NO_3^-. Journal of Applied Geochemistry, 10, 391–405.

Widory, D., Kloppmann, W. Chery, L., Bonnin, J.B., Rochdi, H., Guinamant, J-L., 2004. Nitrate in groundwater—an isotopic multi-tracer approach. Journal of Contaminant Hydrogology, 72, 165–188.

Williams, A.E., Lund, L.J., Johnson, J.A., Kabala, Z.J., 1998. Natural and anthropogenic nitrate contamination of groundwater in a rural community, California. Environmental Science Technology, 32, 32–39.

32

CHAPTER 3.0

DIFFUSION OF AMMONIUM THROUGH GLACIAL CLAY SOILS

ABSTRACT

The objective of this study is to experimentally simulate interactions between liquid manure and soil in diffusion dominant areas beneath earthen manure storage (EMS). A previous radial diffusion cell method was modified to create the anaerobic chamber that employed a plastic glove bag supplied with inert argon gas. The anaerobic conditions were maintained during the entire run time. Little oxidation of ammonium occurred; consequently, nitrate and nitrite concentrations were lower than the detection limit. Chloride (Cl) played a key role in redistribution of major cations and anions resulting from the ammonium diffusion. Linear ammonium and potassium adsorption isotherms were obtained. The resulting distribution coefficients, K_d for ammonium ranged from 0.3 to 0.4 L/kg. Significant ammonium exchange reactions led to an average increase in hardness of 137% in the reservoirs, due to extraction of exchangeable calcium and magnesium. Geochemical mixing modeling using PHREEQC adequately simulated the linear ammonium adsorption at the low dissolved ammonium concentrations (<30mM). The predicted manure volumes to cause ammonium saturation were 1.0 to 1.4 mL/g for the glacial clay soil samples.

33

3.1 INTRODUCTION

The livestock industry in Alberta, including both cattle and hogs, has expanded tremendously in the past 25 years (Alberta Agriculture, Food and Rural Development, 2002). According to the most recent agricultural statistics, Alberta currently produces 40% (5.8 million head, as of Jan. 2004) and 14% (2.1 million head, as of Jan. 2004) of Canada's total beef and hog output, respectively (Agri-Food Statistics, 2004).

Manure produced by intensive livestock operations has been a public concern due to the substantial volume generated. Earthen manure storage (EMS) system, constructed with local geological material, is a common means to store liquid manure in Western Canada. Old EMS systems (older than 20 years), which are scattered throughout Alberta, have no engineered liner or barrier system to prevent the seepage of liquid manure (AGDEX, 2001). Studies of the issue to date have focused on seepage loss of liquid manure and are based on advection and dispersion as a major contaminant transport mechanism (DeTar, 1979; Fonstad and Maule, 1996, 1999; Ham and DeSutter, 1999; Parker, et al., 1999).

The current Alberta specification for EMS strictly enforces the need for an engineered liner system to protect groundwater and surface water resources (AOPA, 2004). Nevertheless, the presence of nitrate and nitrite, which is commonly caused by the leakage of liquid manure from EMS, has frequently exceeded water quality guidelines. In both the Canadian standard (CCME) and the U.S standard (U.S. EPA), 10 mg/L is the maximum contaminant level (MCL) for $N-NO_3$ and $N-NO_2$. In reality, 32 to 87% of the water resources in areas of low to high intensive livestock operation regions in Alberta exceeded the nitrate MCL for aquatic life (CAESA Water Quality Study, 1998, 2004).

34

Moreover, even EMS structures engineered with clay, geosynthetic, or concrete liner systems often leak liquid manure into surrounding hydrogeologic regimes (MPCA, 2001).

In order to evaluate a budget of excess nitrogen under EMS environment, the long-term diffusion effect and the interaction of liquid manure and local soils should be considered, in addition to the seepage loss of liquid manure from EMS facilities. In this study, therefore, diffusion is identified as a major transport process between liquid manure and the local soils used for the construction of EMS. The rationales for the introduction of diffusion are as follows: (1) molecular diffusion, which is the slowest contaminant transport, should be examined for long-term risk assessment and a decommissioning strategy to address unlined old EMS; and (2) EMS in the Canadian Prairies are generally located in glacial clay and/or clay tills with diffusion dominated hydrogeologic regimes.

Ammonium, which is the most abundant form of nitrogen in liquid hog manure, is regarded as an origin of nitrate contamination in aquifers (Fonstad, 2004, Hendry et al., 1984). This is because excessive ammonium can be transported to the aerobic zones of an aquifer and then be oxidized to form nitrate and/or nitrite (Kreitler, 1975, Wassenaar, 1995, Fukada et al., 2004, Hudak, 2000; Widory et al., 2004, Zebarth et al., 1999). According to Fonstad (2004)'s field measurement for fluid throughout EMS, low dissolved oxygen concentrations, ranging from 0.3 to 1.3 mg/L, lead to anaerobic conditions at subsurface areas of the EMS. Eh readings of less than −100 mV, and high organic carbon concentrations of approximately 6,000 mg/L, also cause nitrogen to remain in the ammonium form. Thus, it is necessary to study ammonium that exists in

35

the anaerobic subsurface areas of EMS to better understand the fate of nitrogen compounds within the nitrogen cycle.

Figure 3.1 accounts for the conceptual model of ammonium diffusion along fractured glacial clays and/or clay tills in the Canadian Prairies. The fractures in the glacial deposits play a key role in the long-tem redistribution of ammonium through molecular diffusion and adsorption (D'Alessandro et al., 1997; Parker et al., 1994; Donahue, 1999). Adsorbed and aqueous phase ammonium may prevail between the fractures. Aqueous phase-ammonium in a major facture is gradually attenuated. Significant cation exchange with the clays in contact with ammonium-rich liquid manure can be a primary cause of strong ammonium adsorption. This may lead to changes in pore fluid chemistry due to the replacement of cations present in the clays.

The aims of this study of ammonium diffusion through glacial clays are (1) to simulate a soil-liquid manure system under an artificial anaerobic condition using a radial diffusion cell method (RDC), and (2) to develop geochemical models that simulate the anaerobic RDC experiment and predict the maximum ammonium sorption capacity of the glacial clay soils.

The RDC method is a versatile technique to simulate geochemical interaction problems with low permeable materials (Van der Kamp, 1996). During the interaction of soil and liquid manure in the RDC, three-dimensional radial diffusion of the liquid manure into porous soils will occur but will be retarded by an adsorption process that involves selective ion exchange reactions. The most essential requirements for performing both

36

the RDC experiment and the geochemical modeling are as follows: (1) maintenance of anaerobic conditions; (2) diffusion controlled adsorption (Kithome et al., 1998); (3) cation exchange between ammonium in the liquid manure and major cations on the clay surface; and (4) competition with the co-existing cations in the liquid manure to occupy the limited exchange sites. These four key elements are required to effectively simulate the geochemical environments at the subsurface of EMS on the basis of a conceptual model for ammonium diffusion.

The specific objectives of the study are to

1. Apply the RDC method within anaerobic conditions.

2. Investigate change in pore fluid chemistry through radial diffusion and adsorption

3. Examine adsorption and desorption characteristics of ammonium under the anaerobic conditions

4. Examine cation exchange characteristics under cation competition.

5. Simulate geochemical mix models: manure effluent-soil interaction using PHREEQC

37

3.2 METHODS

3.2.1 Anaerobic radial diffusion cell method

The radial diffusion cells in Figure 3.2 were developed to effectively investigate various aspects of the hydrogeochemistry of pore fluid or groundwater that is in contact with low permeable materials such as aquitards, crystalline rocks, and marine sediments (Van der Kamp et al., 1996; Van Stempvoort and Van der Kamp, 2003). The principle of the method is based on diffusive exchange reactions between pore fluid in the saturated soil sample and the reservoir water placed along the axes of the soil samples (Figure 3.2-[3]). After diffusive equilibrium has occurred, the solution in the central reservoir of the RDC allows for taking the representative pore fluid of the soil samples. By excluding fluid flow in the RDC, the transport mechanism between solutes in the reservoir and soils is governed only by a molecular diffusion process, and not by advection and dispersion. This characteristic of the RDC method allows the examination of a wide range of geochemical reactions related to the soil-manure interaction.

PVC Teflon was used to create the diffusion cells in this experiment (See Figure 3.2-[2]). The PVC Teflon-diffusion cell is to eliminate undesirable geochemical reactions between the pore fluid and the steel of the Shelby tube (See Figure 3.2-[4]). The processes of the modified RDC method for anaerobic conditions are as follows: (1) cell preparation, (2) diffusive equilibrium with pore fluid (65 days), (3) diffusion of ammonium (60 days) and (4) desorption process (60 days).

38

3.2.1.1 Cell preparation

Glacial clay soils were sampled in Ponoka, Alberta (Cell UA1 to 5). Figure 3.2-[4] shows the geometry of the PVC Teflon RDC. To construct a reservoir hole in the soil sample in the RDC, the trimmed top surfaces of the soils were drilled along the central axis of the cylindrical RDC (O.D: 27mm, I.D.: 24mm, H: 70mm). These were not drilled down to the absolute bottom of the cells in order to allow three-dimensional radial diffusion into the porous media (Figure 3.2-[3]). The typical reservoir depth was 70 mm from the top surface, and the average height of all the cells was 90 mm. A polyethylene (PE) porous liner was inserted into the drilled hole. The intact core samples were then enclosed with O-ring seals and with the square-shaped upper-plates of the cells. Prior to inserting the PE liners into the holes, the porous liners were saturated with deionized water for 7 to 8 hours by vacuum pumping. The mass change of the liners, due to water saturation, was recorded for the full mass balance calculation. Porous liners should be hydrophilic and unreactive to soils and liquid manures. Consequently, this experiment employed hydrophilic polyethylene porous liners: X-5306 Porex®-25μ fine. The porous liners were installed to prevent the collapse of the drilled holes during the diffusion period. The cell preparation was conducted as quickly as possible to minimize disturbance of, and moisture loss from, the soil samples.

39

3.2.1.2 Diffusive equilibrium and monitoring reservoir

After setting up the five diffusion cells, each central reservoir, which had an inner volume of 20 mL±0.08, was filled with 20mL-ultra pure water (18.2 MΩ-cm and 0.7 μS/cm, Barnstead). To synthesize the representative pore fluid, diffusive equilibrium time of at least 60 to 90 days was allotted, depending on the types of soil samples (Van der Kamp et al., 1996). In order to confirm diffusive equilibrium time, the electrical conductivity (Orion® 130A) of the reservoir solutions was measured by using a micro electrical probe and the pH change (Accumet® AR50) of the reservoirs was monitored (Van der kamp et al., 1996).

The levels of deionized water in the reservoirs decreased during the equilibrium period. Subsequent injections of deionized water into the reservoirs were conducted to attain water saturation through intact soil samples. Swelling of the clay-rich soil samples would take place during successive injections of deionized water into the reservoirs. Water loss from the reservoirs due to monitoring and evaporation was recorded to ascertain mass balance calculation. The mass balance was considered to include the volume of water successively injected for saturation, evaporation loss, routine measurement loss, and sampling loss. Stagnant electrical conductivity response of the reservoirs was regarded as completing diffusive equilibrium. After equilibrium was achieved, the pore fluids were sampled from the diffusion cells and filtered using syringe filtration (Waterman® nylon membrane filter paper 0.45 μm). Major cations and anions of the pore fluid were analyzed by ion chromatography (IC), Dionex® 2500 (Applied Environmental Geochemistry Research Facility at the University of Alberta).

40

Accordingly, the pore fluid data were (1) pore fluid volume by mass balance, (2) measured electrical conductivity, (3) monitored change of pH, (4) temperature effect, (5) major cation and anion concentrations by IC analysis, and (6) total alkalinity as $CaCO_3$. The obtained data were used to characterize initial pore fluid chemistry, based on speciation calculation by PHREEQC. The initial pore fluid data were also used for geochemical mix modeling.

3.2.1.3 Anaerobic conditions and injection of liquid hog manure

To delineate the anaerobic environment beneath EMS, the four hand-glove bag, shown in Figure 3.2-[1] was adopted. It is a cost-effective method and enables monitoring of the reservoir under anaerobic condition. Argon gas was added to the structured chamber (3 or 5 times per day) to maintain less than 1% oxygen in the glove bag chamber. The anaerobic chamber is to separate the diffusion cells from the atmospheric environment of the laboratory room (O_2 available). Within the chamber, to enable routine monitoring and sampling, were an electrical balance and a spanner to screw the top cap of each cell. It is critically important to maintain a sufficient argon gas level during the routine monitoring program.

After creating the anaerobic chamber, the reservoirs in the five diffusion cells were subjected to 20mL±0.36-raw liquid hog manure, which was collected at the Swine Research and Technology Center (SRTC) at the University of Alberta (March, 2004). In order to obtain the earlier response of the anticipated ion exchange, the effluents of about 20 mL (reservoir volume) were sampled from the reservoirs (~20 mL) after a10-day

41

diffusion period elapsed. Fresh, raw manures were immediately re-injected into the reservoirs. During a 60-day diffusion period, a routine monitoring program was performed to assess the effluent chemistry; this included the measurement of electrical conductivity, pH, temperature, and mass change caused by evaporation and measuring and sampling losses.

After the 60-day diffusion period, the effluents were sampled from all the cells. The conventional water chemistry analysis was conducted for the collected effluent solution, including cation and anion concentration by IC analysis, electrical conductivity, pH, temperature, dissolved oxygen (DO), hardness, alkalinity, total dissolved solids (TDS), and total organic carbon (TOC).

The final step was to account for the desorption process of the ammonium, which means that the ammonium adsorbed during the diffusion period might desorbe from the soils. To do this, 20mL-ultra pure water was injected into each reservoir in contact with the soil samples, thus desorbing ammonium. The average injection error was approximately 0.15%. The desorption duration was planned to continue for a further 60 days. The routine monitoring program and water chemistry analysis were carried out during the desorption-periods.

42

3.2.2 Geochemical mixing models using PHREEQC

PHREEQC interactive version 2.6.0.1 (Parkhurst and Appelo, 1999), developed by the U.S. Geological Survey, was used for the geochemical mixing modeling. The simulations were divided into two modules: (1) SIMPLE MIX MODEL and (2) MIX MODEL. The SIMPLE MIX MODEL refers to the simulation of a single episode of the liquid hog manure injection. Hence, the SIMPLE MIX MODEL described the anaerobic RDC experiment with a single liquid hog manure injection. The MIX MODEL aims to simulate the maximum number of injection episodes to achieve full ammonium saturation in soils.

The specific deliverables for the SIMPLE MIX MODEL are (1) modeled ammonium adsorption isotherm, in terms of pore fluid equilibrium activity; (2) comparison with the adsorption isotherm determined by the anaerobic RDC experiment; and (3) simulation of altered pore fluid chemistry, including anaerobic conditions, sulfate reduction, and ammonium diffusion in competition with major cations. The concept of the SIMPLE MIX MODEL is that the liquid hog manure in the reservoir chemically mixes and reacts with pore fluid in the soils. The key input data is effective pore fluid volume estimated by the mass balance calculation. In this study, the effective pore fluid volume was defined as the sum of the water volume added successively, due to water saturation, and the water volume determined by gravimetric water content. The analytical results of the pore fluid and liquid hog manure were used to determine the initial pore fluid chemistry and contaminant source chemistry, respectively.

43

Because molecular diffusion is a long-term contaminant transport process in low permeable materials, it is hard to determine the maximum amount of ammonium adsorbed on the clays in the laboratory. Thus, the MIX MODELING is a predictive model employed to investigate the injection volume of the liquid hog manure required for full ammonium saturation of the clay soils. In the simulation, liquid hog manure was successively injected into the reservoir until the reservoir equilibrium concentrations would not change. It is assumed that the soils could not adsorb any more ammonium at this point (i.e., there were no reservoir concentration changes).

3.3. MATERIAL CHARACTERIZATION

Material characterization is divided into two sections: (1) soil characteristics that included local geology, classification, clay mineralogy, physical and chemical properties; and (2) geochemical property of the liquid hog manure as a contaminant.

3.3.1 Soils

3.3.1.1 Local geology and sampling

Soils for this study were sampled in east central Ponoka, Alberta, Canada. The surficial geology of the sampling areas is mainly glacial lacustrine deposits (Figure 3.3). The general lithology is glacial clay and clay till at 1.5 to 5.3 m from the surface. Alberta has a semi-arid climate. The Ponoka region uses groundwater as its drinking water resource. The soil samples were collected by Shelby tube and were stored in a moisture room (4°C) prior to being used in the experimental program.

44

3.3.1.2 Characterization of soils

According to the United Soil Classification System (USCS), the sampled soils in this study were classified as sandy lean clay (CL) for Cell UA1 to 2 at 1.5 to 2.3 m depth, and sandy fat clay (CH) for Cell UA3 to 5 at 3 to 5.3 m depth. Table 3.1 indicates the particle-size distribution and classification of the soil samples. The soils consist of 31 to 34% sand and 65 to 68% clay. Both samples are inorganic clay-rich soils, as determined on the basis of A-line plotting (Lambe and Whitman, 1979). Based on the USDA system (U.S. Department of Agriculture), Cell UA1 to 2 and Cell UA3 to 5 were classified as clay loam and clay, respectively (Table 3.1). Hydrometer tests and wet sieve analysis were preformed for the soil classification at the Geotechnical Laboratory at the University of Alberta. The total porosity estimated by gravimetric water content typically ranged from 0.32 to 0.42. Volumetric water contents were 32 to 33% for Cell UA1 to UA2, and 37.5 to 42% for UA3 to 5.

X-ray diffraction (XRD) and Scanning Electron Microscope (SEM) analyses were used to identify the clay mineralogy of the samples. The XRD results indicated that the soil samples were composed of smectite ($[1/2Ca,Na]0.7[Al,Mg,Fe]_4[Si,Al]_8O_{20}[OH]4.nH_2O$), quartz ($SiO_2$) and illite ($KAl_2(OH)_2[AlSi_3(O,OH)_{10}]$), with lesser amounts of plagioclase ($Na[AlSi_3O_8] - Ca[Al_2Si_2O_8]$), chlorite ($(Mg, Fe)_5Al(AlSi_2) O_{10}(OH)_9$), and kaolinite ($Al_4Si_4O_{10}(OH)_8$). Minor quantities of potassium feldspar ($K[SiAl_3O_8]$) were detected as well (See Table 3.1). Elemental identification using SEM revealed the same results as XRD. The soil samples from Ponoka consist of 60% smectite in clay fraction and framework sand/silt. Smectite-rich clays promoted the swelling of soil samples during

45

the diffusive equilibrium. The estimated ratio of bulk to clay fraction from the XRD (Table 3.2) closely met the USCS classification results.

The cation exchange capacity (CEC) of the soil samples is a crucial factor in determining ammonium adsorption, because adsorption of dissolved ions is always part of an exchange reaction (Langmuir, 1997). The cation exchange capacities of the samples were determined by conventional ammonium acetate (NH_4OAc) method (McKeague, 1981): 21.2 meq/100g for Cell UA1 to 2; 43.3 meq/100g for Cell UA3 to 4; and 34.2 meq/100g for Cell UA5 (Table 3.3). The high CEC values reflected the 68% smectite present in the clay fraction of the samples.

A saturated pastes extraction test (Carter, 1993) was conducted to examine geochemical properties of the soil samples (Table 3.3). A 1:1 volume ratio of air-dried soil to deionized water was adopted to create the saturated pastes (Hogg and Henry, 1984). The saturated pastes were then centrifuged to extract the soluble salts. The background ammonium-N concentrations were 4 to 10 mg/L. The leached nitrate-N concentrations ranged from 3.4 to 8.6 mg/L. Nitrite was rarely detected because it rapidly oxidized to nitrate. The measured soil pH typically ranged from 7.9 to 8.2 for the non-saline soils.

3.3.2 Liquid hog manure

Characterization of the initial liquid hog manure is one of the most critical procedures in this process because it provides the initial source concentration (C_0) in the reservoir. The liquid hog manure collected at the SRTC was filtered by centrifugation and syringe filtration (0.45 micron). Table 3.4 shows IC analysis for the initial liquid hog manure.

46

Notably, ammonium was a dominant species of which mole fraction is approximately 45%. Bicarbonate, potassium and chloride were 36%, 7% and 6% in mole fraction, respectively. Calcium, magnesium and sodium in the manure were extremely limited (1 to 4%).

The measured electrical conductivity and pH of the manure were 23 mS/cm (25°C), and 7.9, respectively. The dissolved oxygen (DO) reflected an extremely low level: 0.8 mg/L. Vigilant treatment of liquid hog manure is required to maintain its anaerobic condition as a source contaminant. The saturation index (SI) of calcite ($CaCO_3$), calculated by PHREEQC, was 0.2 for the liquid hog manure; consequently, calcite precipitation is expected during the diffusion periods. CO_2 (g) in the initial liquid hog manure was over saturated with respect to atmospheric CO_2 because the SI value of 0.58 for CO_2 (g) in the initial liquid manure exceeded the SI of -3.51 for atmospheric CO_2 (g). Therefore, degassing of CO_2 (g) from the reservoir is expected to occur during the experimental program, including the sampling and measuring of the reservoir solutions. The degassing of CO_2 (g) from the reservoir will contribute to an increase in the reservoir's pH. As a result of this, degassing of CO_2 may reduce acidity resulting from the exchange reactions between the raw liquid hog manure and the clay soil samples. The speciation calculation based on PHREEQC also indicated that bicarbonate forms aqueous complexes preferably with calcium, magnesium and sodium in the liquid hog manure, and that phosphate forms complexes with hydrogen ($H_2PO_4^-$ and HPO_4^{-2}) in the initial liquid hog manure.

47

3.4 RESULTS AND DISCUSSION

3.4.1 Geochemical interpretation for soil-liquid manure system.

3.4.1.1 Synthetic pore fluid using radial diffusion cell

Prior to sampling equilibrated reservoir solutions that are in contact with the soil samples, the required diffusive equilibrium time was predicted using ChemFlux (Fredlund and Stianson, 2003), which is a comprehensive transport-modeling tool based on the finite element method. Figure 3.4 shows the 3D mesh for the porous media and the 3D diffusion-only modeling result. In the model, a conservative chloride diffuses from the porous media to the reservoir. The negative sign refers to the inverse diffusion direction (porous media → reservoir). The predicted equilibrium time ranged from 55 to 60 days when the equilibrium concentration for chloride reached 20 mg/L. Therefore, the reservoir solutions were sampled when 65 days had elapsed and the pore fluid was regarded as representative of the soil samples. To confirm the diffusive equilibrium time, the electrical conductivity of and the pH change in the reservoir solutions were measured (Van der kamp et al., 1996).

Figure 3.5 shows that the determined diffusive equilibrium time ranged from 53 to 66 days for the Cell UA1, 2 and 5 samples. In the case of Cell UA3 and 4, the reservoir solution was not completely equilibrated within the designed equilibrium time (65 days). The estimated equilibrium time for Cell UA3 and 4 ranged from 66 to 109 days.

The elapsed time to reach equilibrium varied according to soil properties: particle size and clay fraction. As shown in Figure 3.5, it appeared that the soil samples with smaller

48

particle size and more clay fraction resulted in a longer diffusive equilibrium time.

The initial pore fluid concentrations are presented in Table 3.5. Ammonium, nitrate, and nitrite concentrations were lower than detection limits according the IC analysis. The charge balances of total dissolved major cations and anions in the pore fluid ranged from 0.60 to 1.73% in equivalence.

The pH of the reservoir increased with contact time, as shown in Figure 3.6. The value of log P_{CO2} distributed from -1.8 to -1.5 throughout Cell UA1 to UA5. It is possible that developing CO_2 (g) in the pore fluids contributed to an increase in the pH of the reservoir solutions. Calcite ($CaCO_3$) was dissolved in the reservoirs. The saturation index (SI) of calcite ranged from -2.6 to -1.6 in the reservoir solutions, according to PHREEQC calculation. As a result of over saturation of CO_2 (g) and dissolution of $CaCO_3$, the reservoir solutions increased on average from 6.1 to 7.0 (Figure 3.6). Therefore, the pH of 7.0 is regarded as the representative pH of the synthesized pore fluids after diffusive equilibrium periods. The value of pH 7.0 will be used for the initial pore fluid chemistry data for geochemical models.

The monitored temperatures of the reservoirs ranged from 20 to 24.5°C during the 65-day equilibrium periods. The measured reservoir temperature was reasonably stable at the laboratory-room temperature. It was assumed that a change in the reservoir temperature did not affect the initial pore fluid chemistry (Van der Kamp et al., 1996).

In order to complete water saturation, 5 to 17 mL of water was added to the soil samples in the diffusion cells. The added water volume was approximately 1.5 to 4.7% of the

49

total volume of the soil in the cells. The effective pore fluid volume ranged from 130 to 170 mL. This estimation is based on mass balance equations that include 0.01 to 0.07% of the evaporation loss and 0.38% of measurement loss. Both the initial pore fluid chemistry and the effective pore fluid volume were used for the geochemical mix models.

3.4.1.2 Reservoir monitoring during ammonium diffusion

Reservoir concentrations for the 10-day and 60-day periods of diffusion are presented in Table 3.5 and Table 3.6. During the 60-day diffusion periods, a substantial decrease of ammonium (NH_4^+) in the reservoirs occurred under the anaerobic conditions (Table 3.5). After a 10-day period, it was observed that approximately 53% of the initial ammonium amount (mole) in the reservoir had diffused to the soils (Figure 3.8-(a)). Ammonium diffusion, achieved by means of a single injection of liquid hog manure, was almost completed within 60 days (with an average 91% of the initial NH_4^+ diffused into the soil samples). Table 3.7 shows the comparison between measured concentrations on diffusion-day 60 and the diluted concentrations for cations and anions. The diluted concentrations, which represent equilibrium concentrations after the diffusion and desorption processes, were calculated based on the mass balance between the diffused and remaining ions in the reservoirs and the estimated pore fluid volume (130 to 170 mL). In comparison with measured and calculated equilibrium concentrations, ammonium did not reach theoretical equilibrium (Table 3.7 and Figure 3.8). The measured ammonium concentrations in Cell UA1, 4 and 5 were about 55 to 84% lower than the expected equilibrium concentrations. The significant concentration gradient for ammonium between background pore fluid (less than 1 mg/L, Table 3.5) and liquid

50

manure (5241 mg/L) forces a dramatic decrease of effluent concentration in the reservoir. The measured concentrations of ammonium were considerably lower than the equilibrium concentrations. This reflects significant retardation of ammonium through the tortuous paths in the fine materials. Therefore, it is clear that ammonium was the most diffusive and adsorptive cation for the 60-day periods. (It is noteworthy that Cell UA2 data were somewhat odd because some rock materials in the cell blocked manure transport; Cell UA2 data were thus neglected for the most part for this portion of the analysis). During the ammonium diffusion periods, chloride was not equilibrated. As shown Table 3.7, the measured chloride concentrations were higher than the calculated equilibrium concentrations (i.e., 3 and 4 times higher). It is inferred that chloride would not diffuse into the porous media. Chloride (Cl^-) played a key role in achieving charge balance during the ammonium diffusion. Figure 3.8 shows the measured and diluted concentrations of K^+ and Cl^-. Chloride preferentially exists as a binary form with potassium in the effluent. In addition, inverse diffusion of the excess calcium and magnesium caused these elements to pair with chloride as $CaCl_2$ and $MgCl_2$ in the reservoir. As shown Figure 3.8 (c), the charge balance error for Cl^- vs. $K-Ca^{2+}-Mg^{2+}$ pairs ranged from 4 to 9% in the effluent solution. During the desorption process, chloride concentrations were closer to equilibrium. Potassium and sodium diffusion was impacted by cation competition and a lower concentration potential when compared with ammonium. The exchangeable sodium re-diffused from the porous media and the reservoir during the 60-day desorption periods. The differences between measured and equilibrium concentrations of sodium indicated an increase of exchangeable sodium concentrations (See Table 3.7). Exchangeable calcium and magnesium greatly increased in the pore fluids. Calcium concentrations increased up to 26 to 81% of initial

51

concentrations in Cell UA1, 4 and 5. The inverse calcium diffusion from the porous media to the reservoir is attributable to exchange reactions. Calcite precipitation in Cell UA2 and 3 caused the decrease in calcium in the reservoir. Significant magnesium inverse diffusion occurred due to exchange reactions during the 60-day diffusion periods. The calcium and magnesium extracted by exchange reactions led to a substantial increase in the reservoir's hardness (Figure 3.10). Geochemical changes during the diffusion periods were summarized in Table 3.8 and 3.9.

Accordingly, ammonium diffusion caused by chemical potential resulted in a redistribution of major cations and anions in the pore fluid. In particular, chloride, which is typically used as a conservative transport species, is more likely to be retained or re-founded due to charge balancing with potassium, exchanged calcium and magnesium. In addition, it is speculated that significant ammonium adsorption that results from the soil-manure contact may cause the expansion of the clay structure layer due to the relatively high hydrated radius of ammonium.

Maintenance of the anaerobic environment in and around the diffusion cells is a key issue for simulating the reducing conditions of the EMS. For the entire running time, including the desorption process (185 days), the presence of oxygen was strictly limited by adding argon gas into the chamber. As a result, ammonium, the reduced form of nitrogen compounds, was not oxidized to nitrate or nitrite in any of the diffusion cells (Figure 3.7-(b)). This fact is key evidence of the importance of maintaining the anaerobic environment in the diffusion cells. In addition to nitrogen compounds, it is possible for sulfate to be reduced in the cells. Sulfate levels decreased from 46 to 80% of the initial

52

content in all cells (Cell UA1 to 5). The author also smelled hydrogen sulfide during the reservoir sampling of the diffusion cells. A chamber in which sufficient argon gas is supplied can be one of the cost-effective alternatives to the creation of an anaerobic environment in a laboratory (Figure 3.2).

As shown in Figure 3.11, the measured reservoir pH rapidly dropped from 7.9 to 6.2 within the first 40 days, and then increased to 6.6 over the next 20 days. It is understood that the increase in hydrogen ions in the reservoir is due to the diffusion of hydrogen ions from the pore fluid. The pH difference between pore fluid (pH 7) and effluent (pH 7.9) resulted in H^+ diffusion (Reaction 1). The predicted pH value for the effluent was between pH 7 and pH 7.8 at equilibrium; however, the effluent pH was equilibrated at 6.2. It is speculated that cation exchange reactions between NH_4^+ and H^+ (Reaction 2) affect the decrease of pH in the reservoir that contains effluent. When ammonium diffuses into the pore fluids, ammonium concentrations increase in that pore fluid. The ammonium with a high mole fraction is better able to occupy the exchange sites on clay minerals and thus exchange H^+. Consequently, the exchangeable H^+ diffusion may directly impact the pH decrease in the reservoirs.

Reaction 3 in Figure 3.10 shows that ammonium adsorption by cation exchange causes chemical regeneration when major cations exist in pore fluid (Semmens et al., 1977). As ammonium (NH_4^+) occupied the exchange sites (X^-), the major cations (M) on the clays were extracted from the sites. The exchanged cations then formed a complexation with bicarbonate ($MHCO_3$) in the pore fluid. According to the speciation calculation by PHREEQC, calcium, magnesium, and sodium preferably forms complexes with

53

bicarbonate. Eventually, the ammonium adsorption caused by cation exchange results in a decrease in bicarbonate in the reservoir. In reality, as shown Figure 3.11, the measured alkalinity for all the cells decreased remarkably, to 64 from 81% of the initial alkalinity.

The elevated $CaCO_3$ concentration, generated by the exchanged calcium, reacted quickly enough to maintain equilibrium in the reservoir solution (Reaction 4). The SI for calcite by PHREEQC speciation calculation ranged from 0.05 to 0.2; therefore, the calcite precipitation generated by the exchangeable Ca^{2+} diffusion caused a H^+ concentration increase in the effluent reservoir.

In contrast, after 40 days, an increase in pH was observed in all of the reservoirs (Figure 3.11). Exsolution and/or evaporation of CO_2 (g) occurred due to reactions between the exchanged calcium and bicarbonate in the liquid hog manure (Reaction 5). The elevated $CaCO_3$ concentration and the developing CO_2 (g) caused the increase in pH levels in the reservoir after 40 days. The measured reservoir pH increased from 6.2 to 6.6 after 40 days. The substantial decrease in TOC in the reservoirs supported the oxidation of organic compounds (e^- donor) as well as sulfate (e^- acceptor) reduction during the interaction periods (Reaction 6). The measured TOC decreased in the reservoirs, to 63 from 86% of the initially determined TOC. Sulfate (SO_4^{2-}) reduction produced bicarbonate. The by-product of bicarbonate was indicated by an increase in pH after 40 days. Based on the measured pH levels for all reservoirs, pH ranged from 6.6 to 7.9 after 40 days. According to the Eh-pH diagram for the $S-O_2-H_2O$ system, illustrated by Langmuir (1997), H_2S and HS^- will be the dominant sulfur forms in the anaerobic pore fluid at the measured pH levels. Furthermore, clay minerals in the cells will buffer the

54

acidity that is generated by ammonium diffusion. It is known that clays have a mineral-controlled buffer capacity that is remarkably resistant to acidity, particularly in comparison to associated carbonates (Langmuir, 1997).

Consequently, ammonium diffusion resulted in a pH decrease in the pore fluid of all the diffusion cells in addition to a substantial increase in hardness. As shown in Figure 3.10, the initial pore fluid pH 7.0 decreased to between 6.2 and 6.6 because of H^+ diffusion resulting from the initial pH difference, the cation exchange of NH_4^+ for H^+ and Ca^{2+}, and calcite precipitation. Therefore, it is possible that changes in pH and hardness can be simple indicators of the need to investigate ammonium plumes in EMS areas, as shown in figure 3.10.

3.4.1.3 Diffusion controlled adsorption with cation exchange

Using the anaerobic RDC method, linear ammonium and potassium adsorption isotherms (R^2= 99%) were developed in relation to the equilibrium activity of the reservoir (Figure 3.13). Although equilibrium concentration was more commonly adopted, equilibrium activity was used for the adsorption isotherms. This was preferable because geochemical reactions are written in terms of activities (Langmuir, 1997). In addition, equilibrium activity is favored to maintain the consistency of the experiment and for numerical modeling results. The activities were determined by PHREEQC speciation calculation based on the Davies equation for activity coefficients. High cation exchange capacity and diffusion-controlled adsorption primarily affected the linearity of ammonium and potassium adsorption isotherms. It was assumed that the smectite-rich soil samples with

55

high CEC values (21.2 to 43.3 meq/100g) had sufficient exchange sites to adsorb 80 to 90% of the ammonium injected into the cells (Figure 3.7 (a)). Von Breymann and Suess (1988) also showed that a linear relationship exists between adsorbed ammonium and dissolved ammonium concentration. The adsorbent were smectite-rich clay soils with high CEC (i.e., 84.2 meq/100g). The dissolved ammonium concentrations ranged from 5.3 to 36 mM. Additionally, Lumbanraja and Evangelou (1994) obtained a linear *ammonium adsorption in a low dissolved ammonium level (20 mM)* as well; in their experiment, ammonium competed with potassium for the exchange sites on vermiculite and smectite-type clay.

In addition to high CEC, The ammonium adsorption was a function of diffusion time, a result also known as the diffusion-controlled adsorption process. The mechanism of diffusion-controlled adsorption may be divided into five steps (Kithome et al., 1998): (1) diffusion of ammonium through the pore fluid up to the smectite particle; (2) diffusion of ammonium through the smectite particles; (3) chemical exchange between ammonium and exchangeable cations on exchange sites in the interior of the smectite minerals; (4) diffusion of the displaced cations out of the interior of the mineral; and (5) diffusion of the displaced cation through the solution away from the smectite minerals. The diffusion-only process in the cells reflected both the heterogeneity and tortuosity of the intact core samples. Therefore, even when the source ammonium concentration was highly concentrated (5242 mg/L), the ammonium dissolved in pore fluid was equilibrated at the low level concentration.

The clay-rich soil samples selectively adsorbed and/or desorbed major cations in pore fluid. The competition for the limited adsorption sites depended on constituent mole

56

fraction, ionic size, and ionic charge. In particular, ammonium predominated at the adsorption sites because ammonium with a high mole fraction in the source—about 45%—had more chances to occupy the sites compared to other co-existing cations. James and Harward (1964) and Mortland (1968) showed that ammonium adsorption was enhanced in the presence of potassium because adsorbed ammonium tends to expand soil's inter-layer as a result of the ability of ammonium to internally diffuse onto a surface. Lumbanraja and Evangelou (1994) observed that potassium adsorption, when in competition with ammonium, was suppressed, whereas ammonium adsorption was enhanced in binary (NH_4^+-K^+) and ternary (NH_4^+-K^+-Ca^{2+}) systems.

Calcium, magnesium, and hydrogen ions were extracted during cation exchange reactions. Significant magnesium and calcium extraction contributed to a hardness increase in the reservoir (Figure 3.10). Because a calcium and magnesium ion has a smaller hydrated radius than does ammonium or potassium, the aqueous calcium cannot percolate through the collapsed or expanded interlayer of minerals where adsorbed ammonium and potassium are located. According to the two-year column studies on smectite-rich clay-swine effluent, conducted by Fonstad et al., (2001), sodium, magnesium, and calcium on the exchange sites were displaced by potassium and ammonium. This caused an increase in hardness for the long-term soil-effluent interaction. Von Breymann and Erwin (1988) discovered that magnesium was displaced by ammonium exchange in marine sediment within an anoxic environment. The extracted magnesium was approximately 40% of the total adsorbed ammonium. Clay mineralogy and CEC were similar to the soils employed in this experiment.

57

The desorption process was performed by injecting ultra pure water into the reservoirs after the ammonium diffusion. The low ammonium concentration (Table 3.5) detected in the reservoir was caused by a dilution effect at the boundary between the pore fluids and the source reservoir; that is, net desorption did not occur. The dilution effect would be influenced by the high CEC soil sample and the small volume of the injected liquid manure.

3.4.2 Geochemical mix models for the anaerobic RDC method

The ammonium adsorption isotherm simulated by SIMPLE MIX MODEL was in agreement with the RDC experiment result (Figure 3.14). The adsorption simulation had lower and upper limits that were dependent on the estimated effective pore fluid volume. The input pore fluid volume ranged from 130 to 170 mL. Notably, the lower limit simulation was in agreement with the experimental results. Figure 3.14 shows the total adsorbed ammonium, both from the experiment (5.7 mmol/cell) and from the lower limit simulation (6.2 mmol/cell).

Estimated K_d ($\dfrac{mg/kgdrysoil}{mg/solution}$) values for ammonium ranged from 0.3 to 0.4 L/kg under anaerobic conditions and diffusion only process (See Figure 3.14). It was assumed that smectite-rich clay soil samples adsorbed all the diffused ammonium because of their relatively large amount of clay soils with high CEC (21.2 to 43.3 meq/100g, dried 531 to 634 g). However, K_d from radial diffusion cells accounts for a diffusive transport characterized by heterogeneity and tortuosity of in situ soils under competition and

58

reducing conditions. No literature that addresses the distribution coefficients, K_d, for ammonium when dealt with by the anaerobic RDC method was available. However, in recent studies, Fonstad (2004) obtained 0.05 to 0.4 L/kg of K_d; Thornton et al. (2000, 2001) reported 0.06 L/kg to 0.3 L/kg values; Erskine (2000) and Ceazan et al. (1989) showed a 0.5 L/kg value and 0.34 L/kg to 0.87 L/kg values for K_d, respectively. The K_d values of these previous studies vary because of the disparate types of adsorption experiments, the CEC, clay mineralogy, initial ammonium concentration, and running time.

Figure 3.15-(a), (b) and (c) demonstrate the simulation of the pore fluid chemistry during linear ammonium adsorption. The anaerobic condition was maintained in the simulated pore fluid. The nitrate and nitrite was not produced in this model (See Figure 3.15-(b)). The concentrations for nitrate and nitrite were negligible in the simulation. Potassium in competition with ammonium linearly diffused into the pore fluid. Diffusion of calcium and magnesium into the soil samples was not significant in the simulation. Sulfate reduction was also simulated by changes in pore fluid chemistry (See Figure 3.15-(c)).

According to the MIX MODEL results, the predicted liquid manure volumes for ammonium saturation were 1.0 to 1.4 mL/g of soils (706 to 1010 mL/Cell, dilution effect was considered). Figure 3.16 represents the number of mixing simulations that correspond to the required number of source injections of the initial injected ammonium concentration, at 5242 mg/L. Thus, the predicted number of injections ranged from 35 to 40 for sandy lean clays (Cell UA1 and 2) and from 43 to 51 for sandy fat clay samples. About 20 mL of liquid manure per injection was assumed, owing to the inner volume of

59

the source reservoir. As a result, the adsorptive ammonium required for saturation ranged from 0.3 to 0.5 mol/kg, depending on the soil types when the initial ammonium concentration was set to 5242 mg/L.

3.5 SUMMARY AND CONCLUSIONS

Maintenance of an anaerobic environment was the most critical issue in this experiment. For the entire experiment period (185 days), the oxygen level was strictly limited by means of adding argon gas. Nitrate and nitrite levels were lower than the detection limit. Therefore, the reduced condition was established and maintained during ammonium diffusion.

The monitoring program of the reservoir was conducted to investigate geochemical responses of pore fluid with diffusion time. Ammonium diffusion caused by chemical potential resulted in a redistribution of major cations and anions in the pore fluid. Chloride (Cl⁻) played a key role in achieving charge balance during the ammonium diffusion. Ammonium diffusion resulted in a pH decrease in the pore fluid of all the diffusion cells in addition to a substantial increase in hardness.

High cation exchange capacity and diffusion-controlled adsorption primarily affected the linearity of ammonium and potassium adsorption isotherms. The distribution coefficient, K_d, determined by a radial diffusion cell method ranged from 0.3 to 0.4 L/kg under competition with co-existing cations and diffusion only mechanism.

The *SIMPLE MIX MODEL* adequately simulated the linear ammonium adsorption at

60

the low dissolved ammonium concentration (<30mM) and changed pore fluid chemistry. Ammonium saturation capacity predicted by the MIX model ranged from 1.0 to 1.2 L/kg for sandy lean clay samples and 1.4 to 1.7 L/kg for sandy fat clay samples.

In conclusion, the anaerobic RDC method effectively satisfied the key requirements: anaerobic conditions, diffusion controlled adsorption, exchange reactions and competition.

REFERENCES

Agri-Food Statistics Update, Issue No. 70, 2004 Livestock Inventory Estimates - Alberta/Canada

Alberta Agriculture, Food and Rural Development, November 2002. Effects of Manure on Soil and Groundwater Quality

Alberta Agriculture, Food and Rural Development, July. 2001. Earthen Manure Storage Seepage, A study of five typical sites, AGDEX, July. 2001. AGRI-FACTS.

Alberta Agriculture, Food and Rural Development, June 2004. 2004 Reference Guide Agricultural Operation Practices Act (AOPA).

Alberta Agriculture, Food and Rural Development, 1998. Monitoring nitrogen in Alberta's farmland waters.

Alberta Agriculture, Food and Rural Development, March, 2004. Assessing Alberta's water quality (CAESA Study).

Ceazan, M.L., Thruman, E.M., Smith, R.L., 1989. Retardation of ammonium and potassium transport though contaminated sand and gravel aquifer: The role of cation exchange. Environmental Science and Technology, 23(11), 1402–1408.

Carter, M.R., 1993. Soil sampling and methods of analyses. Can. Soc. of Soil Sci., Lewis Publ., Ann Arbor, MI.

D'Alessandro, M., Mousty, F., Bidoglio, G., Guimera, J., Benet, I., Sanchez-Vila, X., Garcia Gutierrez, M., Yllera De Llano, A., 1997. Field tracer experiment in a low permeability fractured medium: results from El Berrocal site. Journal of Contaminant Hydrology, 26,189–201

DeTar, W.R., 1979. Infiltration of liquid dairy manure into soil. Transactions of the American Society of Agricultural Engineers, 22, 520–558.

Donahue, R.B., Barbour, S.L., Headley, J.V., 1999. Diffusion and adsorption of benzene in Regina clay. Canadian Geotechnical Journal, 36, 430–442.

Erskine, A.D., 2000. Transport of ammonium in aquifers: retardation and degradation. Quarterly Journal of Engineering Geology and Hydrogeology, 33, 161–170.

Fonstad, T.A., 2004. Transport and fate of nitrogen from earthen manure storage effluent seepage. Ph.D. thesis, University of Saskatchewan.

Fonstad, T.A., Maule, C.P., 1996. Solute migration beneath earthen hog manure storages in Saskatchewan. ASAE International Meeting, Pheonix, Arizona. July, 1996. Paper presentation, Pub.No.: CSAE paper No. 962049.

Fonstad, T.A., Maule, C.P., 1999. Solute migration and moisture flux beneath cattle feedlot pens. ASAE-CSAE-SCGR Annual International Meeting, Toronto, Ontario, Canada. July 1999. ASAE paper No. 992178; 31.

Fonstad, T.A., Maule, C.P., Barbour, S.L., Donahue, R., Ingram, L., Meier, D., 2001. Fluid movement and chemical transport from an animal waste storage. Preferential Flow, Water Movement and Chemical Transport in the Environment, Proceedings of the 2nd International Symposium, January 2001, Honolulu, Hawaii, USA. ASAE Pub # 701P0006

Freeze, R.A., Cherry, J.A., 1979. Groundwater. Prentice-Hall, Inc., Englewood Cliffs, New Jersey, USA.

Fukada, T., Hiscock, K.M., Dennis, P.F., 2004. A dual-isotope approach to the nitrogen hydrochemistry of an urban aquifer. Journal of Applied Geochemistry, 19, 709–719.

Ham, J. M., DeSutter, T. M., 1999. Seepage losses and nitrogen export from swine-waste lagoons: a water balance study. Journal of Environmental Quality, 28, 1090–1099.

Hendry, M.J., McCready, R.G.L., Gould, W.D., 1984. Distribution, source and evolution of nitrate in a glacial till of southern Alberta, Canada. Journal of Hydrology, 70, 177–198.

Hogg. T.J., Henry, J.L., 1984. Comparison of 1:1 and 1:2 suspensions and extracts with the saturation extract in estimating salinity in Saskatchewan. Canadian Journal of Soil Science, 64, 699–704.

Hudak, P.F., 2000. Regional trends in nitrate content of Texas groundwater. Journal of Hydrology, 228, 37–47.

James, D.W., Harward, M.G., 1964. Competition of NH_3 and H_2O for adsorption sites on clay minerals. Soil Science Society Proceedings, 1964, 636–640.

Jenne, E.A., 1995. Metal adsorption onto and desorption from sediments. Rates in metal speciation and contamination of aquatic sediments, ed H.E. Allen. Ann Arbor, MI: Ann Arbor Press.

Keeney, D.R, Harfield, J.L., 2001. Nitrogen Cycle, Historical Perspective, and Current and Potential Future Concerns. Nitrogen in the Environment: Source, Problems, and Management, 2001 ELSEVIER.

63

Kithome, M., Paul, J.W., Lavkulich, L.M., Bomke, A.A., 1998. Kinetics of ammonium adsorption and desorption by the natural zeolite clinoptilolite. Soil Science Society of America Journal, 62, 622–629.

Kreitler, C.W., Jones, D.C., 1975. Natural soil nitrate: The cause of nitrate contamination of groundwater in Runnels Country, Texas. Groundwater, 13(1), 53–61.

Lambe, T.W., Whitman, R.V., 1979. Soil Mechanics, SI Version. John Wiley and Sons.

Langmuir, D., 1997. Aqueous Environmental Geochemistry. Prentice-Hall, Upper Saddle River, New Jersey.

Lumbanraja, J., Evangelou, V.P., 1994. Adsorption-desorption of potassium and ammonium at low cation concentrations in three Kentucky subsoils. Soil Science Society of America Journal, 157(5), 269–277.

McKeague, J.A., 1981. Manual on soil sampling and methods of analysis. 2nd. ed. Ottawa: Canadian Society of Soil Science.

Minnesota Pollution Control Agency (MPCA), April, 2001. Effects of liquid manure storage systems on groundwater quality—Summary Report.

Mortland, M.M., 1968. Protonation of compounds at clay minerals surfaces. Transactions 9th International Congress Soil Science, 691–699.

Okine, E.K., Basarab J.A., 2003. Livestock feed efficiency as it relates to nutrient balancing: improved nutrient utilization reduces nutrient loss in manure. Manure management 2003 conference, Progress and Opportunities, Lethbridge, Alberta.

Parker, B.C., Gillham, R.W., Cherry, J.A., 1994. Diffusive disappearance of immiscible-phase organic liquids in fractured geology media. Canadian Geotechnical Journal, 32, 805–820.

Parker, D.B., Schulte, D.D., Eisenhauer, D.E., 1999. Seepage from earthen animal waste ponds and lagoons: An overview of research results and state regulations. American Society of Agricultural Engineers, 42(2), 485–493.

Parkhurst D.L., Appelo C.A.J, 1999. User guide to PHREEQC: A computer program for speciation, reaction-path, 1D-transport and inverse geochemical calculations. U.S. Geological Survey Water Resource Inv.

Rich, C.I., Black, W.R., 1964. Potassium exchange as affected by cation size, pH and mineral structure. Journal of Soil Science, 97, 384–390.

Semmens, M.J., Wang, J.T., Booth, A.C., 1997. Biological regeneration of ammonium-saturated clinoptilolite. Mechanism of regeneration and influence of salt

concentration. Environmental Science and Technology, 11(3), 260–265.

Thornton, S.F., Lerner, D.N., Tellam, J.H., 2001. Attenuation of landfill leachate by clay liner materials in laboratory columns: 2. Behavior of inorganic contaminations. Waste Management and Research, 19, 70–88.

U.S. Environmental Protection Agency (EPA). 2004. 2004 Edition of the Drinking Water Standards and Health Advisories.

Van der Kamp, G., Van Stempvoort, D.R., Wassenaar, L.I., 1996. The radial diffusion method. 1. Using intact cores to determine isotopic composition, chemistry and effective porosities for groundwater in aquitards. Water Resources Research, 32, 1815–1822.

Van Stempvoort, D.R., Van der Kamp, G., 2003. Modeling the hydrogeochemistry of aquitard using minimally disturbed samples in radial diffusion cells. Journal of Applied Geochemistry, 18, 551–565.

Von Breymann, M.T., Suess, E., 1988. Magnesium in the marine sedimentary environment: $Mg-NH_4$ ion exchange. Chemical Geology, 70, 359–371.

Wassenaar, L., 1995. Evaluation of the origin and fate of nitrate in the Abbotsford aquifer using the isotopes of ^{15}N and ^{18}O in NO_3^-. Journal of Applied Geochemistry, 10, 391–405.

Widory, D., Kloppmann, W. Chery, L., Bonnin, J.B., Rochdi, H., Guinamant, J-L., 2004. Nitrate in groundwater: an isotopic multi-tracer approach. Journal of Contaminant Hydrology, 72, 165–188

Zebarth, B.J., Paul, J.W., Kleeck, R.V., 1999. The effect of nitrogen management in agricultural production on water and air quality: evaluation on a regional scale. Agriculture, Ecosystems and Environment, 72, 35–52.

Table 3.1 Summary of soil classification and property

Index	Group 1	Group 2	Group 3
Sand (%)	35	32	32
Silt and clays (%)	65	68	68
USCS group symbol	CL	CH	CH
USCS Classification	Sandy lean clay	Sandy fat clay	Sandy fat clay
USDA Classification	Clay loam	Clay	Clay
Total porosity (%)	0.32	0.42	0.38
Volumetric water content (%)	33	42	38
Bulk density (g/cm^3)	1.75	1.46	1.61

NOTE: Group1 denotes Cell UA1 and UA2; Group2: Cell UA3 and UA4; Group3: UA5.

Table 3.2 Summary of X-ray diffraction analyses

Minerals		Bulk fraction (%)	Clay fraction (%)
Weight percent		61	39
Quartz		41	2
Plagioclase Feldspar		15	2
Potassic feldspar		2	1
Clays	Kaolinite	6	4
	Chlorite	6	5
	Illite	21	17
	Illite-Smectite	0	0
	Smectite	10	68
	Total Clay	43	95

Table 3.3 Geochemical properties of the soil samples

Geochemical index		Group 1	Group 2	Group 3
Cation exchange capacity (meq/100g)		21.2	43.3	34.2
Total nitrogen (%)		0.06	0.08	0.04
Organic matter (%)		1.5	1.5	1
Total organic carbon (%)		0.74	0.77	0.48
SPE (mg/L)	Sodium	63	60	61
	Calcium	54	52	73
	Magnesium	23	19	23
	Potassium	6	11	15
	N-Ammonium	4	7	10
	Chloride	67	31	24
	Sulfate	150	102	130
	N-Nitrate	9	3	4
	N-Nitrite	2.5	2	0.96
	pH	7.9	8	8.18
	E.C. (mS/cm)@ 25°C	0.39	0.34	0.38
	SAR	1.83	1.81	1.60
	ESR	0.03	0.03	0.02
	ESP	2.67	2.64	2.34

NOTE
(1) Group 1: Cell UA1 and UA2; Group 2: Cell UA3 and UA4 and Group 3: Cell UA5
(2) SPE denotes saturated paste extraction
(3) E.C.: Electrical Conductivity, SAR: Sodium Adsorption Ratio, ESR: Exchangeable Sodium Ratio, and ESP: Exchangeable Sodium Percent

68

Table 3.4 Geochemical property of the liquid hog manure sample

	Analyte	Results	Unit
Cations	Calcium (Ca)	199	mg/L
	Potassium (K)	1710	mg/L
	Magnesium (Mg)	6.4	mg/L
	Sodium (Na)	611	mg/L
	Ammonium (NH_4)	5241.5	mg/L
Anions	Chloride (Cl)	1380	mg/L
	Sulphate (SO_4)	9	mg/L
	Nitrate-N	1	mg/L
	Nitrite-N	1	mg/L
	Orthophosphate (PO_4-P)	1270	mg/L
Carbonates	Bicarbonate (HCO_3)	14300	mg/L
	Carbonate (CO3)	100	mg/L
	Hydroxide (OH)	<100	mg/L
Iron	Iron (Fe)-Dissolved	4	mg/L
Organic carbon	Dissolved organic carbon (DOC)	4700	mg/L
	Total oragnic carbon (TOC)	6510	mg/L
Geochemical index	pH	7.9	pH
	Conductivity (EC)	23	mS/cm
	Hardness (as $CaCO_3$)	523	mg/L
	Alkalinity	11700	mg/L
	Dissolved oxygen (DO)	0.8	mg/L
	Density	1	g/mL
	Total dissolved solid (TDS)	10900	mg/L

Table 3.5 Reservoir monitoring results for major cations (unit: mg/L)

Major cations	Cell I.D.	Initial pore fluid	Initial liquid manure	Diffusion-day 10	Diffusion-day 60	Desorption- day 60
NH4+	UA Cell 1	< 1.0	5242	2423	508	298
	UA Cell 2	< 1.0	5242	2417	3177	59
	UA Cell 3	< 1.0	5242	1767	1067	35
	UA Cell 4	< 1.0	5242	-	136	18
	UA Cell 5	< 1.0	5242	1093	169	30
K+	UA Cell 1	10	1710	1260	856	20
	UA Cell 2	10	1710	1340	1370	72
	UA Cell 3	6	1710	1260	854	31
	UA Cell 4	6	1710	-	408	23
	UA Cell 5	4	1710	1120	726	42
Na+	UA Cell 1	28	611	530	460	110
	UA Cell 2	<20	611	540	600	60
	UA Cell 3	<20	611	1520	420	90
	UA Cell 4	21	611	-	320	80
	UA Cell 5	<20	611	510	460	90
Ca2+	UA Cell 1	16	199	190	250	110
	UA Cell 2	<10	199	150	80	80
	UA Cell 3	13	199	180	180	120
	UA Cell 4	13	199	-	360	110
	UA Cell 5	<10	199	250	260	120
Mg2+	UA Cell 1	6	6.4	15	89	45
	UA Cell 2	<2	6.4	8	17	36
	UA Cell 3	3	6.4	14	68	34
	UA Cell 4	3	6.4	-	92	29
	UA Cell 5	<2	6.4	28	106	25

Table 3.6 Reservoir monitoring results for major anions (unit: mg/L)

Major anions	Cell I.D.	Initial pore fluid	Initial liquid manure	Diffusion-day 10	Diffusion-day 60	Desorption- day 60
Cl-	UA Cell 1	20	1380	1110	706	135
	UA Cell 2	<20	1380	1150	1040	69
	UA Cell 3	<20	1380	1120	684	101
	UA Cell 4	<20	1380	-	468	131
	UA Cell 5	<20	1380	1040	751	132
PO43-	UA Cell 1	<1	1270	313	294	8
	UA Cell 2	<1	1270	282	199	47
	UA Cell 3	<1	1270	297	199	11
	UA Cell 4	<1	1270	-	41	5
	UA Cell 5	<1	1270	144	80	13
HCO3-	UA Cell 1	200	14300	6670	3890	751
	UA Cell 2	200	14300	8920	11500	704
	UA Cell 3	200	14300	6570	5100	801
	UA Cell 4	200	14300	-	2730	579
	UA Cell 5	100	14300	5810	3260	637
SO42-	UA Cell 1	24	9	3	5	12
	UA Cell 2	6	9	3	2	4
	UA Cell 3	16	9	3	4	1
	UA Cell 4	16	9	-	3	2
	UA Cell 5	6	9	3	5	6
NO2- / NO3-	UA Cell 1	<0.04	1	0.4	D.L	0.3
	UA Cell 2	<0.04	1	0.4	D.L	<2
	UA Cell 3	<0.04	1	0.4	D.L	<0.2
	UA Cell 4	<0.04	1	-	D.L	<0.2
	UA Cell 5	0.05	1	0.4	D.L	<0.2

Table 3.7 Measured concentrations vs. diluted concentrations (equilibrium) unit: mg/L

Analyte	Cell I.D.	Diffusion-day 60		Final pore fluid after desorption	
		Measured conc.	Diluted conc.	Measured conc.	Diluted conc.
NH_4^+	Cell UA1	508	1117	29	1050
	Cell UA2	3177	1106	59	704
	Cell UA3	1067	930	35	815
	Cell UA4	136	559	18	545
	Cell UA5	169	1079	30	1058
K^+	Cell UA1	856	306	20	191
	Cell UA2	1370	291	72	117
	Cell UA3	854	237	31	145
	Cell UA4	408	187	23	148
	Cell UA5	726	269	42	190
Na^+	Cell UA1	460	119	110	57
	Cell UA2	600	109	60	33
	Cell UA3	420	extrac.	90	extrac.
	Cell UA4	320	84	80	53
	Cell UA5	460	100	90	50
Ca^{2+}	Cell UA1	250	42	110	8
	Cell UA2	80	42	80	32
	Cell UA3	180	35	120	16
	Cell UA4	360	33	110	extrac.
	Cell UA5	260	26	120	extrac.
Mg^{2+}	Cell UA1	89	5	45	extrac.
	Cell UA2	17	2	36	0.2
	Cell UA3	68	3	34	extrac.
	Cell UA4	92	3	29	extrac.
	Cell UA5	106	0.1	25	extrac.
Cl^-	Cell UA1	706	244	135	149
	Cell UA2	1040	235	69	103
	Cell UA3	684	194	101	120
	Cell UA4	468	165	131	120
	Cell UA5	751	217	132	135
SO_4^{2-}	Cell UA1	5	23	12	22
	Cell UA2	2	7	4	7
	Cell UA3	4	16	1	15
	Cell UA4	3	15	2	15
	Cell UA5	5	7	6	6

72

Table 3.8 Summary of geochemical indexes after diffusion and desorption (1)

Geochemical Index	Cell I.D.	Initial pore fluid	Initial liquid manure	Diffusion-day 10	Diffusion-day 60	Desorption-day 60
TDS (mg/L)	UA Cell 1	201	10900	6390	4280	803
	UA Cell 2	91	10900	7580	8740	667
	UA Cell 3	121	10900	6330	4720	771
	UA Cell 4	142	10900	-	2990	661
	UA Cell 5	84	10900	5810	3910	728
Hardness as CaCO₃ (mg/L)	UA Cell 1	65	523	536	991	460
	UA Cell 2	1	523	407	270	348
	UA Cell 3	45	523	507	729	440
	UA Cell 4	45	523	-	1280	394
	UA Cell 5	1	523	740	1090	403
Alkalinity as CaCO₃ (mg/L)	UA Cell 1	200	11700	5470	3190	616
	UA Cell 2	100	11700	7310	9390	557
	UA Cell 3	100	11700	5390	4180	656
	UA Cell 4	100	11700	-	2230	475
	UA Cell 5	100	11700	4760	2670	522

73

Table 3.9 Summary of geochemical indexes after diffusion and desorption (2)

Geochemical Index	Cell I.D.	Initial pore fluid	Initial liquid manure	Diffusion-day 10	Diffusion-day 60	Desorption-day 60
E.C. (mS/cm)	UA Cell 1	0.224	23	16	9	8
	UA Cell 2	0.0788	23	19	21	8
	UA Cell 3	0.154	23	16	11	8
	UA Cell 4	0.1541	23	-	6	7
	UA Cell 5	0.0692	23	13	7	8
pH	UA Cell 1	7.03	7.9	7.3	7	8
	UA Cell 2	6.86	7.9	7.7	8	8
	UA Cell 3	7.04	7.9	7.2	7	8
	UA Cell 4	7.06	7.9	-	6	7
	UA Cell 5	7.07	7.9	7.6	7	8
TOC (mg/L)	UA Cell 1	-	6510	-	2380	20
	UA Cell 2	-	6510	-	3060	28
	UA Cell 3	-	6510	-	2090	23
	UA Cell 4	-	6510	-	1050	26
	UA Cell 5	-	6510	-	939	32
DOC (mg/L)	UA Cell 1	-	4700	-	944	18
	UA Cell 2	-	4700	-	1720	19
	UA Cell 3	-	4700	-	1270	22
	UA Cell 4	-	4700	-	314	23
	UA Cell 5	-	4700	-	407	27
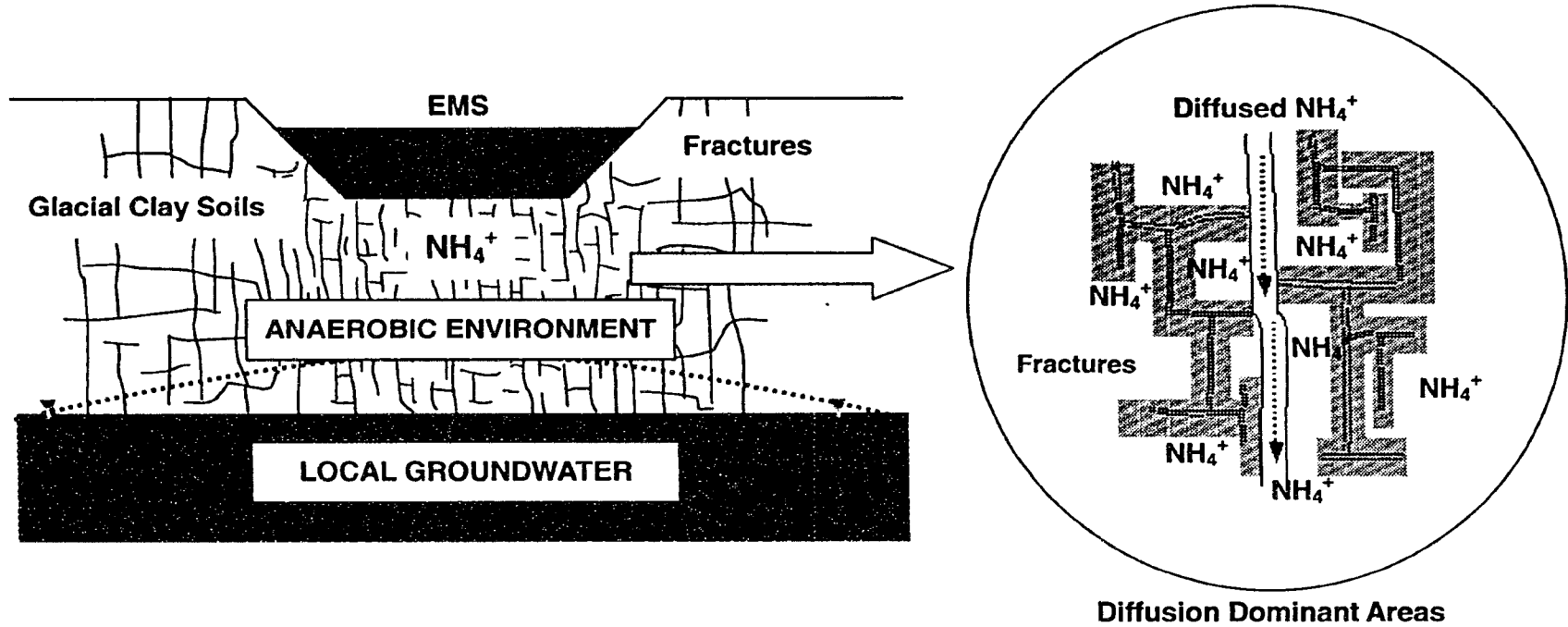
Figure 3.1 Conceptual model for ammonium diffusion along fractured glacial clays and/or clay tills in the Canadian Prairies
* NOTE: EMS denotes Earthen Manure Storage and LHM refers to Liquid Hog Manure
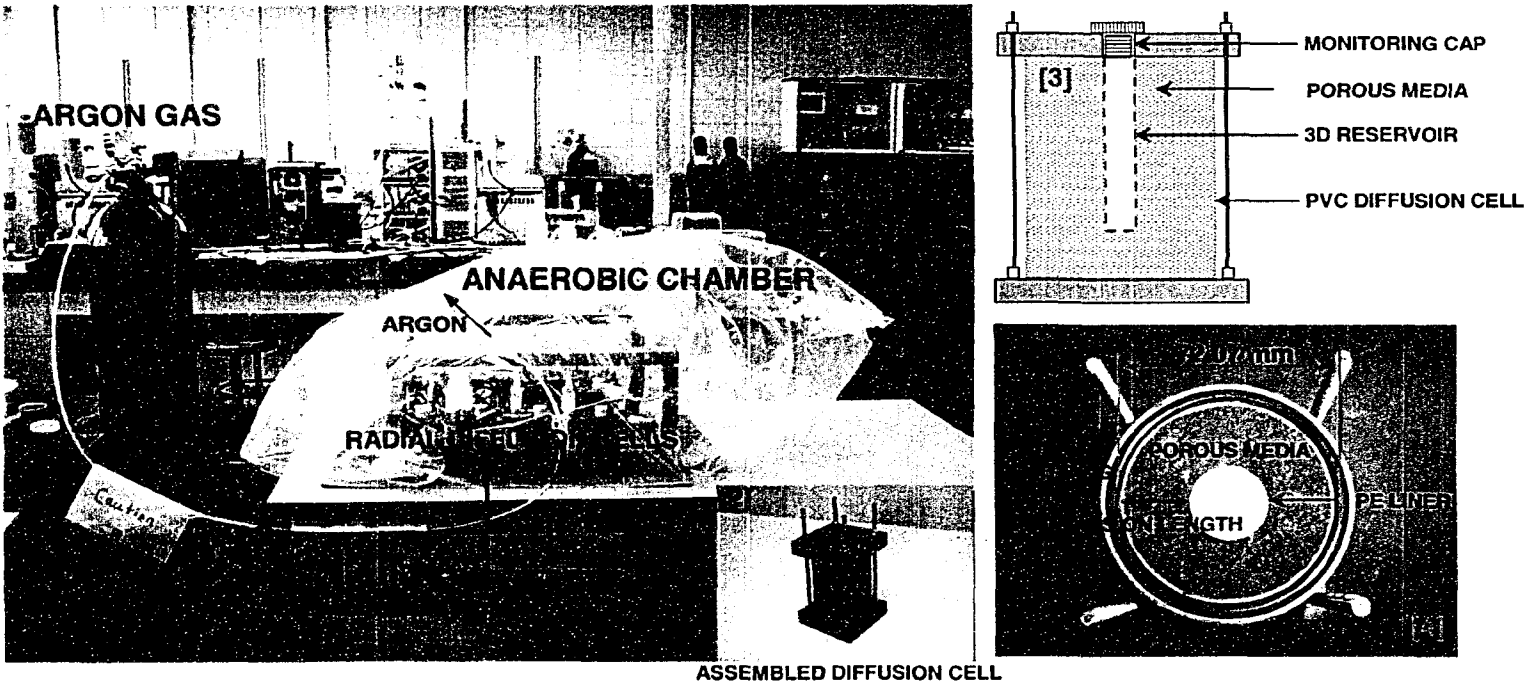
Figure 3.2 Anaerobic radial diffusion cell setting and schematic of a radial diffusion cell

© 2004 Alberta Geological Survey

/\/ NTS Grid	Ice-contact undivided
▓ Lakes	Draped moraine
/\/ Rivers	▓ Stagn. moraine - undulating
▓ Organic	▓ Stagn. moraine - mod. hummocky
Eolian	▓ Stagn. moraine - str. hummocky
Lacustrine - fine	▓ Stagn. moraine - mix. hummocky
Lacustrine - coarse	▓ Ridged end moraine
Fluvial - fine	▓ Ice-thrust moraine

Fluvial - coarse	▓ Ice-thrust & stagn. moraine
▓ Stream/Slopewash	Draped moraine with fluvial
▓ Loess & Fluvial	/// Stagn. moraine with fluvial
▓ Ice-contact lacustrine - coarse	▓ Draped moraine on bedrock
▓ Ice-contact lacustrine - fine	▓ Stagnation moraine on bedrock
▓ Ice-contact fluvial - coarse	▓ L. Tertiary/E. Pleistocene fluvial
▓ Ice-contact fluvial - fine	Bedrock

Figure 3.3 Sampling areas: Ponoka, Alberta, Canada (Alberta Geological Survey, 2004)
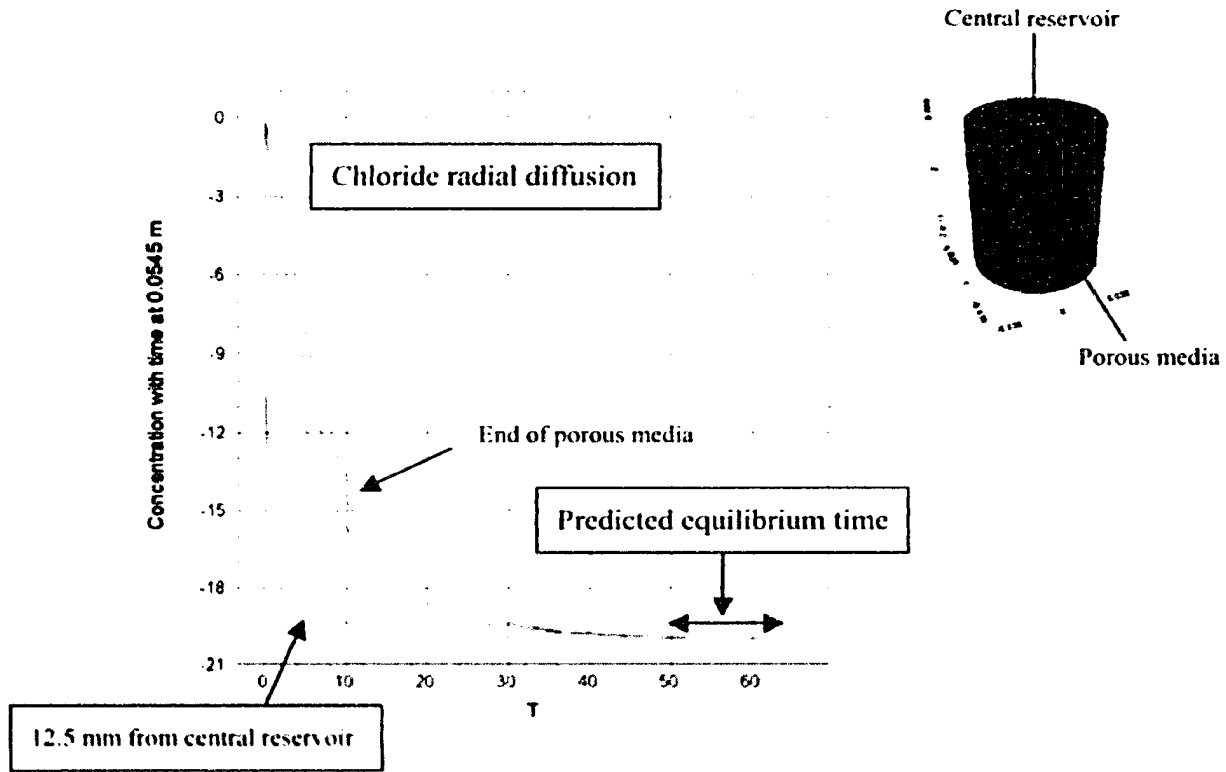
Figure 3.4 Predicted equilibrium time using radial diffusion of chloride through porous media
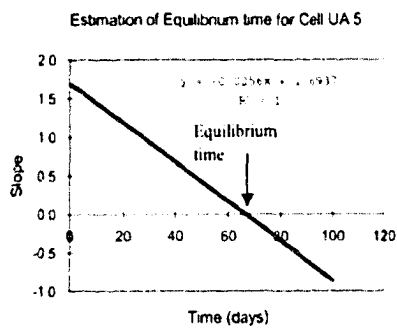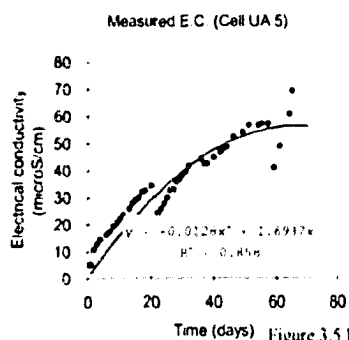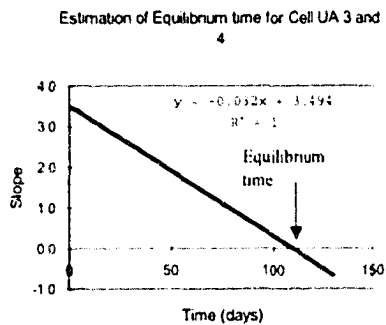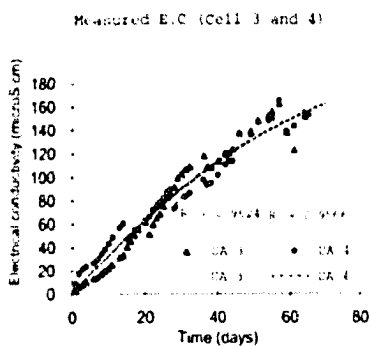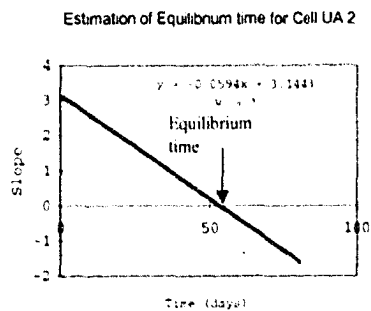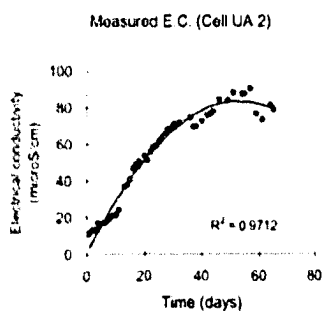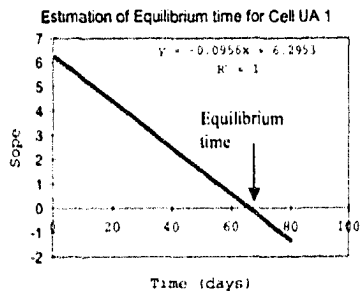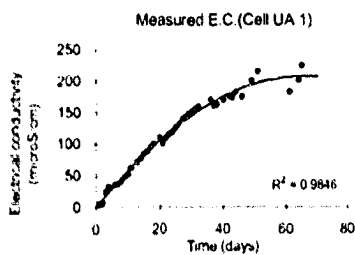
Figure 3.5 Monitored electrical conductivity of the reservoirs during the diffusive equilibrium process

79
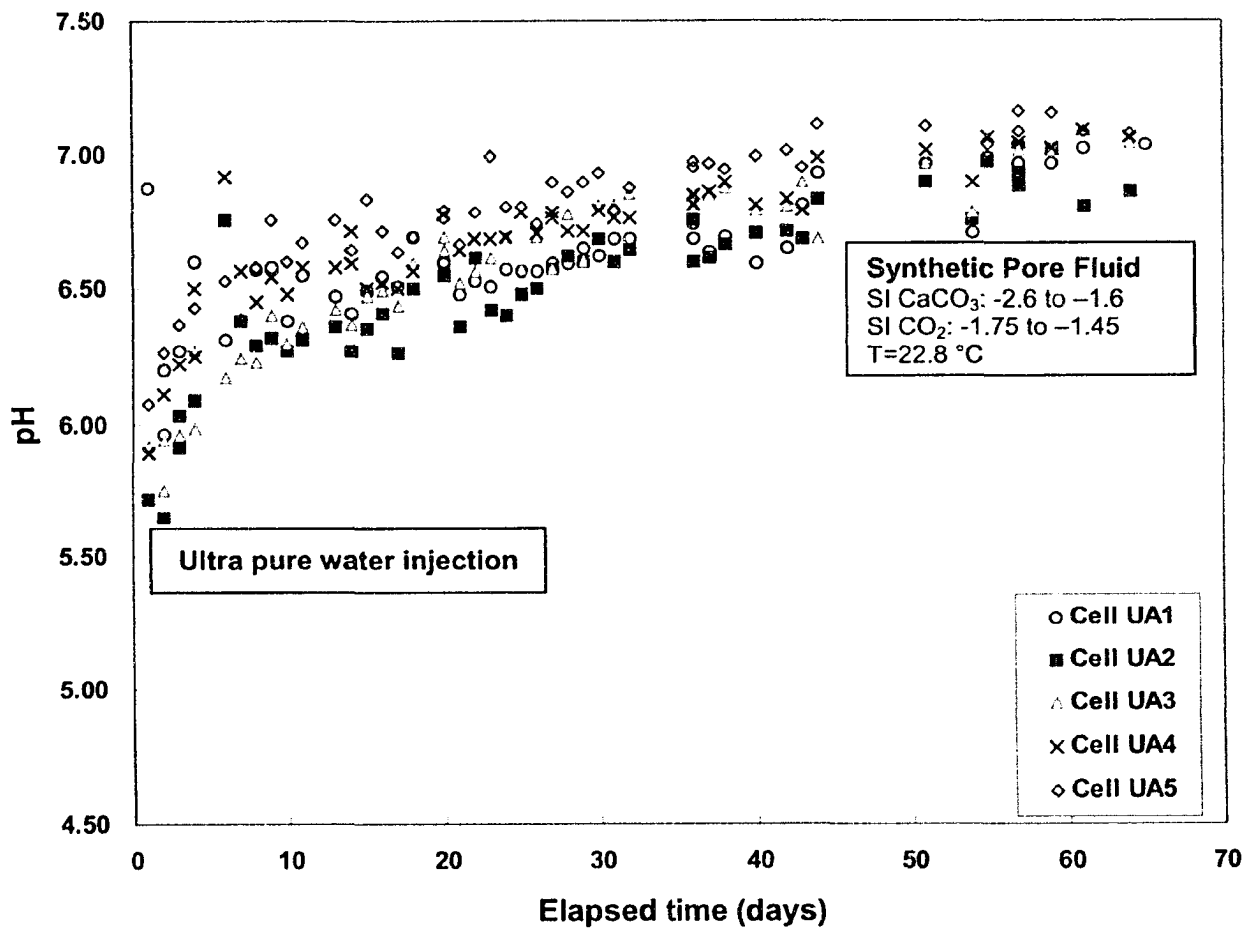
Figure 3.6 Monitored reservoir pH during diffusive the equilibrium process
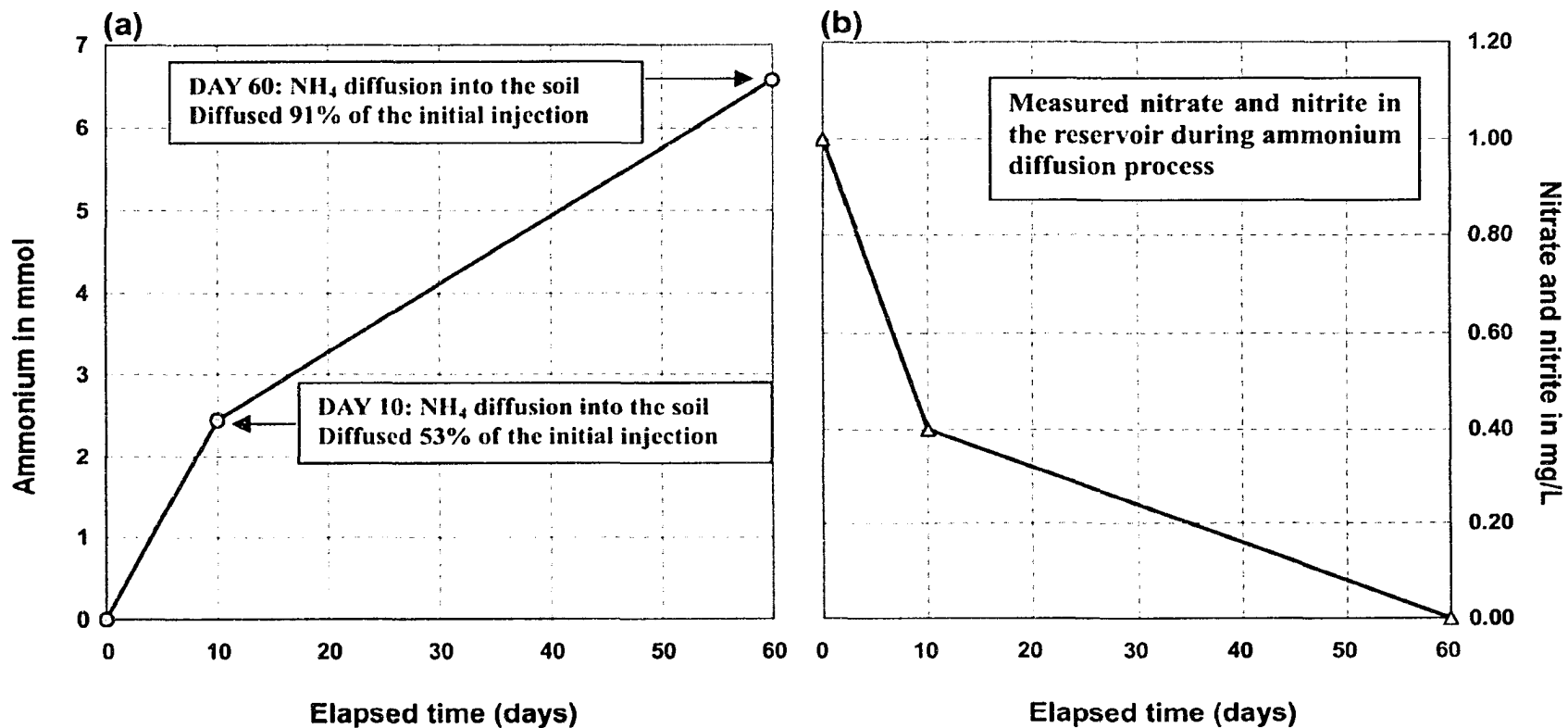
Figure 3.7 (a) Diffused ammonium and (b) maintenance of the anaerobic conditions in the radial diffusion cells
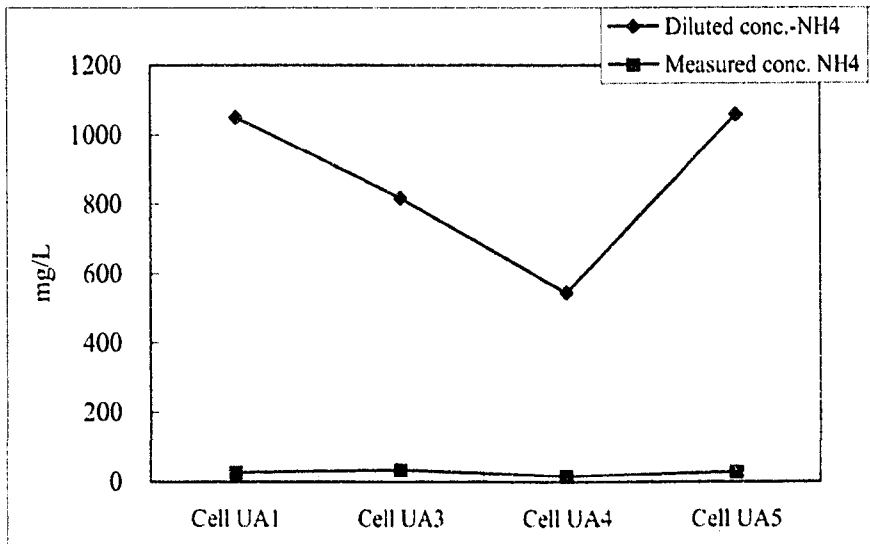
Figure 3.8 (a) Measured vs. diluted ammonium concentration
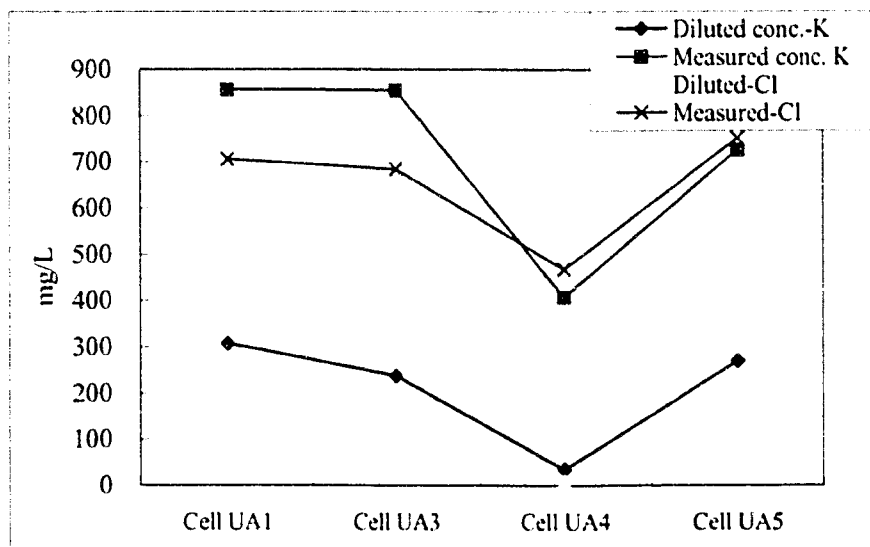
Figure 3.8 (b) Measured vs. diluted potassium and chloride
concentration

82
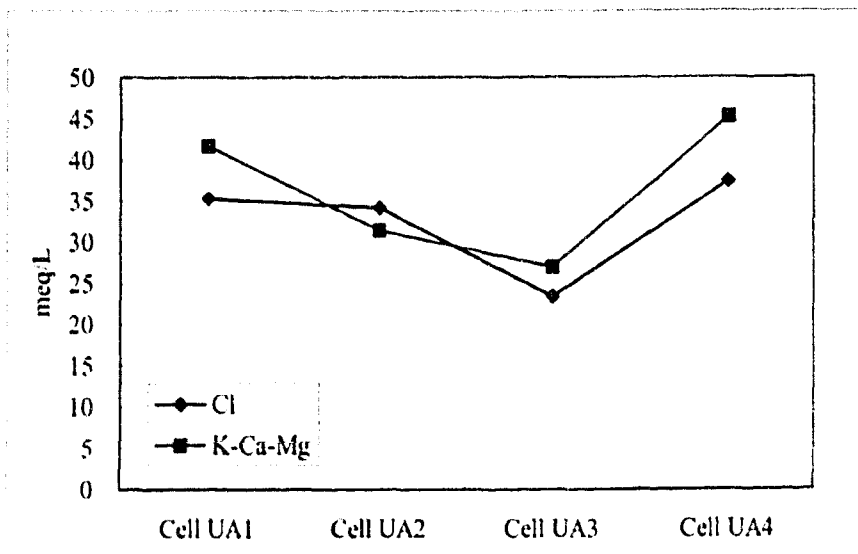
Figure 3.8 (c) Milli-equivalent of Cl⁻ vs. K+, Ca^{2+} and Mg^{2+}
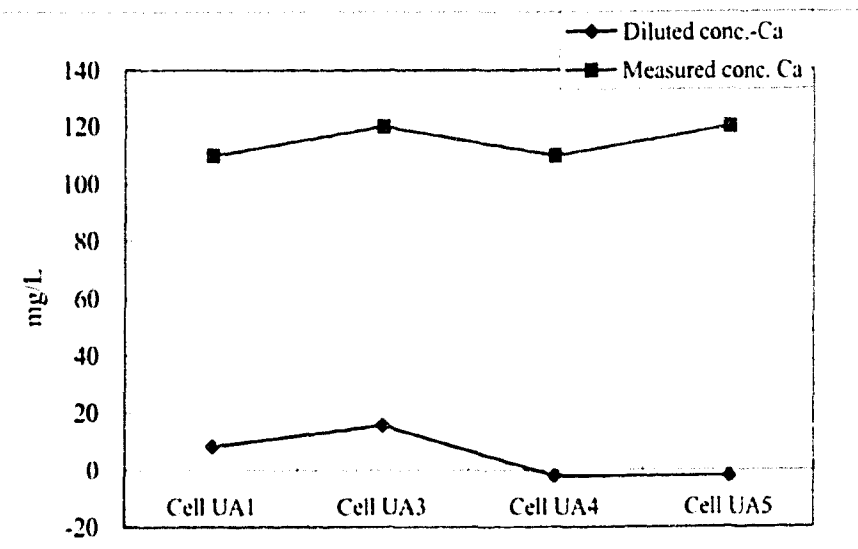
Figure 3.8 (d) Measured vs. diluted calcium concentration

83
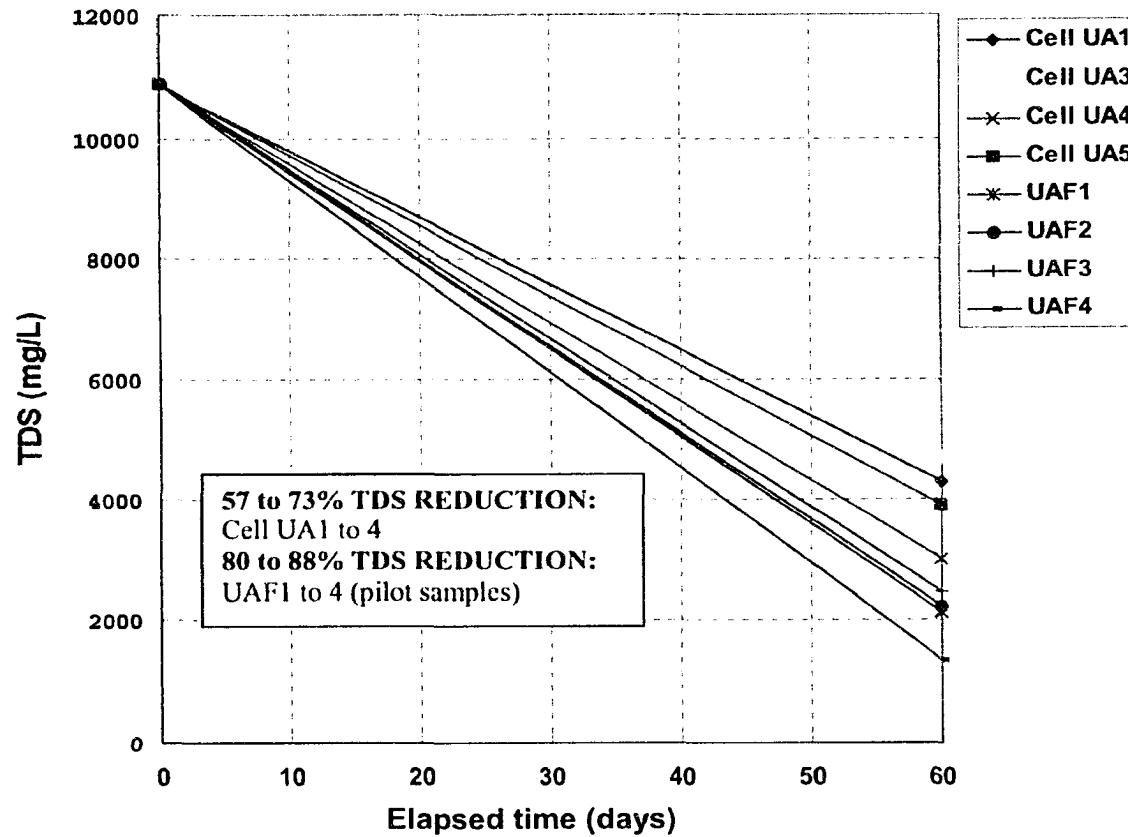
Figure 3.9 Reduction in TDS during the diffusion periods
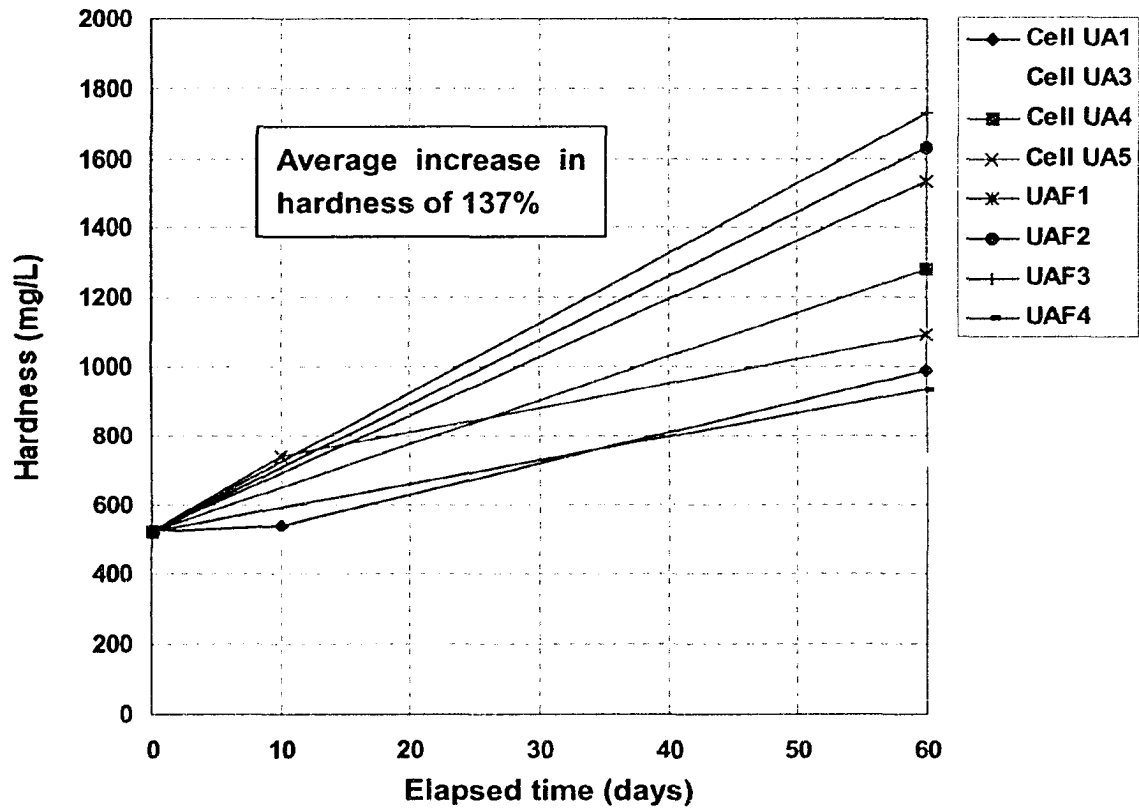
Figure 3.10 Elevated hardness in all the reservoirs during the diffusion process
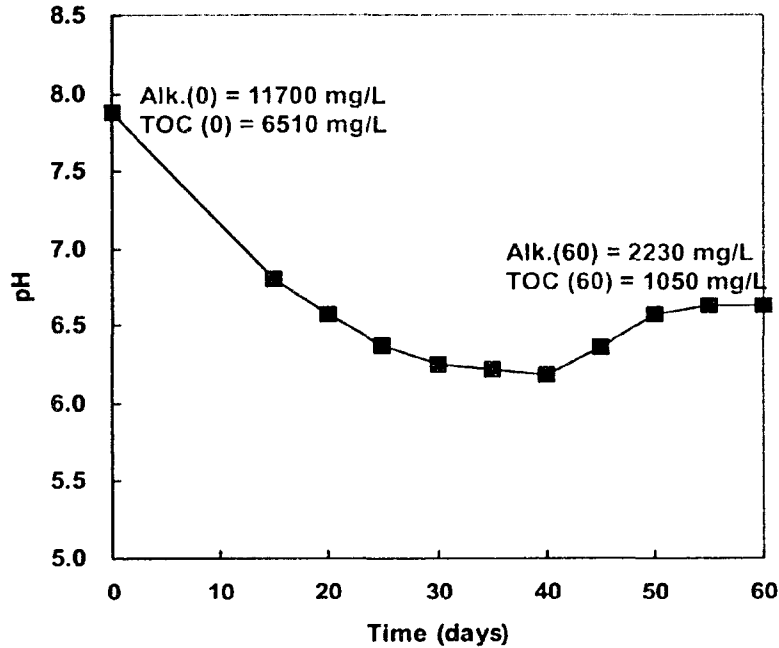
Decrease in pH in the reservoir:

React. [1] H^+ diffusion between pore fluid (pH 7.0) and manure (pH 7.9).

React. [2] $NH_4^+ + HX \Rightarrow NH_4X + H^+ ; K = \dfrac{[NH_4X][H^+]}{[NH_4^+][HX]}$

React. [3] $[X]M^+ + NH_4^+ + HCO_3^- \Rightarrow [X][NH_4^+ + MHCO_3$

React. [3] $[X]M^{+2} + NH_4^+ + 2HCO_3^- \Rightarrow [X]NH_4^+ + M(HCO_3)_2$

React. [4] $Ca^{+2} + HCO_3^- \Rightarrow CaCO_3 + H^+$

Increase in pH in the reservoir:

React. [5] $Ca^{+2} + 2HCO_3^- \Rightarrow CaCO_3 + CO_2(g) \uparrow + H_2O$

React. [6] $2CH_3O + SO_4^{-2} \Rightarrow 2HCO_3^- + H_2S$
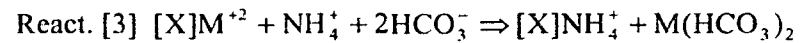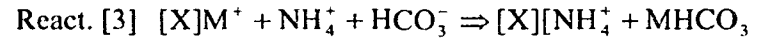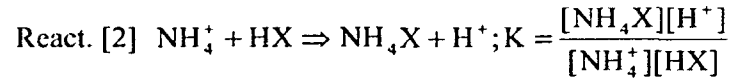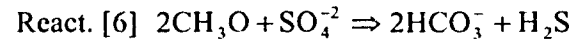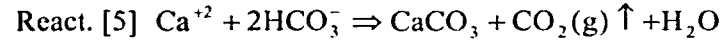
Cf. Eh-pH diagram for S-O_2-H_2O system (Langmuir, 1997).

NOTE
X^-: exchange site with monovalent
M: major cations (Ca, Mg, K, Na)
Alk. (0) and (60): measured alkalinity on day 0 and day 60
TOC (0) and (60): measured TOC on day 0 and day 60.

Figure 3.11 Change in pH during the diffusion periods and related geochemical reactions in the diffusion
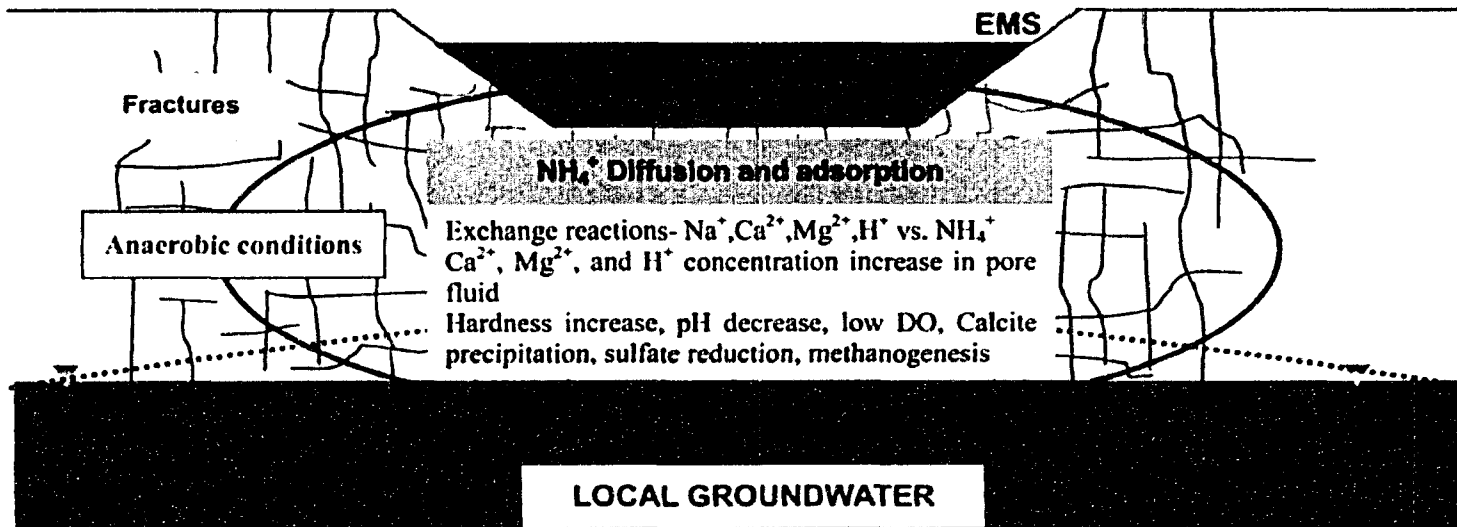
Figure 3.12   Change in pore fluid chemistry resulting from NH_4^+ diffusion

* NOTE: EMS denotes Earthen Manure Storage and LHM refers to Liquid Hog Manure
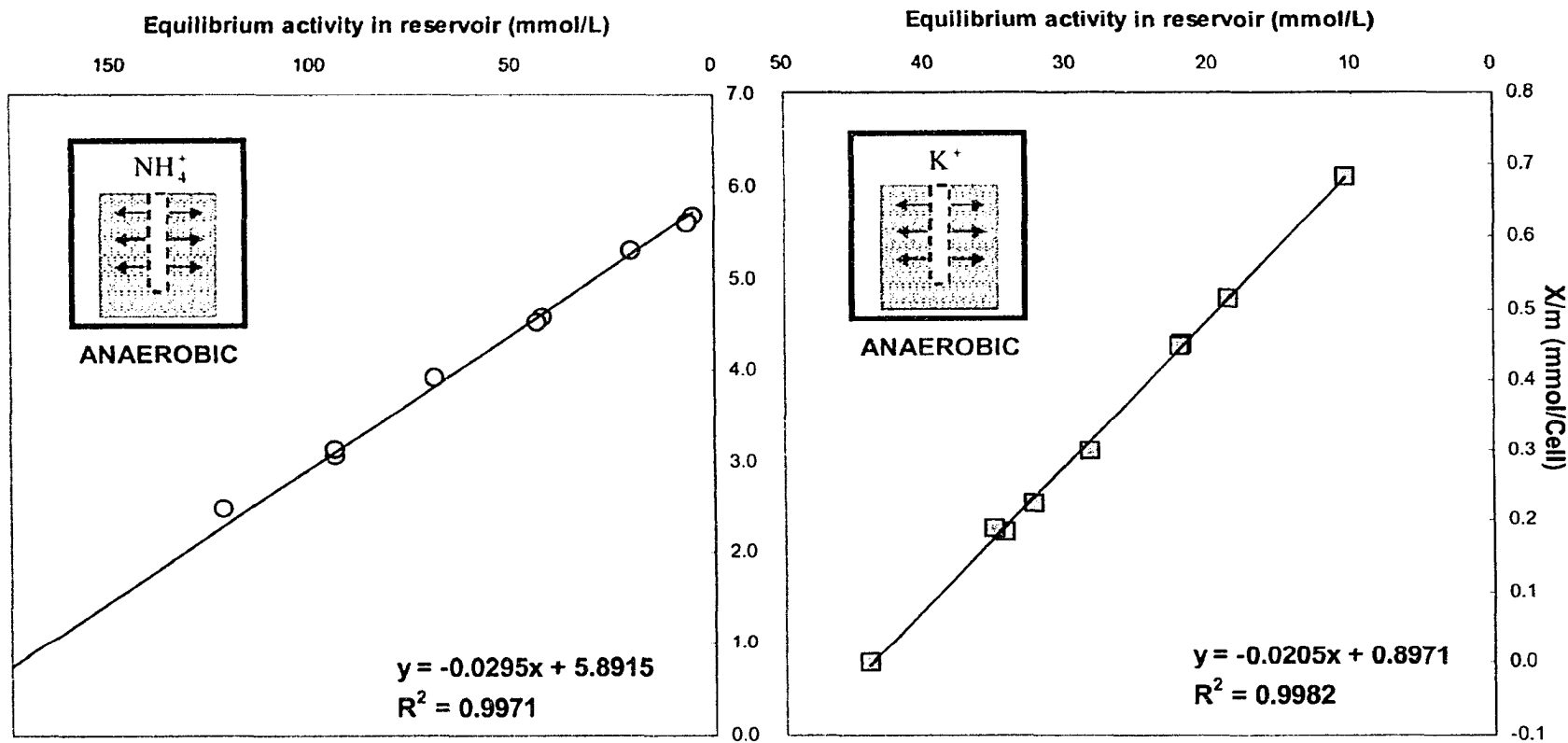
Figure 3.13 Linear ammonium and potassium adsorption isotherms under anaerobic conditions using the RDC method
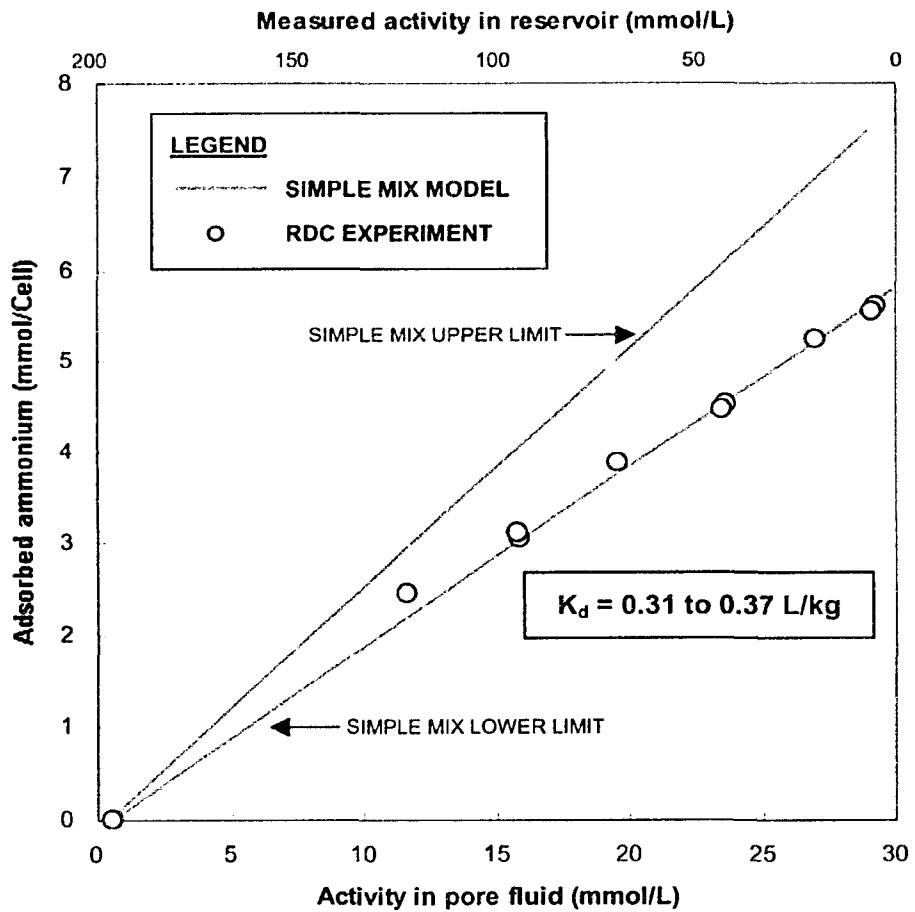
Figure 3.14 Ammonium adsorption determined by the RDC experiment and SIMPLE MIX MODEL
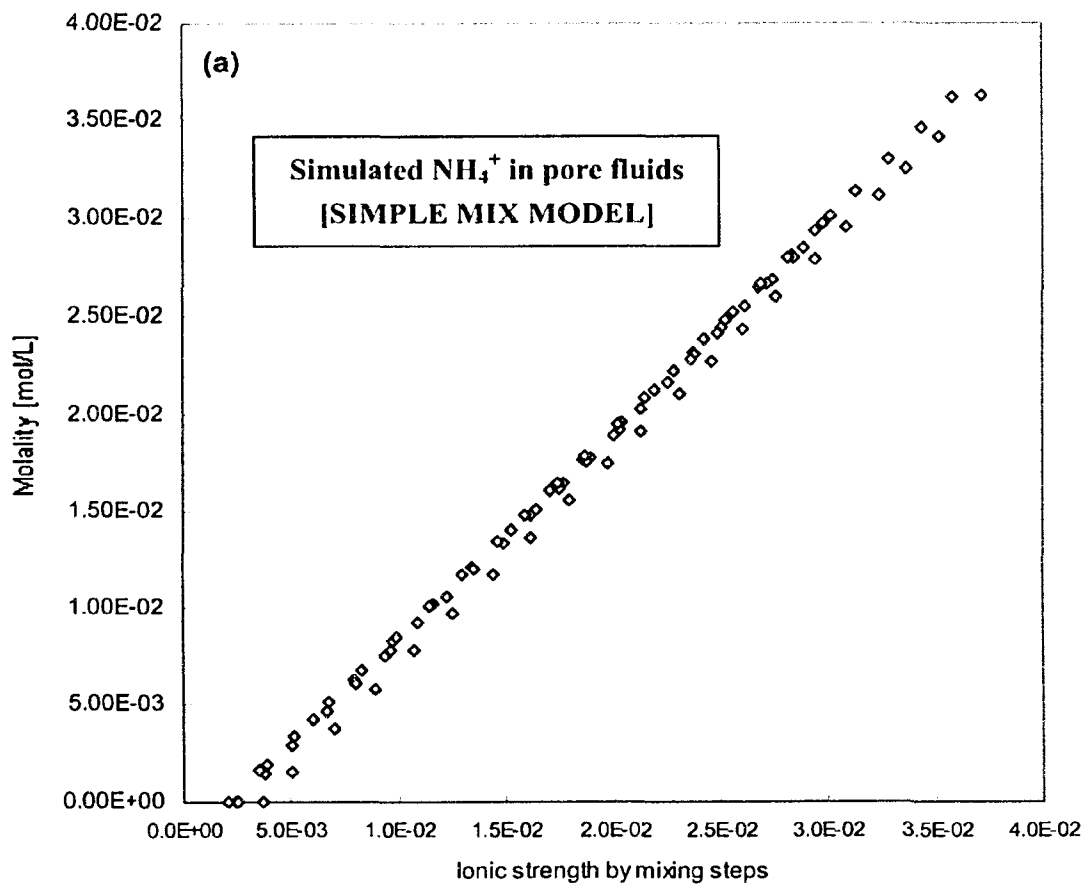
Figure 3.15 (a) NH_4^+ in pore fluids simulated by SIMPLE MIX MODEL
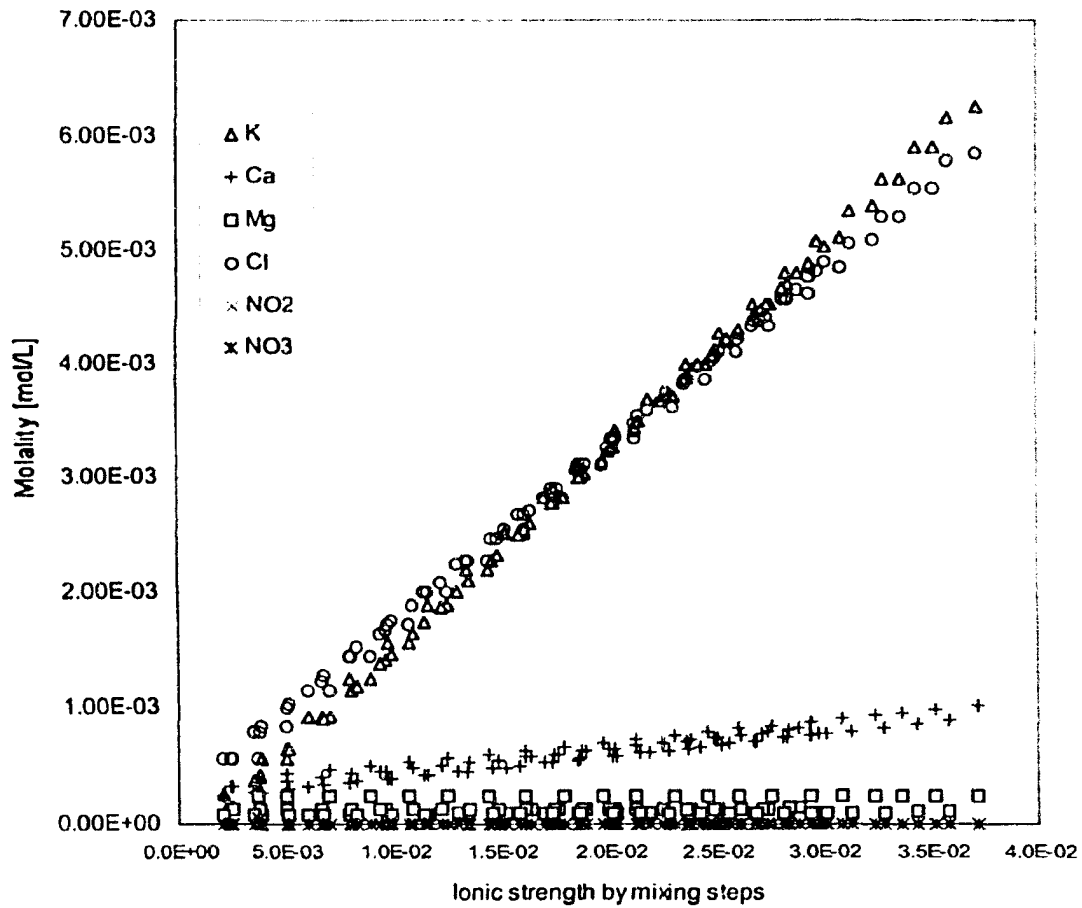
Figure 3.15 (b) change in pore fluid chemistry simulated by SIMPLE MIX MODEL
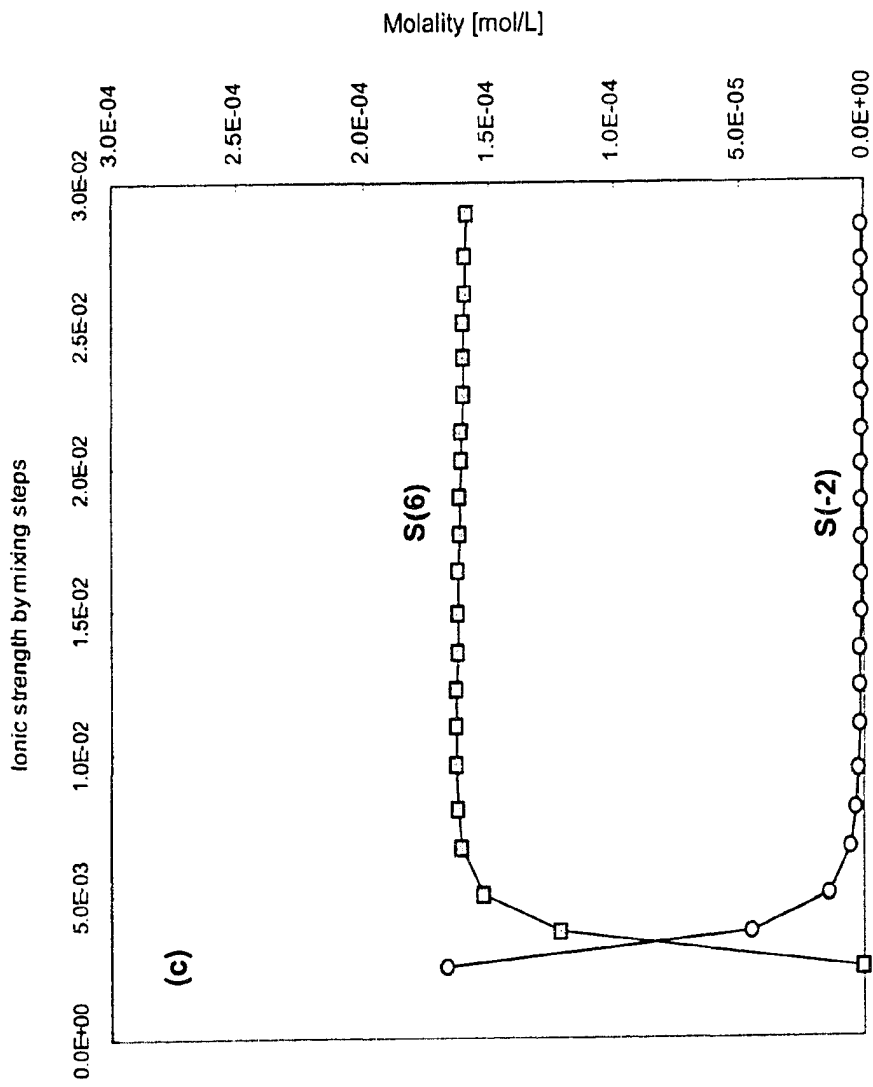
Figure 3.15 (c) S(6) and S(-2) in pore fluid simulated by SIMPLE MIX MODEL

92
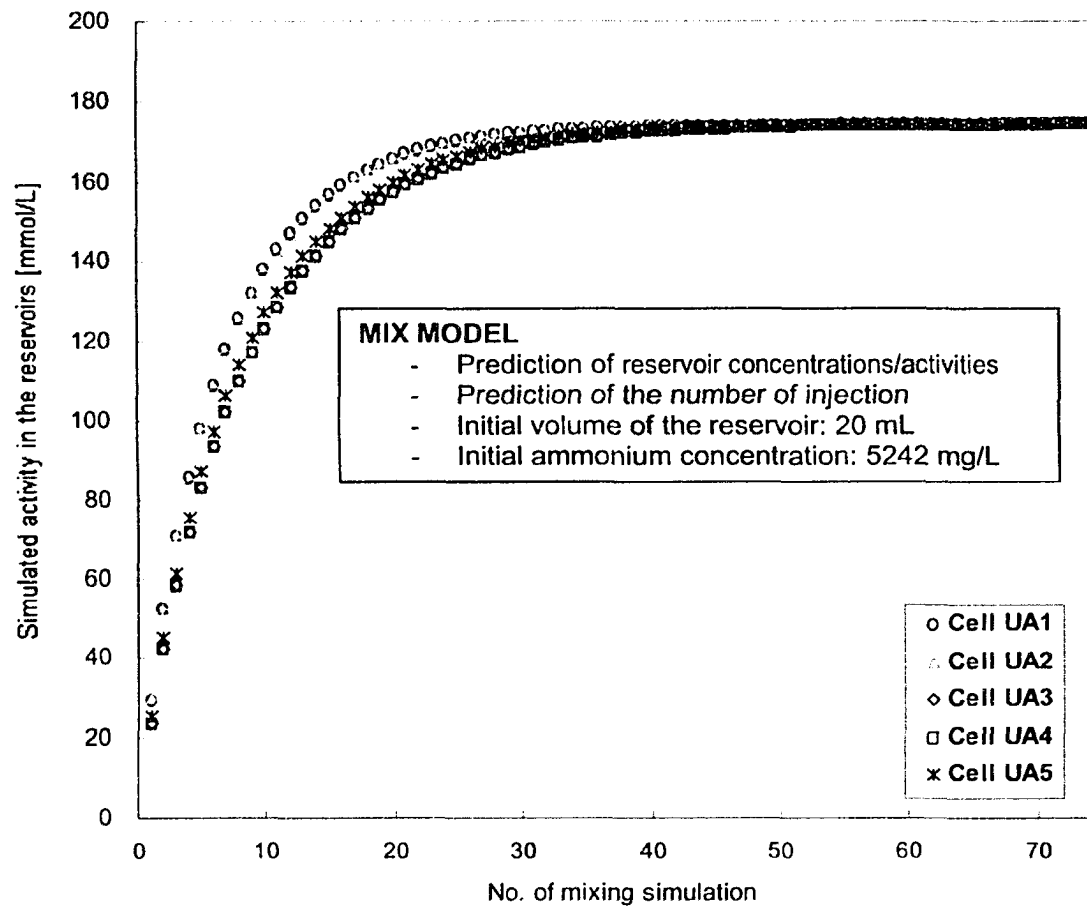
Figure 3.16 Result of the MIX MODEL simulation

CHAPTER 4.0

REACTIVE TRANSPORT MODELING USING THE ANAEROBIC RADIAL DIFFUSION CELL METHOD

ABSTRACT

Reactive transport modeling was conducted to simulate the anaerobic radial diffusion cell experiment for diffusion of ammonium through glacial clay soils. The reactive model developed using PHREEQC code accounts for both radial diffusion of liquid manure through porous media, and change in the pore fluid chemistry response with time. The PHREEQC modeling framework was verified by using ChemFlux, a 3-D finite element model to simulate the radial transport of the unreactive species chloride. After confirmation of radial diffusion, mixing and cation exchange reactions were added to the PHREEQC modeling framework. The reactive transport analysis showed that ammonium was equilibrated at 2411 to 2988 mg/L through the porous media after a 60 day-diffusion period, using a source concentration of ammonium of 5242 mg/L. The exchange reactions were significant in the exchange layer that was approximately 17.5 mm thick near the source. The predicted maximum volumes of liquid hog manure for ammonium full saturation were 0.62 to 1.08 mL/g. The estimated effective diffusion coefficient for chloride ranged from 2.80×10^{-10} to 6.67×10^{-10} m^2/sec. The three-dimensional radial diffusion modeling provided an ammonium effective diffusion coefficient of 2.29×10^{-10} m^2/sec for glacial clay soils collected in Ponoka, Alberta.

94

4.1 INTRODUCTION

4.1.1 Background

Management of earthen manure storage (EMS) has become a public concern due to potential environmental impacts on regional groundwater quality. In particular, the old unlined EMS in Alberta, Canada, have the potential to leach nitrate which is harmful to humans, livestock, surface and groundwater. Nitrate contamination is known to have caused blue baby syndrome in infants, oxygen transport problems for elderly people, the eutrophication of lakes and rivers, and nitrate poisoning in cattle (Comly, 1945; Pauwels et al., 2001; Stoltenow and Lardy, 1998). Excess ammonium beneath EMS can be transported to shallow groundwater by runoff, seepage of liquid manure, flow along fractures, diffusion, seasonal fluctuation of groundwater, or heavy rainfall (Fonstad and Maule, 1996; Ham and DeSutter, 1999). Excess nitrogen-ammonium converts to nitrate because of oxidation in aerobic zones (Follett and Delgado, 2002; Gooddy et al., 2002; Hendry et al., 1984). Nitrate with high mobility in pore fluid can disperse to nearby hydrogeological regimes and eventually connect to many receptors (Astatkie et al., 2001). For these reasons, drinking water standards established by the CCME (Canadian Council Ministers of the Environment) and the U.S. EPA (U.S. Environmental Protection Agency) prescribe maximum concentration levels (MCL) for N-nitrate and N-nitrite, which are 10 mg/L. In addition, Agricultural Operation Practices Act (AOPA) guidelines for EMS construction strictly regulate the preliminary investigation of perspective EMS sites by professional engineers and the installation of engineered liner systems (Alberta Agriculture, Food and Rural Development, 2002). Because of these concerns and

95

guidelines, the net ammonium adsorption capacity for soils used for EMS construction is a key issue for engineers who evaluate excess ammonium beneath EMS facilities.

In this study, a radial diffusion cell method (RDC) was modified to adequately describe the geochemical environment beneath EMS facilities. The experimental results presented in chapter 3 were generated to meet all essential requirements for EMS characterization, including (1) anaerobic conditions; (2) diffusion controlled adsorption; (3) cation exchange; and (4) competition of ions. The anaerobic RDC method provided the advanced distribution coefficients, K_d, which ranged from 0.31 to 0.37 L/kg. Additionally, the geochemical models appropriately simulated ammonium adsorption at low dissolved ammonium concentration (30 mM), and predicted the required maximum liquid manure volume for ammonium saturation (1.0 to 1.4 mL/g). These models, which also enabled pore fluid chemistry simulation, provide unique engineering tools for EMS construction, risk assessment, and decommission. However, a drawback of the models is that they cannot provide the required time to ensure saturation because they are based on the steady state diffusion of the mixing simulation. Therefore, this study aims to develop a reactive transport model that can predict diffusion time because ammonium reacts with pore fluid during radial diffusion through the porous media.

4.1.2 Concept of reactive transport model for the anaerobic RDC method

Recently developed geochemical models for an RDC method dealt separately with (1) the transient diffusion of solutes through porous media, and (2) coupled geochemical reactions. Novakowski and Van der Kamp (1996) derived a semi-analytical radial

diffusion solution based on the Bessel functions and simulated transient radial diffusion. The model provided hydrogeological parameters, such as effective porosities and effective diffusion coefficients. Van Stempvoort and Van der Kamp (2003) simulated the change in hydrogeochemistry during radial diffusion of the solutes. The simulation greatly supported the measured major cation and anion concentrations, and it described aqueous speciation, calcite/atmospheric CO_2 equilibrium, and sulfur/carbon redox reactions.

The anaerobic RDC method used for a soil-manure system consists of liquid manure in the central reservoir of the RDC. The contaminant mixture diffuses radially through the surrounding (Figure 4.1). The liquid manure mixture has a wide range of cation and anions, including ammonium, potassium, sodium, calcium, magnesium, bicarbonate, phosphate, and others. It is clear that ammonium diffusion is influenced by the ions that coexist in the liquid manure mixture (Lumbanraja and Evangelou, 1994). Furthermore, the liquid manure that comes into contact with the porous medium reacts with its pore fluid. In particular, cation exchange between the ammonium in the liquid manure and the clay surface of soils was significant in the anaerobic RDC experiment, as explained in chapter 3. The exchange reactions in pore fluid lead to ammonium adsorption onto the clay minerals of the reactive porous media in the cells. A diffusion process known as diffusion-controlled adsorption governs the transport of solutes, including sorption reactions in an RDC (Kithome et al., 1998). All the conditions and procedures mentioned above should be performed within an oxygen-limited environment to best approximate the conditions below the EMS facility. Hence, the coupled reactive transport model used to simulate ammonium diffusion should include both radial

97

diffusion and cation exchange. The modeling strategy in this study is divided into five steps: (1) development of a radial diffusion model using PHREEQC; (2) verification of the model, using the contaminant transport software ChemFlux; (3) coupling of the model with the cation exchange reaction; (4) simulation of a single liquid manure injection; and (5) determination of the maximum volume of liquid manure that will produce ammonium saturation.

4.2. MATERIALS

The RDC method was developed for use in the investigation of pore fluid chemistry in low-permeable aquitards, fractured rocks, and sediments (Van der Kamp et al., 1996). The diffusion cells were separated from the laboratory environment by the introduction of inert argon gases into an anaerobic chamber. Minimally disturbed in-situ clay-rich soils were used in the diffusion cells. The central reservoir was then subjected to the ammonium rich liquid hog manure mixture. The concentration gradient between the reservoir solution and the pore fluid in the porous media caused diffusive transport and exchange reactions.

4.2.1 Porous media

Soil samples were collected from glacial lacustrine deposits located in Ponoka, in east central Alberta, Canada. Shelby tubes were used to extract the soil. The samples were stored in a moisture room at 4°C until their preparation for the diffusion cells. The five diffusion cells, Cell UA1 to 5 were set up in this way: Cell UA1 and 2 at 1.5 to 2.3 m depth and Cell UA3 to 5 at 3 to 5.3 m depth. According to USCS classification, the soil

98

samples were sandy lean clay (CL) in Cell UA1 and 2, and sandy fat clay (CH) in Cell UA3 to 5. The gravimetric water content of the samples ranged from 18.3 to 28.9%. The estimated total porosity, assuming 100% saturation, was 0.32 to 0.42. The background concentration of soluble salts was determined by saturated paste extraction (SPE) tests. N-Ammonium concentrations ranged from 4 to 10 mg/L throughout the soil pastes. The N-nitrate and N-nitrite concentrations ranged from 3.4 to 8.6 mg/L, and from 0.96 to 2.49 mg/L, respectively. The clay fraction of the in-situ soil comprised 68% smectite, 17% illite, and 15% kaolinite and chlorite, according to XRD (X-ray diffraction) and SEM (Scanning Electron Microscope) analysis. The smectite-rich soil samples resulted in high cation exchange capacities of 21.2 to 43.4 meq/100g (ammonium acetate method, NH_4OAc).

4.2.2 Contaminant

In the anaerobic RDC experiment, the central reservoir contained a volume of 20 ± 0.08 mL of raw liquid hog manure. The manure that came in contact with the glacial clays in the diffusion cells was collected at the Swine Research Center at the University of Alberta in Edmonton. Ion chromatography (IC) analysis determined that the manure consisted of 45% ammonium, 36% bicarbonate, 7% potassium, 6% chloride, and 1-4% sodium, calcium and magnesium. The dissolved oxygen (DO) level in the manure was 0.8 mg/L which is below the detection limit of the DO probe. The measured alkalinity (as $CaCO_3$) was 11700 mg/L and pH of the samples was 7.9.

4.3 METHODS

PHREEQC interactive version 2.6.1, developed by USGS (U.S. Geological Survey), was used to simulate a radial diffusive transport with exchange reactions. A radial diffusion domain is a converted strip-shape diffusion cell with both chemical and physical properties of porous media (Figure 4.3). This is a key technique employed to approximate a symmetric radial diffusion in the reactive model.

In this study, the modeling framework is defined as the unreactive radial diffusion of a conservative chloride through the radial diffusion domain. ChemFlux, which is a finite element contaminant transport model, was used to verify the modeling results (Figure 4.3 and Figure 4.8). After verification of the model, the exchange reactions were added to the radial diffusion framework. In addition, ChemFlux was used to predict effective diffusion coefficients for chloride and to simulate the three-dimensional radial diffusion of ammonium through the porous media.

4.3.1 Numerical models

4.3.1.1 PHREEQC

PHREEQC interactive is a geochemical modeling tool used to simulate geochemical reactions such as ion exchange equilibria, advection, dispersion, and diffusion transport processes in natural or contaminated water. PHREEQC is based on equilibrium chemistry of aqueous solutions as they interact with minerals, gases, solid solutions, exchangers, and sorption surfaces. One limitation of the program is that the aqueous

100

model may not be appropriate at high ionic strengths of aqueous solutions because PHREEQC adopted ion-association and Davies equation in order to model the non-ideality of aqueous solutions (Parkurst and Appelo, 1999).

PHREEQC provides a one-dimensional diffusive transport process with an advection-reaction-dispersion equation as follows:

$$\frac{\partial C}{\partial t} = -v\frac{\partial C}{\partial x} + D_L\frac{\partial^2 C}{\partial x^2} - \frac{\partial q}{\partial t}$$
Eq.4-1

In the Eq.4-1, C is the concentration of water (mol/kgw), t is time (in days), v is pore water flow velocity (m/days), x is distance (m), and q is the concentration of the solid phase in the pores expressed as mol/kgw. D_L is the longitudinal hydrodynamic dispersion coefficient (m^2/days) that is defined as $D_L = D^* + \alpha_L v$, where D^* is the effective diffusion coefficient (m^2/days), and α_L is the dispersivity (m) (Freeze and Cherry, 1979). In this study, it is assumed that the advection term, $-v\frac{\partial C}{\partial x}$, is neglected because the pore fluid velocity (or average linear velocity) is equal to zero for diffusion-only transport processes. Thus, the longitudinal hydrodynamic dispersion coefficient depends only on the effective diffusion coefficient $(D_L = D_e)$.

4.3.1.2 ChemFlux

ChemFlux is a comprehensive contaminant transport-modeling tool based on the finite element method (FEM). It is feasible for the model to simulate complicated two-dimensional or three-dimensional contaminant transport problems. Static pore pressure

101

should be calculated by using SVFlux, which is a finite element seepage model, prior to the injection of contaminants into porous media in ChemFlux. The static pore pressures can then be transferred into ChemFlux for the simulation of contaminant transport through the porous media (Fredlund and Stianson, 2003).

The governing equation, which is an advection-dispersion equation for a three-dimensional diffusion problem, is as follows:

$$\frac{\partial C}{\partial t} = D \cdot \frac{\partial^2 C}{\partial x^2} + D \cdot \frac{\partial^2 C}{\partial y^2} + D \cdot \frac{\partial^2 C}{\partial z^2} - R \qquad \text{Eq.4-2}$$

The nomenclatures are the same as for Eq. 4-1. R denotes retardation factor, $R = 1 + \frac{\rho_d}{\theta} K_d$, where ρ_d is bulk density (ML^{-3}), and θ is volumetric water content. In the equation, advection and dispersion were excluded to simulate a diffusive transport.

4.3.2 Reactive transport modeling

4.3.2.1 Static pore pressure and diffusive equilibrium

Prior to diffusive equilibrium modeling, the geometry of the porous media, soil properties, and boundary conditions were defined using SVFlux. Figure 4.2 illustrates the developed three-dimensional mesh based on the actual RDC geometry. Even though hydraulic conductivity does not account for diffusion-only simulations, the saturated hydraulic conductivity of the in-situ soils was set to 2.4×10^{-1} m/day for the input data. Specific gravity, G_s, determined by the ASTM D 854 standard method, was set to 2.624

102

for the input. As a result, the static pore pressure in the porous media was simulated on the basis of steady state diffusion (Figure 4.2).

Using ChemFlux to simulate the three-dimensional diffusive equilibrium, the measured chloride concentration of the pore fluid was regarded as a background concentration of the porous media. This generated a concentration gradient between the porous media with chloride ($C_c \neq 0$) and the reservoir with pure water ($C_R = 0$). Consequently, the chloride was radially diffused from the porous media to the reservoir. The inverse diffusion, which is a diffusion from the porous media to the source, provided the effective diffusion coefficient of chloride for the porous media because the modeled diffusive equilibrium time fit the experimental equilibrium time.

4.3.2.2. Ammonium diffusion only

Using ChemFlux, three-dimensional radial diffusion of ammonium was simulated for the anaerobic RDC experiment. In this 3D simulation, ammonium was capable of being transported only by diffusion process. It was assumed that no reactions occurred during ammonium diffusion through the porous media. After the static pore pressures were calculated, the reservoirs were subjected to the ammonium ion. The ammonium concentration defined in the model was based on the initial liquid hog manure chemistry characterized by the IC analysis.

The boundary conditions of the reservoirs allowed 3D radial diffusion. A radial segment and no-flux boundary conditions were assigned along the top surface of the reservoir. A

103

lateral radial diffusion boundary, with a direction perpendicular to that of the surface plane of the cylindrical reservoir, was defined along the planes. The radial segment and surface boundary conditions were allocated at the end of the reservoir.

The concentration gradient between the porous media (C=0) and the reservoir ($C_R \neq 0$) caused ammonium mass transfer from the reservoir to the porous media. The distribution ratios (C/C_R), estimated in the 60-day diffusion-only simulation, were compared to the breakthrough ratio (C/C_0) generated by the experimental analysis. This process provides an effective diffusion coefficient for ammonium with respect to the porous media.

4.3.2.3 Modeling framework

The modeling framework allows for radial diffusive transport in PHREEQC. The radial diffusion domain, containing effective pore fluid volume and pore fluid chemistry information, plays a key role in the framework before adding mixing and cation exchange reactions. To model the radial diffusion domain, it is assumed that (1) the porous media is homogenous, (2) the porous media is completely water saturated and diffusively equilibrated (S=1), (3) solutes diffuse symmetrically into the porous media, and (4) the direction of solute diffusion is perpendicular to the surface of the central reservoir.

Figure 4.3 presents a radial slice of the diffusion domain with angle, θ, radius, R, and unit height (1 cm). The joints, J_n, were allocated on the divided elements and they contain the representative concentrations corresponding to their elements. The volume of

104

each element is based on the estimated effective pore volume, n_pV_n. Total pore volume,

$\sum_1^n n_pV_n$, is equivalent to the pore volume of the slice, where n_p denotes total porosity

and is determined by the gravimetrical water content. The pore volume ratio, n_pVR_n =

V_n / V_{n-1}, increases with the number of divided elements in the slice. The trend of the

volume ratio change reflects the radial geometry of porous media (cf. n_pVR_1 is equal to

1). By using n_pVR_n, the slices can be converted to the radial diffusion domain with

effective diffusion lengths (Figure 4.3). In the framework model, a conservative chloride

was injected into the radial diffusion domain. The results were compared with diffusion-

only simulation, using ChemFlux in order to verify the model.

4.3.2.4 Coupled reactive modeling

After verification of the radial diffusion domain, the coupled mixing and cation

exchange reactions were added to create a reactive transport model (Figure 4.4). The

model is divided into two categories: (1) a model to simulate the radial diffusion that

accompanies cation exchange reactions and results from single injections of liquid hog

manure with a volume of 20 mL, and (2) prediction of the manure volume required to

cause ammonium saturation in the porous media (500-day simulation). With category (1),

the results were compared with the anaerobic RDC experimental results produced with a

single injection of liquid hog manure.

The exchange sites for NH_4X, KX, NaX, CaX_2, and MgX_2 were normalized in

equivalent fraction on the basis of a simple ion exchange model (Langmuir, 1997). The

equivalent fractions for the cations, determined by the anaerobic RDC experiment, takes

105

into account the following key requirements: anaerobic conditions, diffusion dominant, adsorption by cation exchange, and cation competition. The X^- refers to the monovalent exchange site (Jenne, 1995). It was assumed that the smectite-rich soil samples with high CEC values (21.2 to 43.3 meq/100g) had sufficient exchange sites to adsorb 80 to 90% of the ammonium injected into the cells. As a result, exchange reactions occurred as liquid hog manure diffused through the radial diffusion domain.

4.4 RESULTS AND DISCUSSION

4.4.1 Simulation of diffusive equilibrium and effective diffusion coefficients

For the diffusive equilibrium simulation, it was assumed that the porous media is completely saturated by water (S=1), that there is no dispersion process—so that the longitudinal hydrodynamic dispersion coefficient is equal to the effective diffusion coefficient ($D_L = D^*$), that porous media cannot adsorb a conservative chloride with a negative charge (R=0), and that chloride inversely diffuses into the reservoir, which means radial diffusion from porous media to reservoir.

The background chloride concentration was set to 20 mg/L, on the basis of the representative pore fluid chemistry. Figure 4.5 shows the change in the reservoir concentrations as determined by the diffusive equilibrium simulation. The negative sign in the reservoir concentration, C_R (mg/L), denotes the inverse diffusion of chloride. The effective diffusion coefficients (D^*) determined by the model varied with the soil samples. In the case of Cell UA1, 2, and 5, the effective coefficients ranged from

106

5.17 $\times 10^{-10}$ to 6.67 $\times 10^{-10}$ m^2/sec. For Cell UA3 and 4, the effective diffusion coefficients ranged from 2.80$\times 10^{-10}$ to 2.85$\times 10^{-10}$ m^2/sec. The lower D* of Cell UA3 and 4 resulted from their comparatively higher clay fraction and longer equilibrium times in the radial diffusion experiment. According to the particle size distribution, determined by a hydrometer test and wet sieve analysis, Cell UA3 and 4 had more clay fraction than Cell UA1 and 2. Cell UA3 and 4 comprised 47% clay, 35% silt, and 18% sand fraction. Cell UA1 and 2 contained 34% clay, 30% silt and 36% sand. The equilibrium times simulated by the model were 53 to 66 days for Cell UA1, 2 and 5, and 106 to 109 days for Cell UA3 and 4.

The results supported Novakowski and Van der Kamp's speculation (1996) that the diffusive equilibrium time is sensitive to the value of an effective diffusion coefficient and is influenced by pore geometry (or tortuosity). Coarse and unconsolidated materials with irregular pore geometry can cause a shorter equilibrium time and higher effective diffusion coefficients, and vice versa (Novakowski and Van der Kamp's speculation, 1996).

The values of the effective diffusion coefficients, 5.17$\times 10^{-10}$ to 6.67$\times 10^{-10}$ m^2/sec, for Cell UA 1, 2, and 5 were higher than those of Shackleford and Daniel (1991). Shackleford and Daniel (1991) obtained 4.4 to 6.0 $\times 10^{-10}$ m^2/sec for the chloride effective diffusion coefficient by simulating leachate spiked with ZnCl$_2$. The total porosity, plastic index (PI), and cation exchange capacity (CEC) of the soil samples were equal to 51 to 60%, 23, and 5 meq/100g, respectively. The chloride concentration was set to 213 to 448 mg/L in the source solution, with pH 3.7 to 6.7 in Shackleford and

107

Daniel's (1991) experiment.

Baron et al. (1990) conducted a diffusion test to investigate an effective diffusion coefficient for chloride. Baron et al. (1990)'s effective diffusion coefficients for chloride ranged from 5.6 to 7.5×10^{-10} m^2/sec. The values of D* were slightly higher than those determined for Cell UA1, 2, and 5. In Baron et al.'s diffusion test (1990), the soil samples were composed of 45% clay and 43% silt. PI, CEC, and soil pH were equal to 27, 10 meq/100g, and 8.1, respectively. The chloride concentration and pH in the source were 1000 mg/L and 7.0, respectively.

A diffusion test on shale and mudstone by Barone et al. (1989; 1992a) yielded relatively low values of D*, ranging from 1.5 to 1.8×10^{-10} m^2/sec. Shackleford and Daniel (1991) also reported the same values of D*, 1.5 to 1.8×10^{-10} m^2/sec, for clay-rich soils with PI of 43. The diffusive equilibrium simulation in this study also provided lower values of D* for clay-rich soil samples. For Cell UA3 and 4, which had more clay fraction than Cell UA1 and 2, the values of D* ranged from 2.80×10^{-10} to 2.85×10^{-10} m^2/sec and were lower than those of Cell UA1 and 2. It is clear that the porous media with a longer equilibrium time in a radial diffusion cell experiment produces lower effective diffusion coefficients.

4.4.2 Three-dimensional radial diffusion of ammonium without reactions

The radial diffusion effect was suppressed beneath the central reservoir level according to the three-dimensional radial diffusion transport analysis. Figure 4.6 represents the

108

proposed three-dimensional radial diffusion contour and simulated distribution ratio

(C/C_R) in the RDC method. The radial diffusion predominately moved in a lateral

direction away from the reservoir source, as shown in Zone☐of Figure 4.6. Novakowski

and Van der Kamp (1996) developed the semi-analytical solutions for the radial

diffusion of solutes through porous media. The developed governing equation in

geological materials is as follows:

$$\frac{\partial C}{\partial t} = \frac{D^{\bullet}\partial^2 C}{R\partial r^2} + \frac{D^{\bullet}\partial C}{Rr\partial r} - \frac{\lambda}{R}C \qquad r_R < r < r_C \qquad Eq.4\text{-}3$$

In Eq.4-3, C denotes resident concentration, r is the radial distance from the center of the

reservoir, $D^{\bullet}$ is the effective diffusion coefficient, R is the retardation factor, λ is the

decay constant, r_R is the radial distance from the origin to the reservoir boundary, and r_C

is the radial distance from the reservoir boundary to the end of the porous media. As

presented in Eq.4-3, the resident concentration is a function of radius and time in a

circular cylindrical domain (Crank, 1975). It was observed that in zone☐, the trend of

the solute diffusion typically followed Novakowski and Van der Kamp's (1996)

analytical solution based on the Bessel functions. The equilibrium concentration for

ammonium increased as the radial diffusion rate increased. The equilibrium time for

non-reactive species in zone☐was estimated by the numerical simulation to be 40 days.

However, as is shown in zone☐, the change in distribution ratio was influenced less by

an increase in radius with diffusion time. It is likely that the radial effect significantly

declined in zone☐. As a result, the solute was retarded and the equilibrium time was

prolonged by 60 days. The implication is that the three dimensional RDC experiment

109

causes longer equilibrium times when compared to the results reported by Novakowski and Van der Kamp (1996) for 2D lateral radial diffusion with increasing radius.

Approximating the distribution ratio (C/C_R), as determined experimentally with three-dimensional radial diffusion, the effective diffusion coefficient for ammonium was determined to be $2.29 \times 10^{-10}\,m^2/sec$ for the clay-rich soil samples collected in Ponoka, Alberta. Figure 4.7 shows transient radial diffusion of ammonium through the porous media. The reservoir source concentration for ammonium was set to 5242 mg/L. The required distribution ratio (C/C_R), on the basis of the experimental result, was 0.66 and 0.91 for 10 days and 60 days, respectively. The 60-day simulation for the anaerobic RDC experiment resulted in an average C_{NH4} / C_R value of 0.91. This was calculated based on investigations of the equilibrium concentrations on the three surfaces, including the top, middle, and bottom of the reservoir, and at thirty points in the finite elements (Figure 4.7). To obtain the ammonium effective diffusion coefficient, it was assumed that ammonium diffuses symmetrically in the effected zone.

The value of D^* for ammonium for the 3D RDC simulation was lower than the D^* of $5.7 \times 10^{-10}\,m^2/sec$ reported by Rowe et al. (1995). The soil samples in Rowe et al.'s (1995) diffusion test were composed of 45% sand, 42% silt, and 23% clay. Total porosity and PI were equal to 32% and 11, respectively. The ammonium concentration in the source was 957 mg/L. The lower value of D^* in this study may be the result of higher clay factions (34% from XRD) and a higher ammonium concentration in the source (5242 mg/L). These features cause retardation of solutes through tortuous paths and longer equilibrium times.

110

However, the three-dimensional radial diffusion model cannot account for reactive transport during diffusion periods. In reality, the ammonium reacts with the pore fluid and the clay minerals during the diffusion period. In particular, cation exchange reactions should be considered during the simulation to effectively investigate ammonium diffusion in the EMS subsurface environment. Moreover, the smectite-rich clay samples with high CEC substantially adsorb and fix ammonium (Fonstad 2004; Hopkins et al., 1991). During the reactions, ammonium competes with other co-existing cations to occupy the adsorption sites. Apparently, although the three-dimensional radial diffusion simulation can serve as an alternative means to obtain an ammonium effective diffusion coefficient, it cannot satisfy the key requirements for EMS characterization.

4.4.3 Diffusive transport analysis with cation exchange

The methodology for the reactive radial diffusion model is divided into four components: (1) Development of a modeling framework for the radial diffusion domain; (2) verification of the modeling framework; (3) addition of reaction to model the anaerobic RDC experiment; and (4) prediction of maximum volume of liquid hog manure required to achieve ammonium saturation.

4.4.3.1 Modeling framework verification

The modeling framework developed in this study is a unique method used to describe radial diffusion using PHREEQC. The radial diffusion domain created here was subjected to a conservative chloride source with a concentration of 1380 mg/L. It was assumed that the chloride diffused radially along the domain without reactions.

111

In order to verify the modeling framework, the results were compared to radial diffusion from ChemFlux, as shown in Figure 4.8. The model explicitly described the radial diffusion of solutes through the radial diffusion domain. The equilibrium concentration for chloride was set to 1150 mg/L, which is 0.83 of the distribution ratio (C/C_R) for the 100-day simulation. The effective length of the radial diffusion domain was based on the pore volume ratio ($n_p V R_n$) and was estimated using the mass balance calculation.

4.4.3.2 Reactive radial diffusion transport analysis

The cation exchange reactions caused by ammonium diffusion through the porous media should be considered in order to develop an accurate reactive transport. The ammonium exchange reactions enable those cations that are on the exchange sites initially, such as calcium, magnesium, and sodium, to be extracted to the bulk solution in the pores. In addition, Langmuir (1997) found that adsorption is always part of an exchange reaction that involves a competing ionic species. As a result, the exchange reactions that occur during interaction of the liquid manure and clayey soils lead to ammonium adsorption and fixation on clay minerals or in interlayers of clays.

To model ammonium adsorption behavior, reactions such as aqueous mixing and cation exchange were added to the modeling framework. In the reactive model, the solutes react with the pore fluid before being transported to the next element in the radial diffusion domain (See Figure 4.4).

112

Figure 4.9 and 4.14 show the simulated ammonium radial diffusion, which includes cation exchange reactions and its contour in the RDC. The reactive ammonium diffusion successfully reflected not only the symmetrical radial effect, but also the ammonium adsorption that resulted from exchange reactions. According to the simulation results, it was anticipated that after the 100-day diffusion periods the dissolved ammonium concentration in the pore fluid would be attenuated from 43 to 54% of the initial ammonium concentration in the source reservoir (5241.5 mg/L). The simulated equilibrium concentrations of ammonium in the pore fluid ranged from 2411 to 2988 mg/L, corresponding to 32.5 and 12.5 mm distance from the source. In contrast, the unreactive model little ammonium was attenuated and equilibrated at 4682 to 4728 mg/L after a 100-day simulation (cf. the two contours as shown in Figure 4.7 and 4.14).

Unlike the unreactive modeling, the reactive transport analysis embodied NH_4-K-Na–Ca-Mg diffusion in competition to occupy exchange sites. The co-existing potassium and sodium also diffused radially into the porous media. Ammonium was the major affined species, potassium was the second species, and these were followed by sodium; the liquid hog manure sample consisted of 79% ammonium, 12% potassium, 7% sodium, 1% calcium and 1% magnesium in major competitive cations. Ammonium dominated the diffusion process because it had greater opportunity to occupy the exchange sites. Figure 4.9 to 4.14 show the 100-day simulation for the anaerobic RDC experiment. The distribution ratio for ammonium ($C_{NH4,[day\ 100]}/C_{R,NH4}$) ranged from 0.57 to 0.46 when it was 12.5 mm (the point near the source) and 32.5 mm (the end of the cell) from the source (See Figure 4.9). The values of the distribution ratios (C/C_R) for ammonium were normalized by the initial reservoir concentration for ammonium ($C_{R,\ NH4}$: 5242 mg/L)

113

because the equilibrium pore fluid concentrations for ammonium were negligible in all the diffusion cells (See Table 4.1, $C_{0,NH4}$ < 1.0 mg/L for Cell UA1 to 5). With respect to potassium, the values of $C_{K,[day\ 100]}/C_{0,K}$ ranged from 84 to 39 when it was 12.5 and 32.5 mm from the source (See Figure 4.10). The $C_{Na,[day\ 100]}/C_{0,Na}$ ranged from 6.8 to 2.7 at 12.5 and 32.5 mm, respectively (See Figure 4.11). The values of the distribution ratios (C/C_0) for potassium and sodium were normalized by the equilibrium pore fluid concentrations as determined by the IC analysis.

In the reactive model, magnesium and calcium were exchanged and then extracted from the exchange sites because of the significant ammonium exchange reactions. The reactive transport analysis supported the diffusion-controlled adsorption mechanism (Kithome et al., 1998). In the mechanism, as ammonium occupies the sorption sites by displacing exchangeable cations, the exchanged cations re-diffuse from the exchange sites to the pore fluid. In the RDC experiment, the exchanged calcium and magnesium initially present in the nearby reservoir were re-diffused through the pores and then extracted from the porous media. This resulted in a substantial increase of the hardness of the reservoirs (See Figure 4.15). A change in hardness was a simple indicator used to monitor changing levels of calcium and magnesium in the reservoirs. During the 60-day contact time, the hardness in the reservoirs increased to 137% of the initial reservoir solution hardness. This resulted directly in elevated calcium and magnesium concentrations in the central reservoirs (See Table 4.1). In the reactive model, the dissolved calcium concentration in the pore fluid increased by as much as 233% of its initial concentration in the pore fluid. As shown in Figure 4.12, $C_{ca,[day60]}/C_{0,ca}$ for calcium ranged 2.94 to 6.41 in the pore fluids. The values of the distribution ratios

114

$(C_x/C_{0,x})$ were also normalized by the equilibrium pore fluid concentrations. Notably, the displacement rate of magnesium was more significant than that of calcium given an increase in the diffusion time (Table 4.1). As a result, $C_{Mg, [day\ 60]}/C_{0,\ Mg}$ ranged from 13.3 to 53.7 in the pore fluids (See Figure 4.13). Fonstad et al. (2001) reported the similar displacement of calcium and magnesium on exchange sites during soil-manure contact. The soils with smectite were sampled from an EMS site near Saskatoon, Saskatchewan, Canada. Soil was ponded with swine effluent for a period of two years. As a result of ion exchange, potassium and ammonium displaced sodium, calcium, and magnesium on the exchange sites and produced a hard water front that advanced at the front of the plume.

The maximum effective exchangeable layer was approximately 17.5 mm thick from the source reservoir according to the reactive model. Figure 4.14 illustrates the contoured ammonium radial diffusion and the simulated exchange layers. When ammonium diffused radially through the porous media, ammonium displaced calcium and magnesium within the approximated exchange layers at a length of 17.5 mm (See Figure 4.12 and 4.13). The exchange layers expanded with diffusion time. As shown in Figure 4.14, calcium and magnesium presented in the exchange layer [1] at a distance of 12.5 mm from the source and were extracted until approximately day 24. After 24 days of diffusion, magnesium extraction then took place in the exchange layer [2]. It was inferable that ammonium would be considerably retarded and adsorbed within the exchange layers. It was also observed that the radial diffusion of potassium and sodium were suppressed within the exchange layers, as shown in Figure 4.10 and 4.11.

115

The reactive model for manure effluent with cation exchange was validated by means of comparing the experimental and unreactive model results (See Table 4.2 and Table 4.3). The central reservoir, containing the initial source liquid manure, had 98% NH_4-K-Na and 2% Ca-Mg in mole fraction.

After 60-day diffusion periods, the measured ammonium (NH_4^+) concentration was 509 mg/L in the reservoir. The predicted ammonium concentration in the reservoir was 484 mg/L and 437 mg/L in the unreactive and reactive model, respectively. The adsorbed ammonium in the experiment was estimated to be 5.3 mmol for the single manure injection. The reactive model calculated 5.4 mmol for the adsorbed ammonium (See Table 4.2). The total distribution ratio (C'/C_R), determined by the mass balance equation, was 0.91, 0.91, and 0.92 in the experiment, the unreactive model, and the reactive model, respectively.

The predicted potassium (K^+) concentration in the reactive model was consistent with the measured potassium concentration in the experiment, as shown in Table 4.2. The measured potassium concentration was 856 mg/L in the experiment. The reactive model calculated a potassium concentration of 859 mg/L. The adsorption and distribution ratios calculated by the reactive model were also similar to the values determined by the experiment. The adsorbed potassium was 0.45 mmol for the single injection in both the reactive model and the experiment. The distribution ratios for potassium were 0.52, 0.58, and 0.51 in the experiment, and the unreactive and reactive models, respectively. In the case of sodium (Na^+), the predicted sodium concentration after the 60-day diffusion was 505 mg/L, and the distribution ratios were 0.27, 0.39 and 0.25 in the experiment, the

116

unreactive model, and the reactive model, respectively.

The exchangeable calcium (Ca^{2+}) and magnesium (Mg^{2+}) diffusion were also predicted in the reactive model. The reactive model calculated that 0.13 mmol of the exchangeable Ca^{2+} would be adsorbed and that 0.03 mmol Ca^{2+} would be extracted to the reservoir in the diffusion duration. In the experiment, 0.12 mmol of Ca^{2+} was adsorbed, and 0.02 mmol of Ca^{2+} was extracted to the reservoir during the same diffusion periods (See Table 4.3). Magnesium was slightly overestimated in the reactive model: the extractable magnesium was 0.07 mmol and 0.18 mmol in the experiment and reactive model, respectively.

The advantage of the reactive model is that the model can include radial diffusion, cation exchange, and cation competition (NH_4-Na-K-Ca-Mg) at the same time. Such efficiency is beneficial because the reactive model can both simulate radial diffusion with cation exchange and it can predict changes in pore fluid chemistry under anaerobic conditions. In addition, the results of the reactive model were in reasonable agreement with the experimental data. Consequently, the coupled simulation that occurred in the reactive model is applicable to the manure effluent and soil interaction problem.

4.4.3.3 Prediction of net ammonium capacity using the reactive transport model

In the predictive model, liquid hog manure was successively injected into the source element on the radial diffusion domain until the pore fluid concentration of ammonium reached equilibrium. Figure 4.16 shows the 500-day reactive simulation used to predict

117

the maximum liquid manure volume. The initial injection concentration for ammonium was set to 5242 mg/L, and was determined from the IC analysis. The volumes of the liquid hog manure predicted to achieve full ammonium saturation was 0.8 mL/g for sandy lean clay samples (Cell UA1 and 2), and 1.27 to 1.36 mL/g for sandy fat clay samples (Cell UA3, 4, and 5). Thus, the net amounts of ammonium able to be adsorbed were 0.23 mol/kg for sandy lean clay samples, and 0.38 mol/kg for sandy fat clay samples. Because 20 mL was set as the single injection-volume of liquid manure, 27 and 40 injections were required to achieve ammonium saturation in the sandy lean clay samples and the sandy fat clay samples, respectively. Based on the apparent diffusion length of 34.7 mm in the RDC, the predicted net diffusion time (equilibrium time for each manure injection-episode was not included in the estimation) is 110 days for the sandy lean clay samples, with the ammonium effective diffusion coefficient (D^*) equal to 2.29×10^{-10} m^2/sec, and 185 days for the sandy fat clay samples, with D^* equal to 2.29×10^{-10} m^2/sec.

The 500-day reactive simulation embodied anaerobic conditions. There was no production of nitrate or nitrite due to the oxidation of the added ammonium. In the case of the anaerobic RDC experiment, nitrate and nitrite concentrations were below the detection limit during the entire running period of 185 days. The developed anaerobic conditions led to sulfate reduction in the pore fluid, as shown in Figure 4.17. In the anaerobic RDC experiment, sulfate concentrations also decreased from 1.91 mM to 0.38 and 0.56 mM in the reservoir solutions.

118

The change in pH in the simulated pore fluid was in agreement with the measured reservoir pH for 25 elapsed days; however, after 25 days, the simulated pH did not follow the measured pH trends. The decrease of pH is associated with the exchange reactions between the ammonium and the cations presented at the exchange sites (Semmens, 1977). In particular, the hydrogen ion (H^+) displaced from the exchange sites, located in the exchange layers, directly impacted the decline of pH in the reservoir (Figure 4.17). Yet, as ammonium reacted with the pore fluid, the soil exhibited its own buffering capacity against acidity (Langmuir, 1997). In the experiment with the single injection of the liquid hog manure, the pH declined until day 40 then increased to 6.8 at equilibrium due to the soil's buffering capacity. The PHREEQC model was not programmed to account for the soil's buffering capacity during the successive injections of liquid hog manure. Mineral weathering, solubility, and acid buffering by clay mineral were beyond the scope of the research program.

4.5 SUMMARY AND CONCLUSIONS

The model suggests that the effective diffusion coefficient for porous media depends on the clay fraction of in-situ soils and the diffusive equilibrium time. The proposed effective diffusion coefficients for chloride ranged from 5.17×10^{-10} to 6.67×10^{-10} m^2/sec for sandy lean clay and 2.80×10^{-10} to 2.85×10^{-10} m^2/sec for sandy fat clay samples collected in Ponoka, Alberta.

According to the three-dimensional radial diffusion results, the three-dimensional RDC experiment suppressed the radial effect below the central reservoir level. The weak

119

radial effect prolonged equilibrium time in comparison to the original RDC method in which only lateral radial diffusion was analyzed by Novakowski and Van der Kamp (1996).

The three-dimensional radial diffusion modeling provided an ammonium effective diffusion coefficient of 2.29×10^{-10} m^2/sec by excluding advection and dispersion in both the experiment and simulation. However, the dissolved ammonium concentrations simulated by the unreactive 3D radial diffusion model were overestimated when compared to the reactive model. The dissolved ammonium concentrations were, on average, 58% higher than those from the reactive model, due to the absence of the cation exchange reactions.

The modeling framework effectively embodied the radial effect for reactive diffusion transport. It can be applied to simulate other reactive radial diffusion problems using a RDC experiment.

By integrating the mixing and exchange reactions into the modeling framework, the reactive model properly simulated ammonium radial diffusion in competition with co-existing potassium and sodium. Potassium and sodium radially diffused through porous media as well; however, ammonium diffusion was the most significant species and had the greatest opportunity to occupy the exchange sites. NH$_4$-K-Na reactive diffusion was evaluated by means of mass balance between the source liquid hog manure and the amount diffused into the porous media. The estimation was agreed with the anaerobic RDC experiment results with respect to the distribution ratio (C/C$_R$).

120

Based on the reactive model, the cation exchange reactions significantly attenuated ammonium diffusion through the porous media. The highly concentrated ammonium-rich liquid hog manure (5242 mg/L) was diluted by 43 to 53% of the initial manure concentration during the reactive diffusion transport.

The exchange reactions occurred in the exchange layer, which was approximately 17.5 mm thick near the source. When ammonium transport was retarded in the exchange layer, calcium and magnesium were displaced from the exchange sites. Magnesium extraction was more significant. The exchange layer expanded with diffusion time. The reactive model also supported this chemical redistribution as an effect of diffusion-controlled adsorption.

The net amounts of ammonium able to be adsorbed were 0.23 mol/kg for sandy lean clay samples, and 0.38 mol/kg for sandy fat clay samples. The simulated net time for saturation by ammonium ranged from 110 to 185 days when the initial ammonium concentration at the source was set to 5242 mg/L. The reactive model predicted the anaerobic conditions during the successive addition of the liquid hog manure into the RDC. This led to the reduction of sulfur compounds.

The reactive modeling with transient diffusion satisfied the key requirements to simulate the geochemical environment in EMS subsurface: (1) anaerobic conditions, (2) diffusion controlled adsorption, (3) cation exchange, and (4) competition. The reactive model is able to provide both radial diffusion transport, including reactions, and the change in pore fluid chemistry. The reactive analysis demonstrates that the long-term diffusion

121

effect should be considered in a budget of nitrogen loss in subsurface areas of earthen manure storage facilities.

REFERENCES

Alberta Agriculture, Food and Rural Development, 2002. Beneficial Management Practices: Environmental Manual for Hog Producers in Alberta.

Astatkie, T., Madani, A., Gordon, R., Caldwell, K., Boyd, N., 2001. Seasonal variation of nitrate-nitrogen in the soil profile in a subsurface drained field. Canadian Biosystems Engineering, 43, 1.1–1.6.

Crank, J., 1975. The mathematics of diffusion, 2nd Ed. Clarendon Press. Oxford.

Baron, F.S., Rowe, R.K., Quigley, R.M., 1990. Laboratory determination of chloride diffusion coefficient in an intact shale. Canadian Geotechnical Journal, 27, 177–184.

Baron, F.S., Rowe, R.K., Quigley, R.M., 1992b. A laboratory estimation of diffusion and adsorption coefficients for several volatile organics in a natural clayey soil. Journal of Contaminant Hydrogeology, 10, 225–250.

Baron, F.S., Yanful, E.K., Quigley, R.M., and Rowe, R.K., 1989. Effect of multiple contaminant migration on diffusion and adsorption of some domestic waste contaminants in a natural clayey soil. Canadian Geotechnical Journal, 26(2), 189–198.

Comly, H.H., 1945. Cyanosis in infants caused by nitrates in well water. Journal of the American Medical Association, 129,112.

Follett, R.F., Delgado, J.A., 2002. Nitrogen fate and transport in agricultural systems. Journals of Soil and Water Conservation, 57(6), 402–408.

Fonstad, T.A., 2004. Transport and fate of nitrogen from earthen manure storage effluent seepage. Ph.D. thesis, University of Saskatchewan.

Fonstad, T.A., Maule, C.P., 1996. Solute migration beneath earthen hog manure storages in Saskatchewan. ASAE International Meeting, Pheonix, Arizona. July, 1996. Paper presentation, Pub.No.: CSAE paper No. 962049.

Fonstad, T.A., Maule, C.P., Barbour, S.L., Donahue, R., Ingram, L., Meier, D., 2001. Fluid movement and chemical transport from an animal wastes storages. Preferential Flow, Water Movement and Chemical Transport in the Environment, Proceedings of the 2nd International Symposium, January 2001, Honolulu, Hawaii, USA. ASAE Pub

701P0006

Fredlund, M., Stianson, J., 2003. ChemFlux Theory Manual, SoilVision Ltd.

Fredlund, M., Stianson, J., 2003. SvFlux Theory Manual, SoilVision Ltd.

Freeze, R.A., Cherry, J.A., 1979. Groundwater. Prentice-Hall, Inc., Englewood Cliffs, New Jersey, USA.

Gooddy, D.C., Clay, J.W., Bottrell, S.H., 2002. Redox-driven changes in porewater chemistry in the unsaturated zone of the chalk aquifer beneath unlined cattle slurry lagoons. Journal of Applied Geochemistry, 17, 903–921.

Ham, J.M., DeSutter, T.M., 1999. Seepage losses and nitrogen export from swine-waste lagoons: a water balance study. Journal of Environmental Quality, 28, 1090–1099.

Hendry, M.J., McCready, R.GL., Gould, W.D., 1984. Distribution, source and evolution of nitrate in a glacial till of southern Alberta, Canada. Journal of Hydrology, 70, 177–198.

Hopkins, K., Byrne, J., Mckenzie, R., 1991. Assessing nitrate pollution potential from intensive animal husbandry operations. Water Resource Institute, the University of Lethbridge, Occasional Paper No. 2.

Jenne, E.A., 1995. Metal adsorption onto and desorption from sediments. □. Rates. In Metal speciation and contamination of aquatic sediments, ed. H.E. Allen. Ann Arbor, MI: Ann Arbor Press.

Kithome, M., Paul, J.W., Lavkulich, L.M., Bomke, A.A., 1998. Kinetics of ammonium adsorption and desorption by the natural zeolite clinoptilolite. Soil Science Soceity of America Journal, 62, 622–629.

Lanmuir, D., 1997. Aqueous Environmental Geochemistry. Prentice Hall: Upper Saddle River, New Jersey, USA.

Lumbanraja, J., Evangelou, V.P., 1994. Adsorption-desorption of potassium and ammonium at low cation concentrations in three Kentucky subsoils. Soil Science Society of America Journal, 157(5), 269–277.

Novakowski, K.S., Van der Kamp, G, 1996. The radial diffusion method 2. A Semianalytical model for the determination of effective diffusion coefficients, porosity, and adsorption. Water Resources Research, 32(6), 1823–1830.

Parkhurst D.L., Appelo C.A.J., 1999. User guide to PHREEQC—A computer program for speciation, reaction-path, 1D-transport and inverse geochemical calculations. U.S. Geological Survey Water Resource Inv.

123

Pauwels, H., Lachassagne, P., Bordenave, P., Foucher, J. C., Martelat, A., 2001. Temporal variability of nitrate concentration in a schist aquifer and transfer to surface waters. Journal of Applied Geochemistry, 16, 583–596.

Rowe R.K., Quigley, R.M., Booker, J.R., 1995. Clayey barrier systems for waste disposal facilities, 1st ed., E & FN SPON. London, U.K.

Semmens, M.J., Wang, J.T., Booth, A.C., 1997. Biological regeneration of ammonium-saturated clinoptilolite □. Mechanism of regeneration and influence of salt concentration. Environmental Science and Technology, 11(3), 260–265.

Shackleford C.D., Daniel, D.E., 1991. Diffusion in saturated soil□: Results for compacted clay. Journal of Geotechnical Engineering, ASCE, 117(3), 485–506.

Stoltenow, C., Lardy, G., 1998. Nitrate poisoning of livestock. North Dakota State University Extension Service Publication, Vol. 839.

Van der Kamp, G., Van Stempvoort, D.R., Wassenaar, L.I., 1996. The radial diffusion method. 1. Using intact cores to determine isotopic composition, chemistry and effective porosities for groundwater in aquitards. Water Resources Research, 32, 1815–1822.

Van Stempvoort, D.R., Van der Kamp, G., 2003. Modeling the hydrogeochemistry of aquitard using minimally disturbed samples in radial diffusion cells. Journal of Applied Geochemistry, 18, 551–565.

Table 4.1 Reservoir monitoring results for major cations (unit: mg/L)

Major cations	Cell I.D.	Initial pore fluid	Initial liquid manure	Diffusion-day 60
NH_4^+	UA Cell 1	< 1.0	5242	508 ↓
	UA Cell 2	< 1.0	5242	3177 ↓
	UA Cell 3	< 1.0	5242	1067 ↓
	UA Cell 4	< 1.0	5242	136 ↓
	UA Cell 5	< 1.0	5242	169 ↓
K^+	UA Cell 1	10	1710	856 ↓
	UA Cell 2	10	1710	1370 ↓
	UA Cell 3	6	1710	854 ↓
	UA Cell 4	6	1710	408 ↓
	UA Cell 5	4	1710	726 ↓
Na^+	UA Cell 1	28	611	460 ↓
	UA Cell 2	<20	611	600 ↓
	UA Cell 3	<20	611	420 ↓
	UA Cell 4	21	611	320 ↓
	UA Cell 5	<20	611	460 ↓
Ca^{2+}	UA Cell 1	16	199	250 ↑
	UA Cell 2	<10	199	80 ↓
	UA Cell 3	13	199	180 ↓
	UA Cell 4	13	199	360 ↑
	UA Cell 5	<10	199	260 ↑
Mg^{2+}	UA Cell 1	6	6.4	89 ↑
	UA Cell 2	<2	6.4	17 ↑
	UA Cell 3	3	6.4	68 ↑
	UA Cell 4	3	6.4	92 ↑
	UA Cell 5	<2	6.4	106 ↑

Table 4.2 Comparison of experimental, unreactive, and reactive models results

Major ions	Initial mole fraction in reservoir	Diffusion models	Initial (mg/L)	Diffusion (mg/L) (60 days)	Adsorption (mmol)	Total Distribution ratio (C'/C_R)	Exchange reactions	Cation competition	Anaerobic conditions	Radial diffusion
			Reservoir	Reservoir	Soils	Soil / Reservoir				
NH_4^+	45%	Experiment	5242	508	5.33	0.91	O	O	O	O
		Unreactive	5242	484	N.A.	0.91	×	×	×	O
		Reactive	5242	437	5.43	0.92	O	O	O	O
K^+	7%	Experiment	1710	856	0.45	0.52	O	O	O	O
		Unreactive	1710	736	N.A.	0.58	×	×	×	O
		Reactive	1710	859	0.45	0.51	O	O	O	O
Na^+	4%	Experiment	611	460	0.18	0.27	O	O	O	O
		Unreactive	611	433	N.A.	0.39	×	×	×	O
		Reactive	611	505	0.25	0.25	O	O	O	O

Table 4.3 Exchangeable calcium and magnesium in the experiment and the reactive model

Major ions	Initial mole fraction in reservoir	Diffusion models	Initial	Diffusion (60 days)	Exchange
			Reservoir (mmol)	Reservoir (mmol)	Reservoir (mmol)
Ca^{2+}	1%	Experiment	0.10	0.12	-0.02
		Reactive	0.10	0.13	-0.03
Mg^{2+}	1%	Experiment	0.01	0.07	-0.07
		Reactive	0.01	0.19	-0.18

UNIT: MM

(a)

23.3

71.4

89

72

(b)

34.7

Vol. 20 ± 0.8 mL
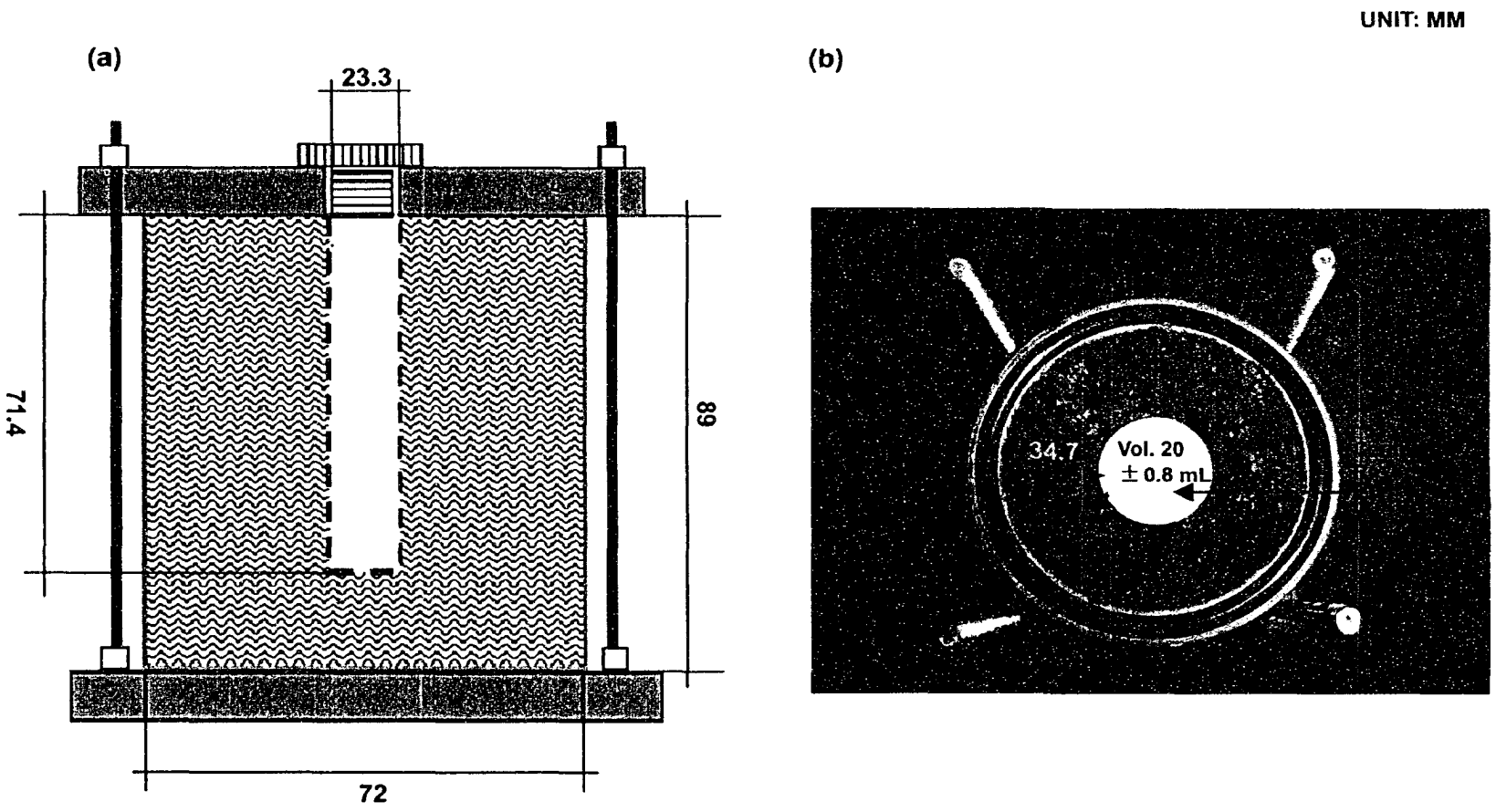
Figure 4.1 (a) Vertical schematic of a RDC and (b) apparent diffusion length and the inner volume of the reservoir
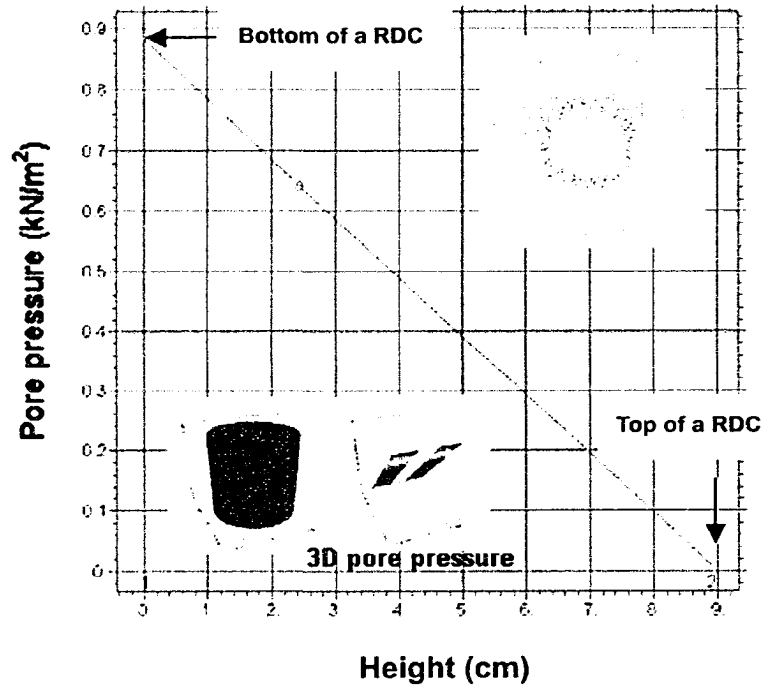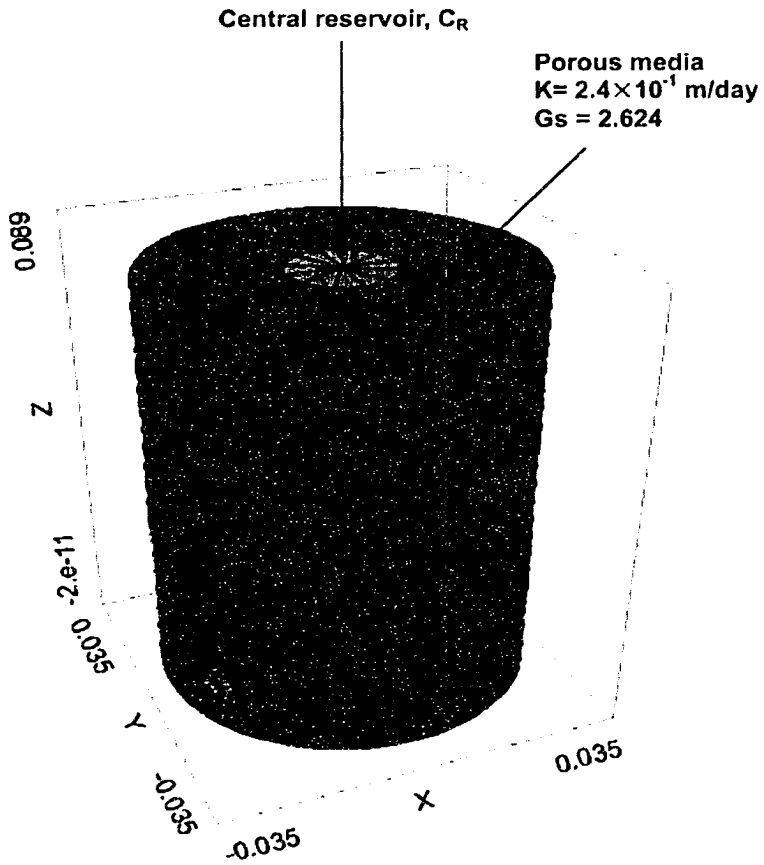
Figure 4.2 3-D mesh for a RDC and static pore pressure in the porous media

3D RADIAL DIFFUSION DOMAIN

RADIAL DIFFUSION DOMAIN

RADIAL SLICE

$$\sum_{1}^{n} n_p V_n$$

RADIAL DIFFUSION DOMAIN

[**Adding pore fluid chemistry information**]

n_pVR_1 n_pVR_2 n_pVR_3 n_pVR_4 n_pVR_5

J_1 J_2 J_3 J_4 J_5
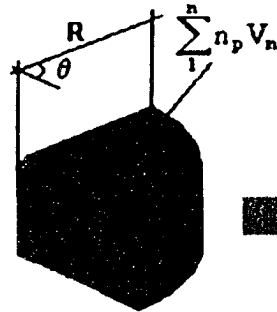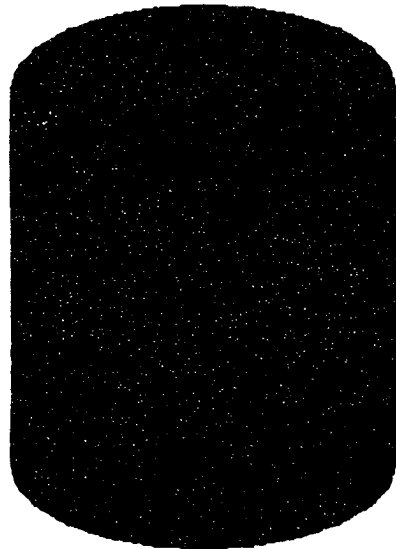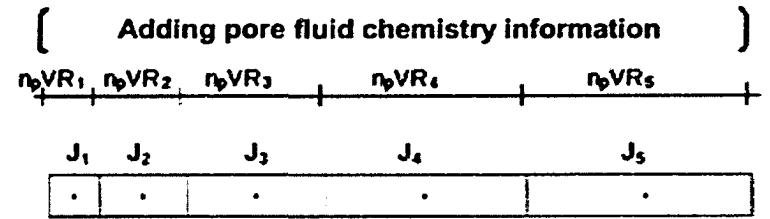
FRAME MODELING

Diffusion only

VERIFICATION
[using ChemFlux]

RADIAL DIFFUSION TRANSPORT

REACTIVE MODELING

Diffusion + Reaction

LEGEND

•   Element joint in diffusion domain

⟹   Diffusion transport component

ⓐ   Reaction component

Figure 4.3 Radial diffusion domain

MODELING FRAME WORK
→ Radial diffusion

REACTION TERMS
→ Mix with pore fluids
→ Exchange reactions
→ Adsorption

ASSUMPTIONS
-Homogeneous porous media
-Symmetric diffusion
-External diffusion
-Limited exchange sites

RESERVOIR

POROUS MEDIA

130
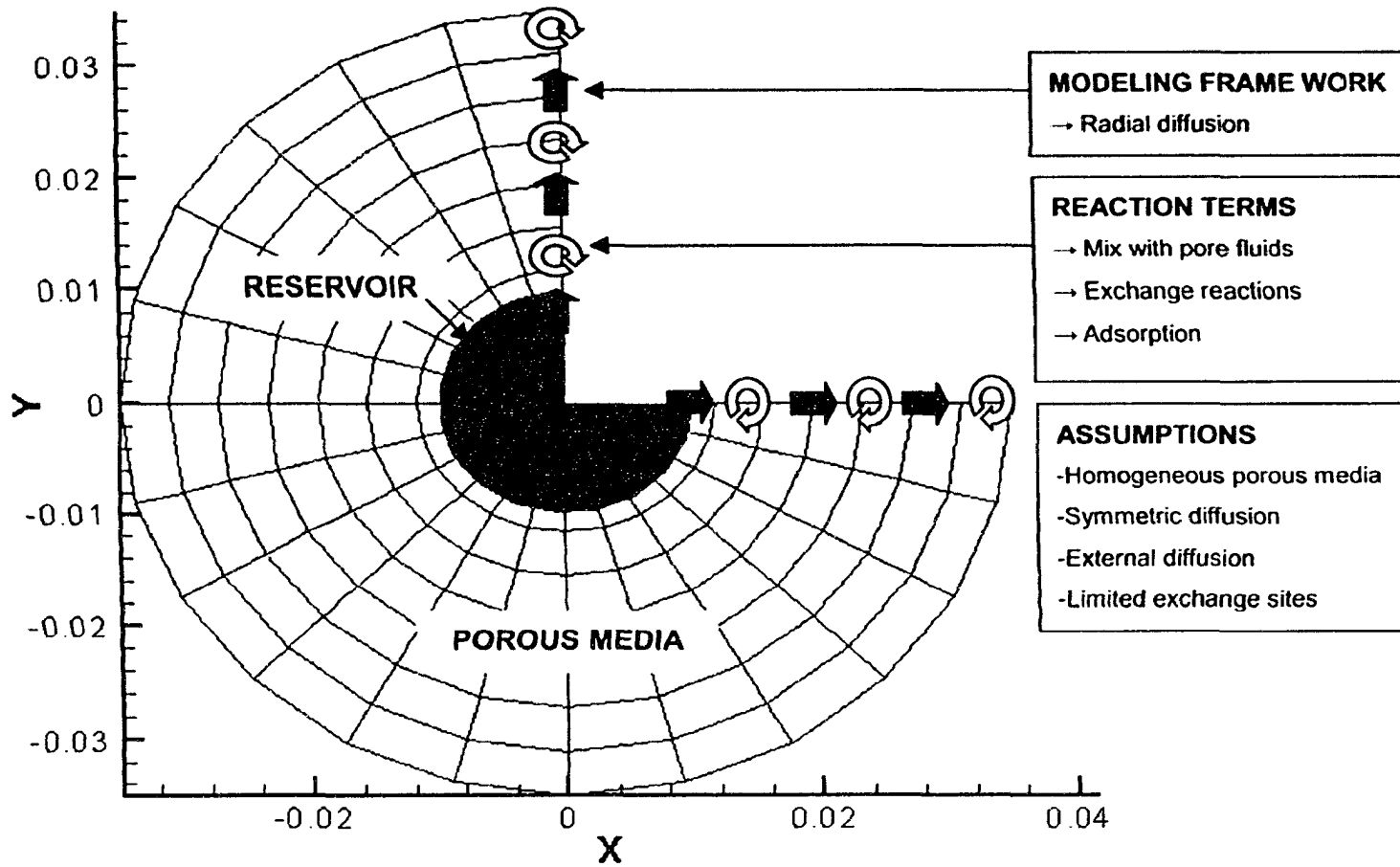
Figure 4.4 Conceptual model for the reactive transport model
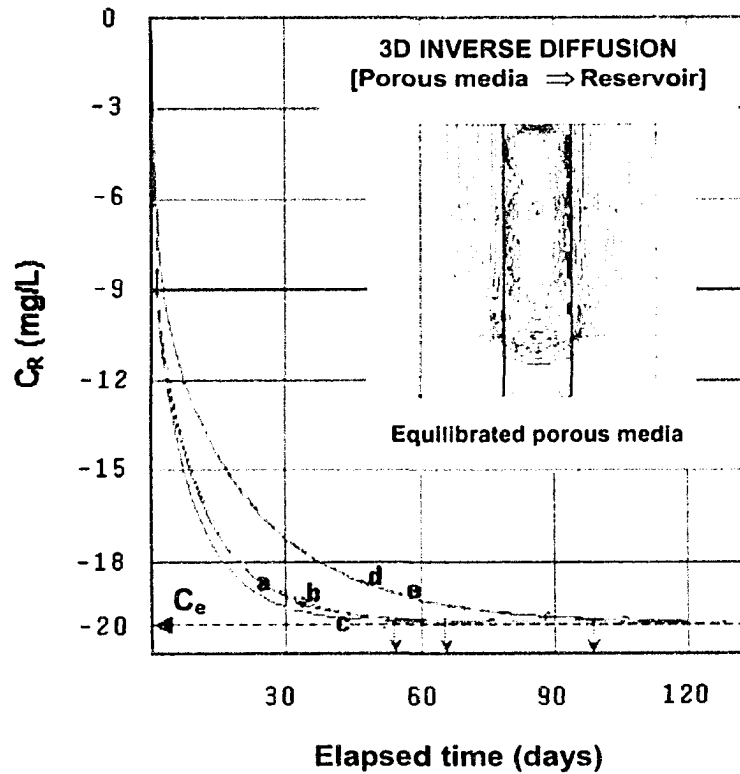
RESULTS

Cell UA1: **a** curve
Equilibrium time: 66 days
D^* :   5.17E-10 m2/sec
Cell UA2: **c** curve
Equilibrium time: 53 days
D^* :   6.67E-10 m2/sec
Cell UA3: **d** curve
Equilibrium time: 109 days
D^* :   2.80E-10 m2/sec
Cell UA4: **e** curve
Equilibrium time: 106 days
D^* :   2.85E-10 m2/sec
Cell UA5: **b** curve
Equilibrium time: 66 days
D^* :   5.23E-10 m2/sec

Figure 4.5 Diffusive equilibrium simulation results using ChemFlux

131
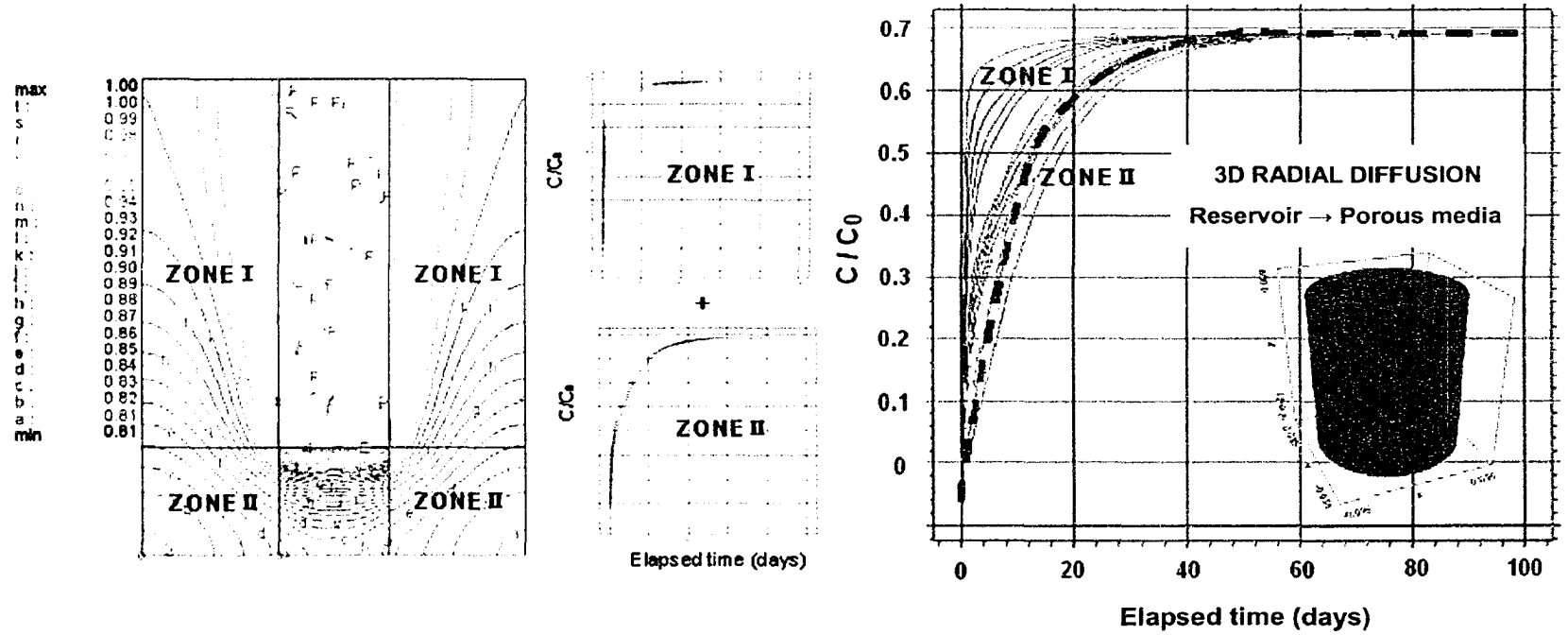
Figure 4.6 Three-dimensional radial diffusion in homogeneous porous media

132
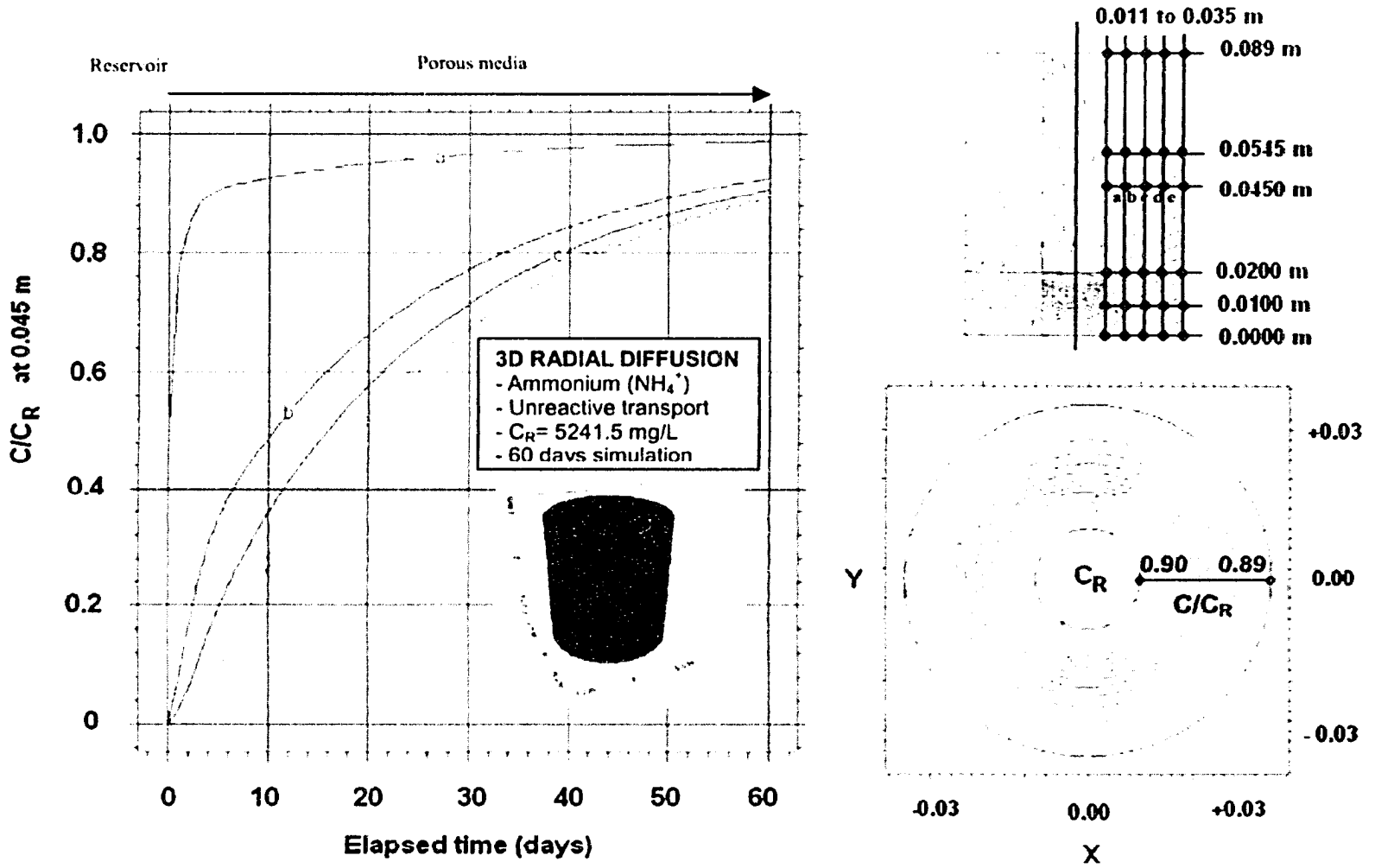
Figure 4.7 3-D radial diffusion of ammonium without reactions
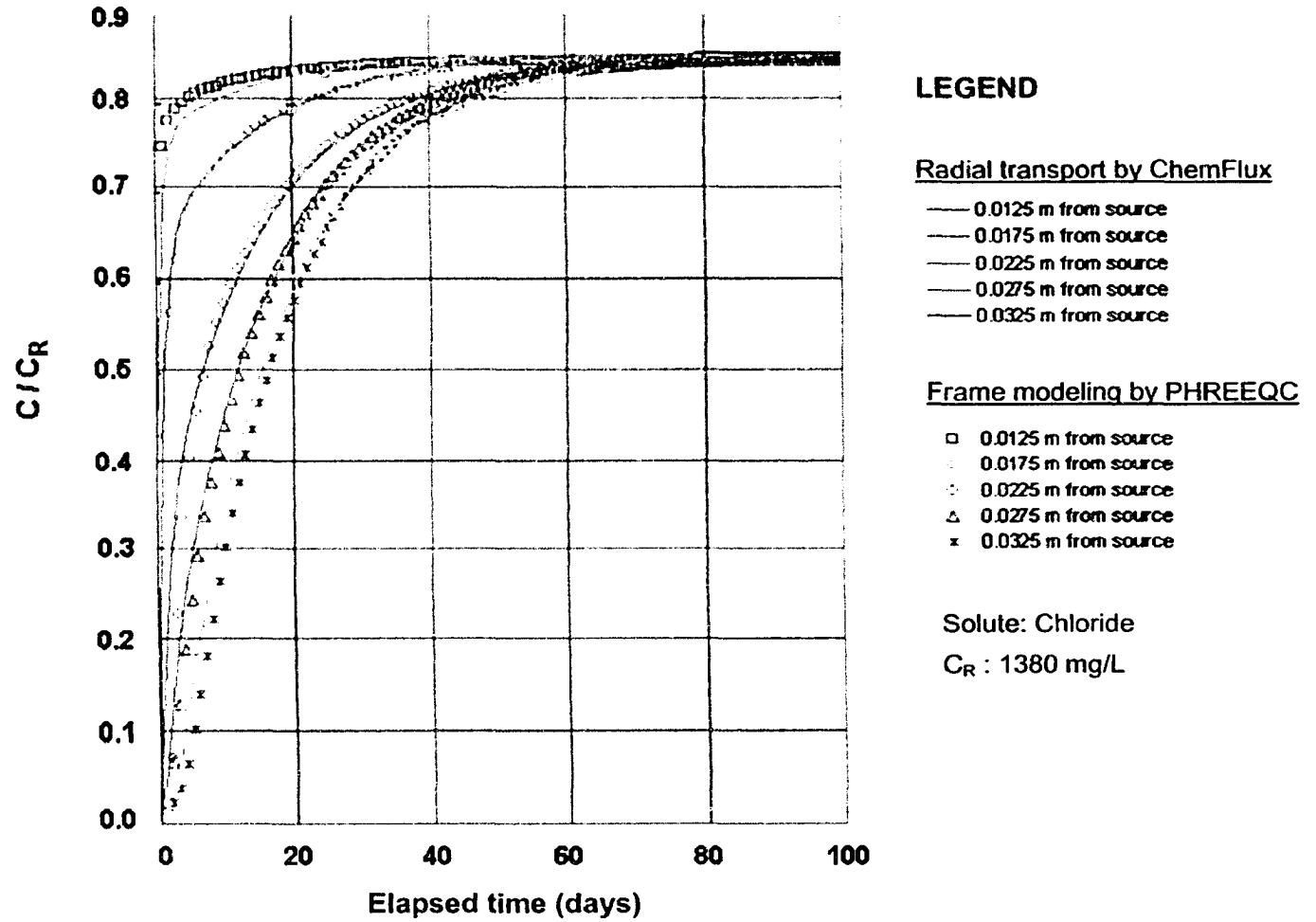
Figure 4.8 Verification for the modeling framework by using a finite element model, ChemFlux

134
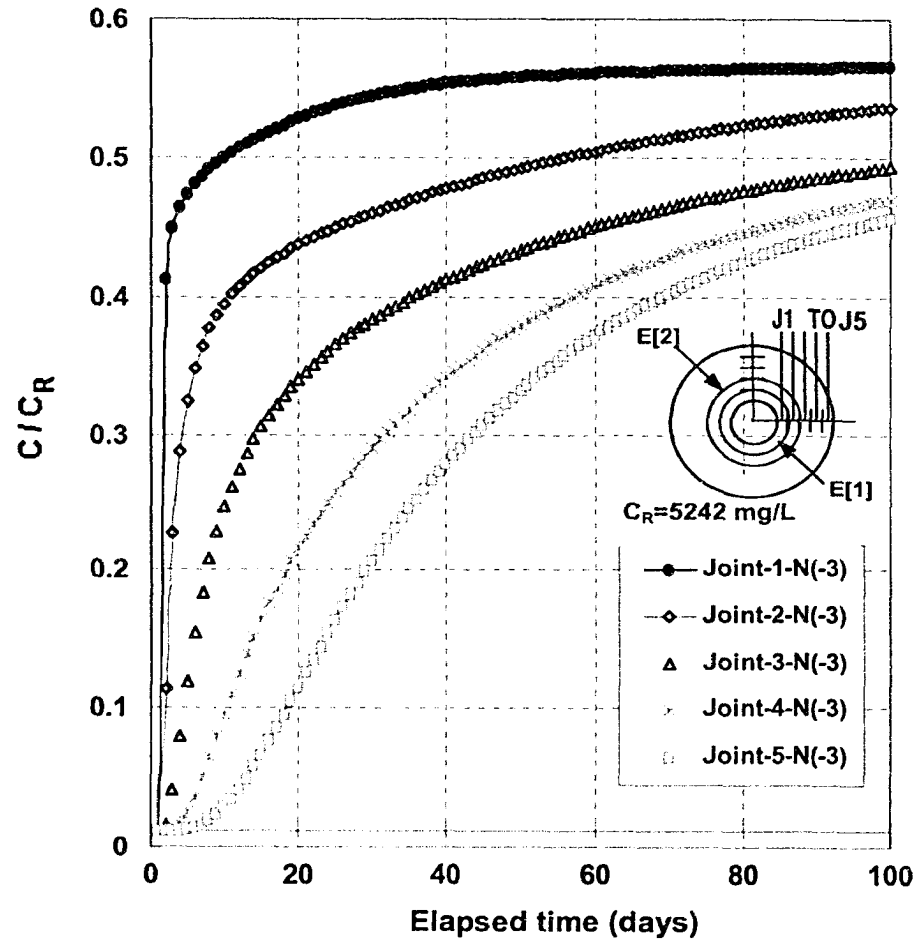
Figure 4.9 Reactive ammonium transport with radial diffusion + cation exchange + competition

136
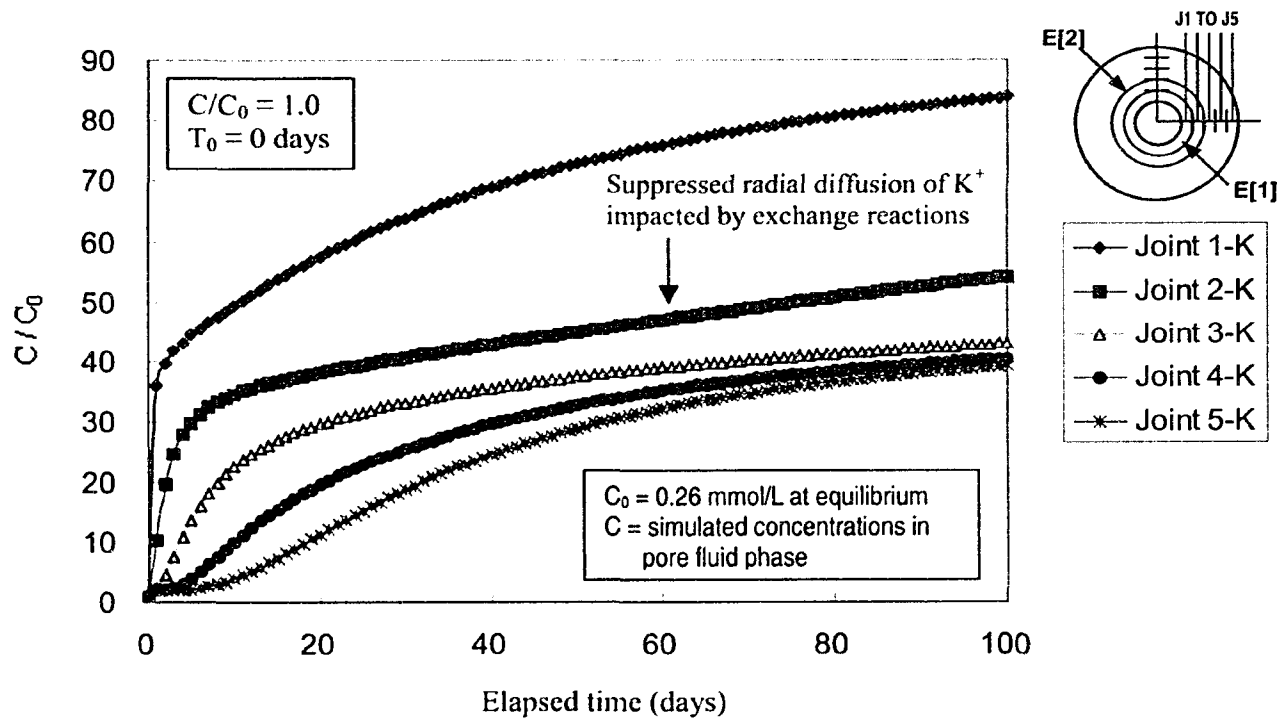
Figure 4.10 Reactive radial diffusion of potassium (radial diffusion + exchange + competition)
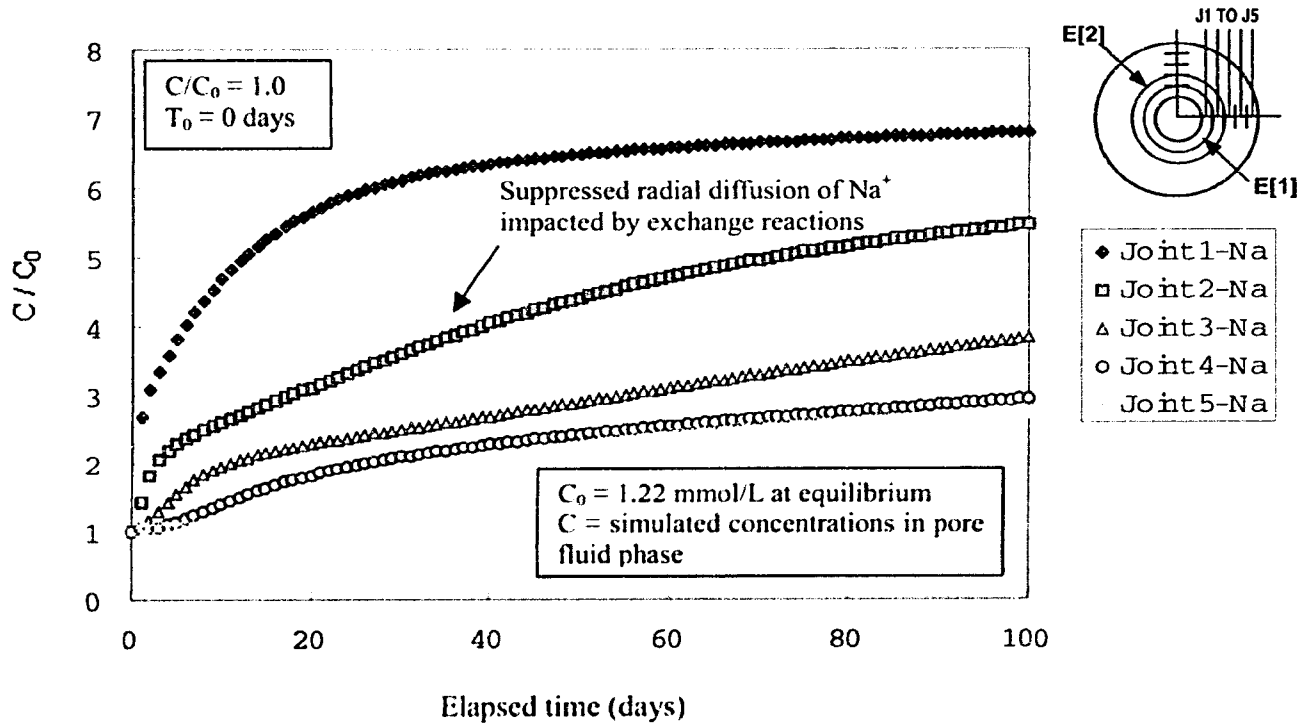
Figure 4.11 Reactive radial diffusion of sodium (radial diffusion + exchange + competition)
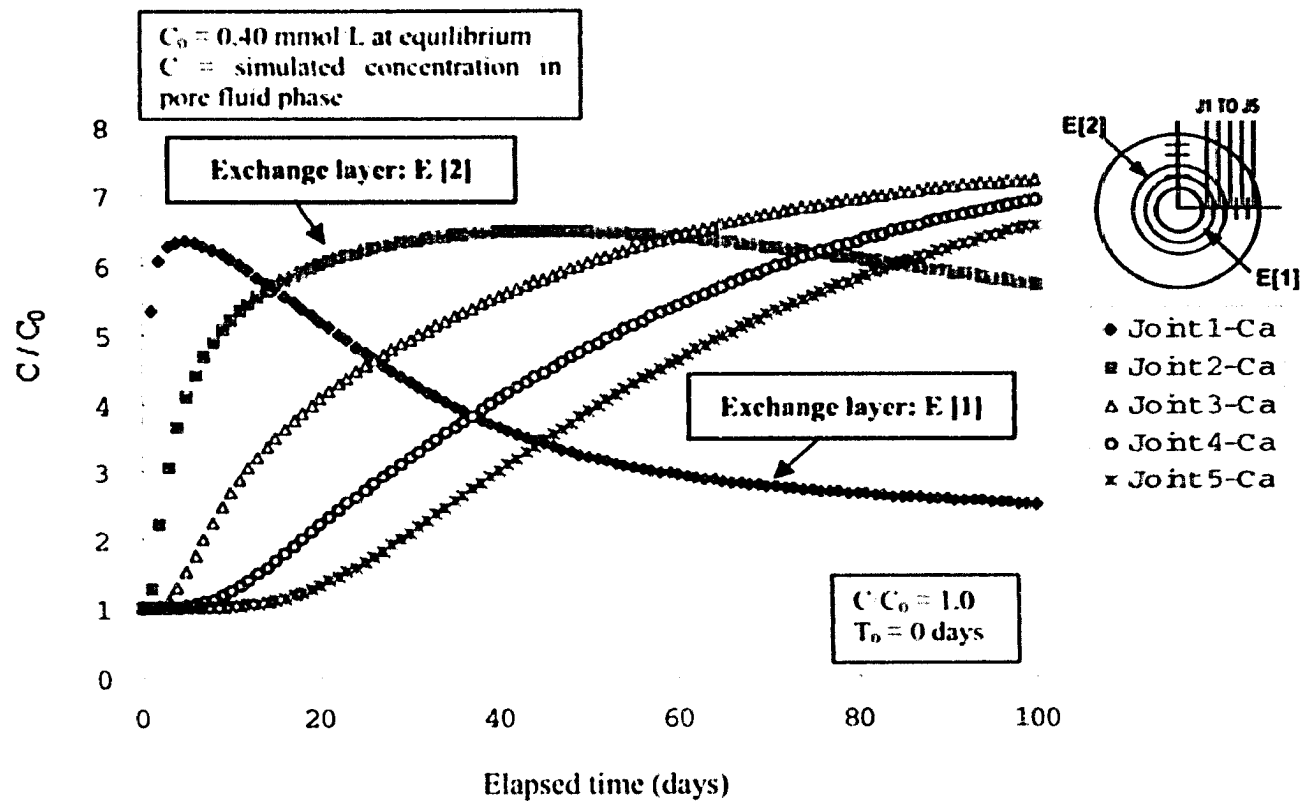
Figure 4.12 Reactive radial diffusion of calcium (radial diffusion + exchange + competition)

139
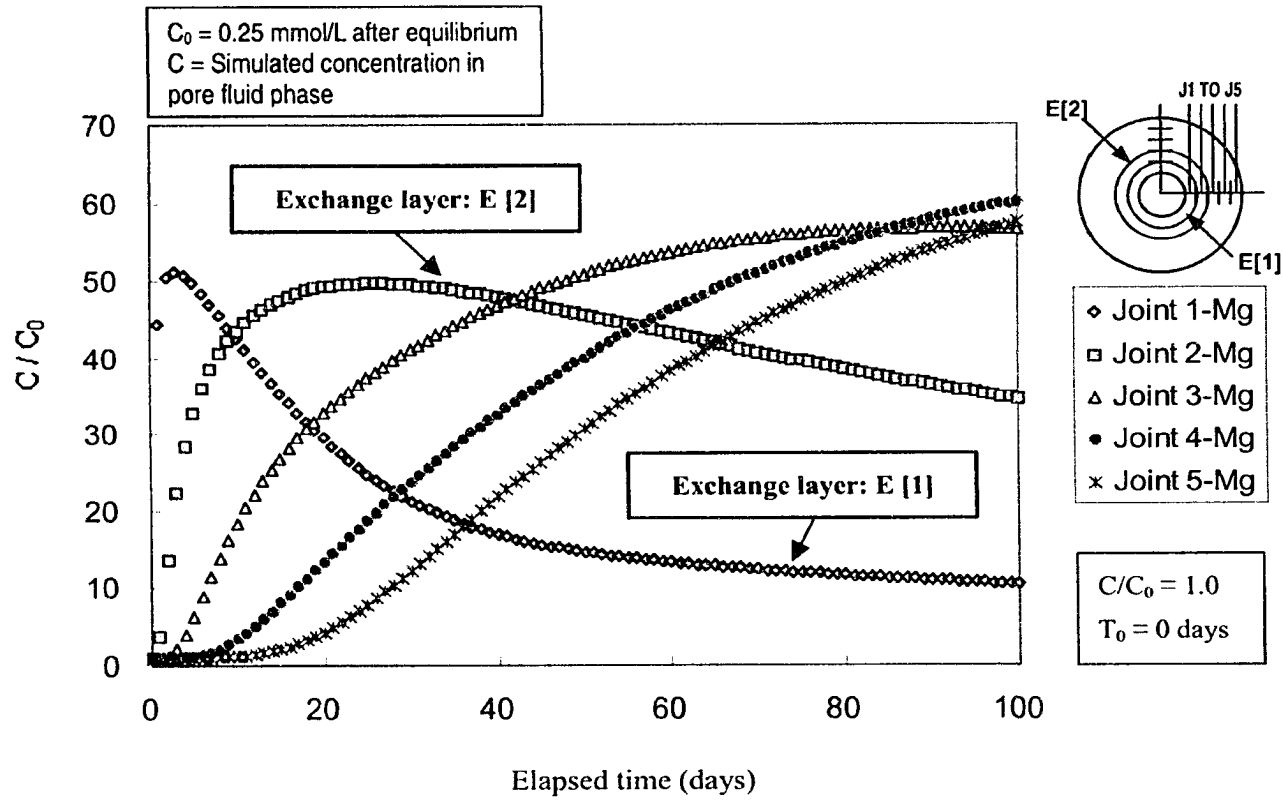
Figure 4.13 Reactive radial diffusion of magnesium (radial diffusion + exchange + competition)
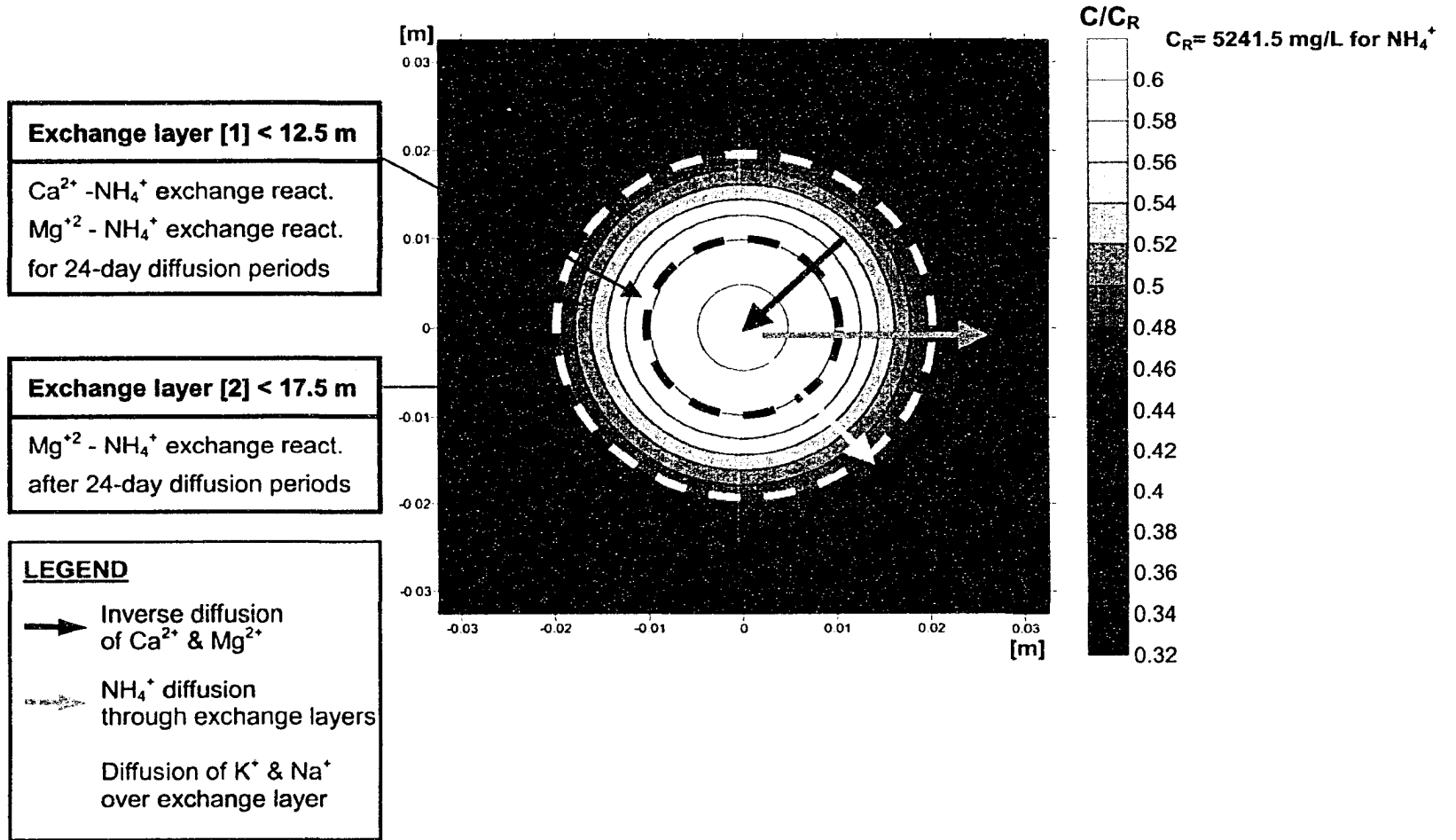
Figure 4.14 Contour of reactive transport for ammonium
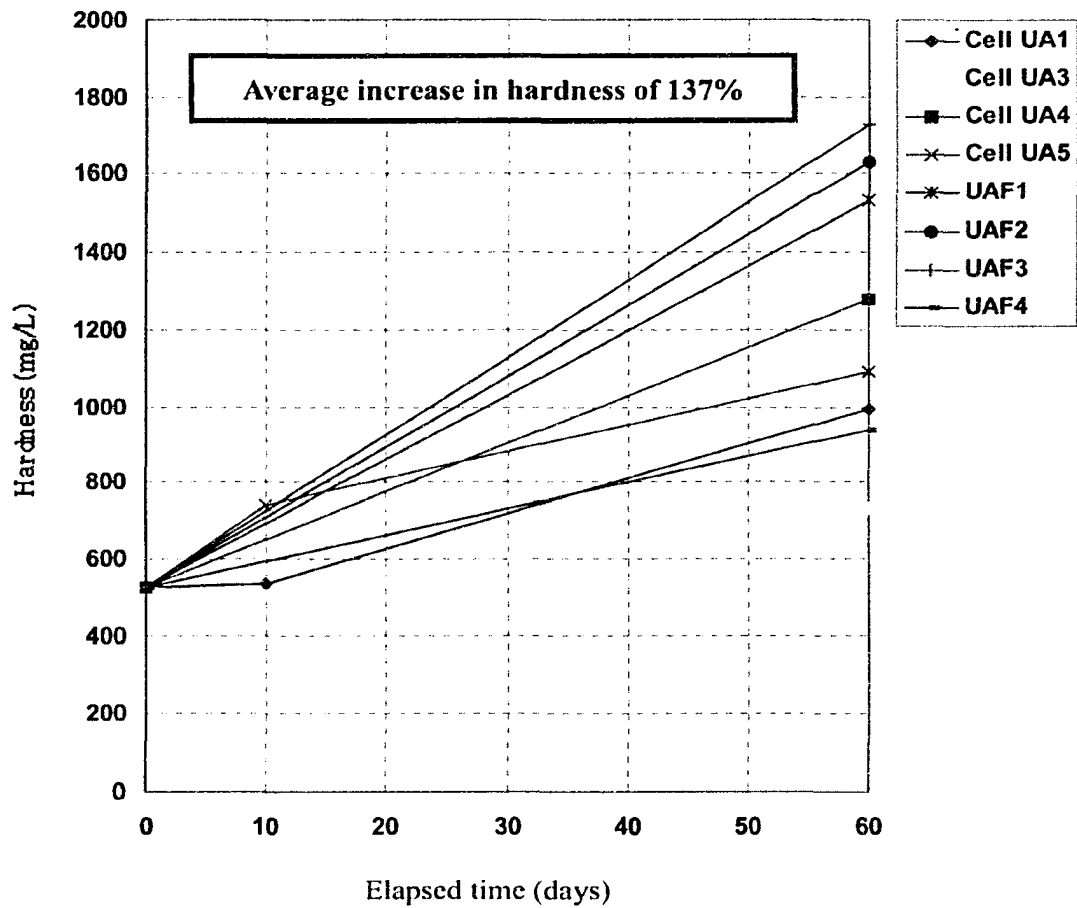
Figure 4.15 Elevated hardness in all the reservoirs during the diffusion process
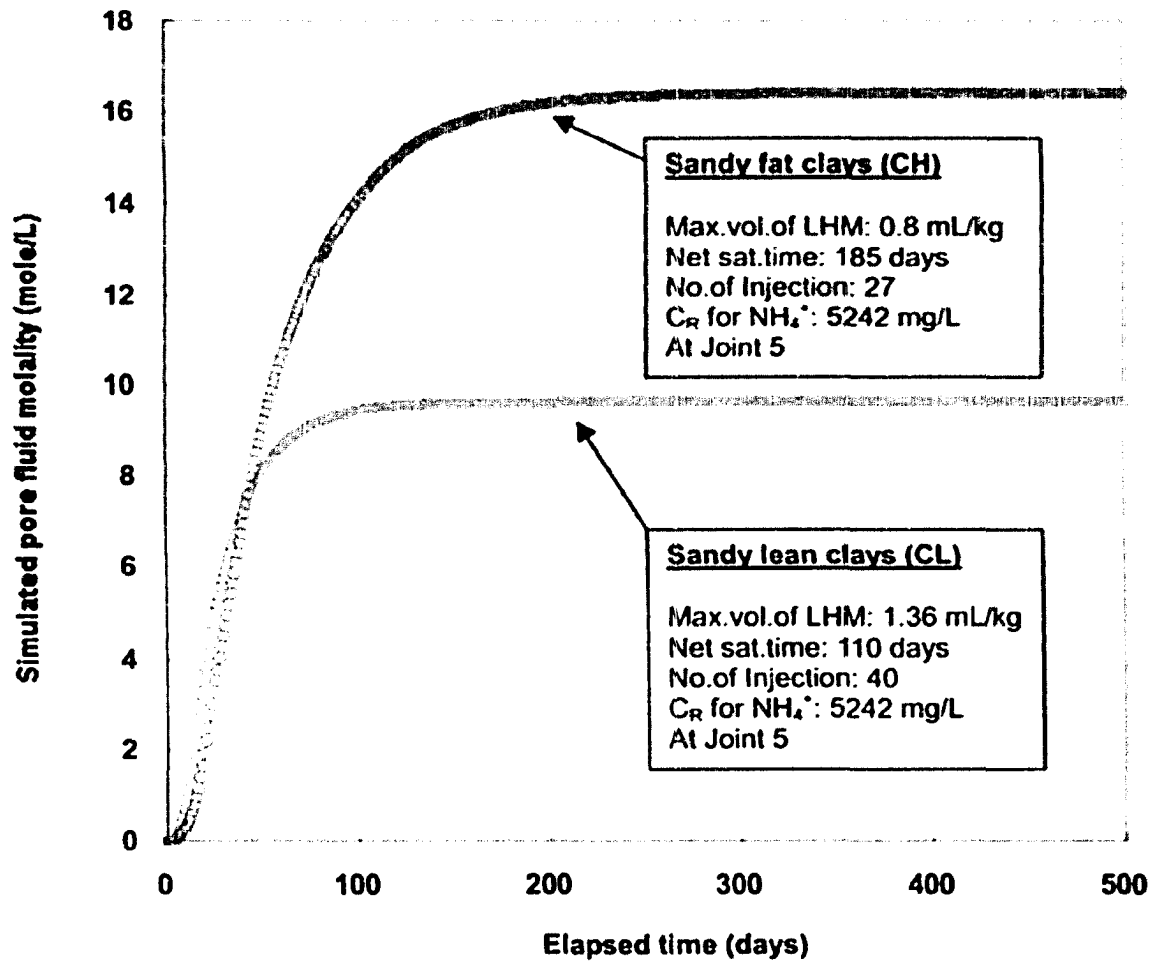
Figure 4.16 Prediction for ammonium saturation by 500-day reactive simulation
NOTE: LHM denotes Liquid Hog Manures for the reservoir sources
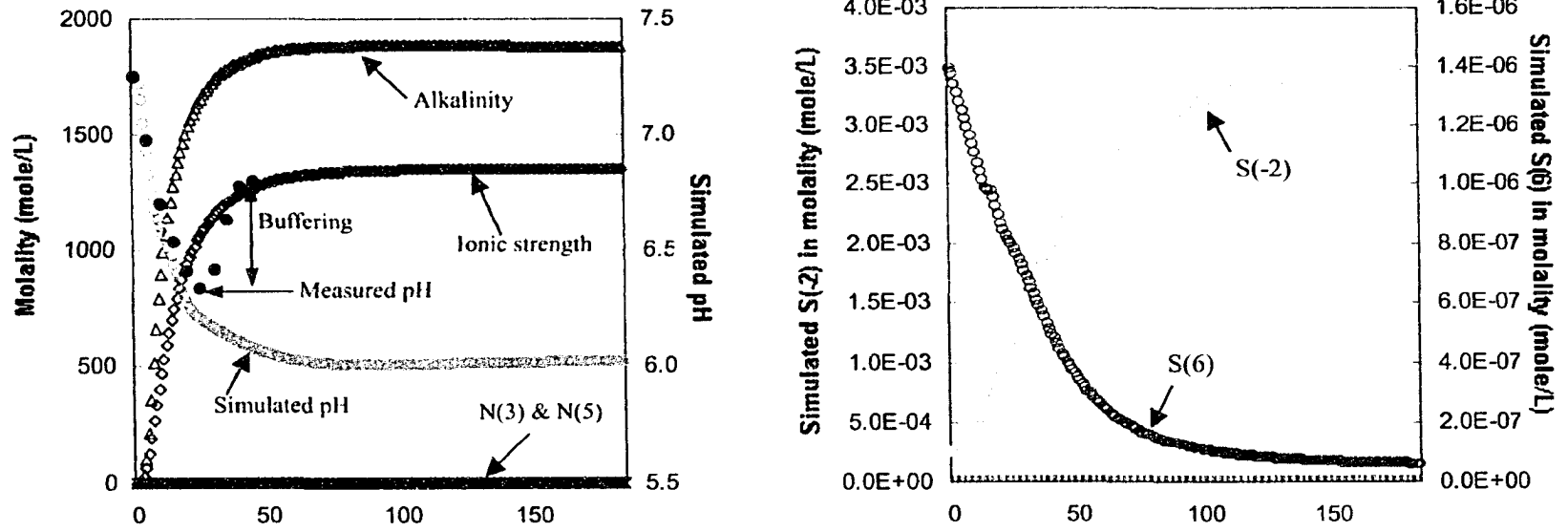
Figure 4.17 Predicted change in pore fluid chemistry

143

CHAPTER 5.0 SUMMARY AND RECOMMENDATIONS

5.1 DIFFUSION OF AMMONIUM THROUGH GLACIAL CLAY SOILS

The main objectives of the research program were (1) to experimentally simulate a soil-liquid manure diffusion under anaerobic conditions, (2) to develop in situ cation exchange geochemical models to simulate the anaerobic RDC experiment, and (3) determine maximum ammonium sorption capacity of the clayey soils.

The key findings are as follows:

- *Synthetic pore fluid chemistry using the anaerobic radial diffusion cell method*

  - Estimated time to reach diffusive equilibrium ranged from 53 to 66 days for sandy lean clay samples (Cell UA1 and 2), and 66 to 109 days for sandy fat clay samples (Cell UA3 to 5).

  - The soil samples with smaller particle size and higher clay fraction had longer diffusive equilibrium times.

  - The pH of the reservoir increased with contact time. The initial pore fluid pH was 7.0

  - Calcite ($CaCO_3$) was dissolved in the pore fluids. The saturation index (SI) of calcite, estimated by PHREEQC speciation calculation, ranged from -2.6 to

-1.61. The value of log P_{CO2} ranged from -1.75 to -1.45 throughout all the cells.

- The effective pore fluid volume ranged from 130 to 170 mL. This estimation is based on mass balance equations that include 0.01% to 0.07% of the evaporation loss and 0.38% of measurement loss.

● *Reservoir monitoring during ammonium diffusion*

- Ammonium, the most reduced form of nitrogen compounds, was not oxidized to nitrate and nitrite in all of the diffusion cells. This is the key evidence that the anaerobic environment in the diffusion cells was maintained.

- The anaerobic chamber in which sufficient argon gas is supplied can be one of the cost-effective ways to create an anaerobic environment in a laboratory.

- The measured reservoir pH rapidly dropped from 7.9 to 6.2 during the first 40 days elapsed and then increased to 6.6 for the remaining 20 days

- Ammonium diffusion caused by chemical potential resulted in a redistribution of major cations and anions in the pore fluid. Chloride (Cl') played a key role in achieving charge balance during the ammonium diffusion.

- The extracted calcium and magnesium from the soils substantially increased the hardness in the reservoir by up to 137%. Sulfate reduction occurred in the reservoir after approximately 40 days also causing the pH of the reservoir to increase.

- Inverse diffusion of the excess calcium and magnesium caused these elements to pair with chloride as $CaCl_2$ and $MgCl_2$ in the reservoir.

- *Diffusion controlled adsorption and desorption with cation exchange*

  - Linear ammonium and potassium adsorption isotherms (R^2=99%) were developed in terms of the equilibrium activity of the reservoir. High cation exchange capacity and diffusion-controlled adsorption primarily affected the linearity of ammonium and potassium adsorption isotherms.

  - The clay-rich soil samples selectively adsorbed and/or desorbed major cations. The competition for the limited adsorption sites depended on constituent mole fraction, ionic size, and ionic charge. In particular, ammonium predominated at the adsorption sites because ammonium with a high mole fraction in the source.

  - The ammonium adsorption was a function of diffusion time, a result also known as the diffusion-controlled adsorption process.

  - The dilution effect would be influenced by the high CEC soil sample and the small volume of the injected liquid manure.

- *Geochemical mix model for anaerobic RDC method*

  - The SIMPLE MIX MODEL adequately simulated the linear ammonium adsorption at the low dissolved ammonium concentration (<30mM).

  - The total adsorbed ammonium both from the experiment (5.7 mmol/cell) and from the lower limit simulation (6.2 mmol/cell).

  - The estimated distribution coefficient, K_d, for ammonium ranged from 0.3 to 0.4 L/kg under anaerobic conditions and diffusion In addition to high CEC.

  - According to the MIX MODEL results, the predicted liquid manure volumes for ammonium saturation were 1.0 to 1.4 mL/g of soils (706 to 1010 mL/Cell,

dilution effect was considered).

- The predicted number of injections ranged from 35 to 40 for sandy lean clays (Cell UA1 and 2) and from 43 to 51 for sandy fat clay samples.

- The adsorptive ammonium required for saturation ranged from 0.3 to 0.5 mol/kg (input NH_4^+ concentration: 5242 mg/L)

5.2 REACTIVE TRANSPORT MODELING USING THE ANAEROBIC RADIAL DIFFUSION CELL METHOD

The aim of this research was to develop a reactive transport model accounting for radial diffusion and exchange reactions in order to investigate and predict net ammonium adsorption capacity and change in pore fluid chemistry. The geochemical environment in the subsurface of EMS facilities should be taken into consideration in the reactive model. The developed model would also be applicable for other exchange reaction problems based on a radial diffusion cell method.

The key findings are as follows:

- The proposed effective diffusion coefficients for chloride ranged from 5.17×10^{-10} to 6.67×10^{-10} m²/sec for sandy lean clay and 2.80×10^{-10} to 2.85×10^{-10} m²/sec for sandy fat clay samples, collected in Ponoka, Alberta.

- The three-dimensional RDC experiment suppressed the radial effect below the central reservoir level according to the three-dimensional radial diffusion simulation. The weakened radial effect could prolong equilibrium time.

- The three-dimensional radial diffusion modeling provided an ammonium

147

effective diffusion coefficient of 2.29×10^{-10} m²/sec by excluding advection and dispersion in both the experiment and the simulation.

- The reactive ammonium diffusion successfully reflected not only the symmetrical radial effect, but also ammonium adsorption resulting from exchange reactions

- During the unreactive modeling little ammonium was attenuated and equilibrated at 4681 to 4728 mg/L after 100-days given a source concentration of ammonium of 5242 mg/L.

- During the reactive transport modeling, ammonium equilibrated from 2411 to 2988 mg/L through the porous media (32.5 to 12.5 mm from the source) given a source concentration of ammonium was 5242 mg/L

- Unlike the unreactive modeling, the reactive transport analysis embodied NH_4-K-Na diffusion under competition in the pore fluid. Changes in the pore fluid concentration ratio for ammonium ($C_{NH4}/C_{0,NH4}$) ranged from 582 to 470 corresponding to distance of 12.5 and 32.5 mm from the source

- In the case of potassium, the value of $C_K/C_{0,K}$ ratio was 39 to 84 and the ratio for sodium, $C_{Na}/C_{0,Na}$, was 2.7 to 6.8 through the porous media. The equilibrium pore fluid concentrations for potassium ($C_{0,K}$) and sodium ($C_{0,Na}$) were 10 and 28 mg/L, respectively.

- The maximum effective exchangeable layer was approximately 17.5 mm thick from the source reservoir. As ammonium ions diffused through the porous media, ammonium displaced calcium and magnesium from the sorption sites to a distance of 12.5 mm from the source. After 24-days of diffusion, the

148

magnesium extraction layer extended over 17.5 mm in ammonium diffusive transport.

- The volumes of the liquid hog manure predicted to achieve full ammonium saturation was 0.8 mL/g for sandy lean clay samples (Cell UA1 and 2), and 1.27 to 1.36 mL/g for sandy fat clay samples (Cell UA3, 4, and 5). Thus, the net amounts of ammonium able to be adsorbed were 0.23 mol/kg for sandy lean clay samples, and 0.38 mol/kg for sandy fat clay samples.

- The simulated net diffusion time to saturate the soil with ammonium ranged from 110 to 185 days given that the initial ammonium concentration at the source was set to 5142 mg/L.

- The reactive modeling with transient diffusion satisfied the key requirements to describe the geochemical environment in EMS subsurface including: (1) anaerobic condition, (2) diffusion controlled adsorption, (3) cation exchange and (4) competition.

5.3 RECOMMENDATIONS

- Ammonium saturation predicted by the MIX MODEL and reactive transport modeling need to be compared with the required maximum volume of liquid manure obtained by a radial diffusion cell method under anaerobic conditions. The predicted successive number of injections for the liquid manure into the cell should be taken into account as well.

- The ammonium adsorption isotherm needs to be determined after the completion of ammonium saturation using the anaerobic radial diffusion cell method. The Langmuir

149

isotherm will be evaluated for accuracy based on the distribution coefficients for the full-scale adsorption of ammonium.

- The desorption process of ammonium is recommended after full ammonium saturation is achieved in order to obtain the net adsorption capacity at the full-scale.

- Further study for change in selectivity coefficient with diffusion time is required for the reactive transport model for a radial diffusion cell method.

150

APPENDIX A. Experimental Results

A-1 Mass balance calculation- Routine measurement

Cell UA1 to Cell UA5 (from page 161 to 165)

Cell UA1 (unit: g)

Days	W	Evp	Af mea W.	Mea. LS	WA	Mea. New W	Actual WA	Af mea W. 2	Mea. LS. 2	Res. Water	Water into soil
1	1710.83	0.00	1710.73	0.10	0.00	1710.73	0.00	1710.73	0.00	20.00	0.00
2	1710.74	-0.01	1710.72	0.02	7.00	1717.71	6.99	1717.63	0.08	26.99	6.99
3	1717.61	0.02	1717.49	0.12	0.00	1717.49	0.00	1717.49	0.00	26.99	0.00
4	1717.52	-0.03	1717.45	0.07	0.00	1717.45	0.00	1717.45	0.00	26.99	0.00
6	1717.43	0.02	1717.30	0.13	0.00	1717.30	0.00	1717.30	0.00	26.99	0.00
7	1717.30	0.00	1717.17	0.13	0.00	1717.17	0.00	1717.17	0.00	26.99	0.00
8	1717.18	-0.01	1717.09	0.09	0.00	1717.09	0.00	1717.09	0.00	26.99	0.00
9	1717.13	-0.04	1717.00	0.13	0.00	1717.00	0.00	1717.00	0.00	26.99	0.00
10	1716.98	0.02	1716.83	0.15	0.00	1716.83	0.00	1716.83	0.00	26.99	0.00
11	1716.84	-0.01	1716.76	0.08	0.00	1716.76	0.00	1716.76	0.00	26.99	0.00
13	1716.74	0.02	1716.71	0.03	0.00	1716.71	0.00	1716.71	0.00	26.99	0.00
14	1716.69	0.02	1716.60	0.09	0.00	1716.60	0.00	1716.60	0.00	26.99	0.00
15	1716.58	0.02	1716.45	0.13	0.00	1716.45	0.00	1716.45	0.00	26.99	0.00
16	1716.46	-0.01	1716.30	0.16	0.00	1716.30	0.00	1716.30	0.00	26.99	0.00
17	1716.33	-0.03	1716.09	0.24	0.00	1716.09	0.00	1716.09	0.00	26.99	0.00
18	1716.09	0.00	1716.00	0.09	0.00	1716.00	0.00	1716.00	0.00	26.99	0.00
20	1715.98	0.02	1715.87	0.11	5.00	1720.87	5.00	1720.71	0.16	31.99	5.00
21	1720.72	-0.01	1720.58	0.14	0.00	1720.58	0.00	1720.58	0.00	31.99	0.00
22	1720.57	0.01	1720.40	0.17	0.00	1720.40	0.00	1720.40	0.00	31.99	0.00
23	1720.42	-0.02	1720.25	0.17	0.00	1720.25	0.00	1720.25	0.00	31.99	0.00
24	1720.27	-0.02	1720.13	0.14	0.00	1720.13	0.00	1720.13	0.00	31.99	0.00
25	1720.09	0.04	1719.94	0.15	0.00	1719.94	0.00	1719.94	0.00	31.99	0.00
26	1719.95	-0.01	1719.82	0.13	0.00	1719.82	0.00	1719.82	0.00	31.99	0.00
27	1719.80	0.02	1719.64	0.16	0.00	1719.64	0.00	1719.64	0.00	31.99	0.00
28	1719.64	0.00	1719.49	0.15	0.00	1719.49	0.00	1719.49	0.00	31.99	0.00
29	1719.50	-0.01	1719.30	0.20	0.00	1719.30	0.00	1719.30	0.00	31.99	0.00
30	1719.33	-0.03	1719.18	0.15	0.00	1719.18	0.00	1719.18	0.00	31.99	0.00
31	1719.20	-0.02	1719.10	0.10	0.00	1719.10	0.00	1719.10	0.00	31.99	0.00
32	1719.09	0.01	1718.88	0.21	0.00	1718.88	0.00	1718.88	0.00	31.99	0.00
36	1718.89	-0.01	1718.71	0.18	2.50	1721.22	2.51	1721.08	0.14	34.50	2.51
37	1721.07	0.01	1720.96	0.11	0.00	1720.96	0.00	1720.96	0.00	34.50	0.00
38	1720.94	0.02	1720.82	0.12	0.00	1720.82	0.00	1720.82	0.00	34.50	0.00
40	1720.83	-0.01	1720.72	0.11	0.00	1720.72	0.00	1720.72	0.00	34.50	0.00
42	1720.70	0.02	1720.46	0.24	0.00	1720.46	0.00	1720.46	0.00	34.50	0.00
43	1720.47	-0.01	1720.27	0.20	0.00	1720.27	0.00	1720.27	0.00	34.50	0.00
44	1720.23	0.04	1720.08	0.15	0.00	1720.08	0.00	1720.08	0.00	34.50	0.00
46	1720.15	-0.07	1719.97	0.18	0.00	1719.97	0.00	1719.97	0.00	34.50	0.00
49	1719.97	0.00	1719.85	0.12	0.00	1719.85	0.00	1719.85	0.00	34.50	0.00
51	1719.79	0.06	1719.56	0.23	0.00	1719.56	0.00	1719.56	0.00	34.50	0.00
54	1719.48	0.08	1719.42	0.06	0.00	1719.42	0.00	1719.42	0.00	34.50	0.00
55	1719.47	-0.05	1719.35	0.12	0.00	1719.35	0.00	1719.35	0.00	34.50	0.00
57	1719.40	-0.05	1719.29	0.11	2.00	1721.21	1.92	1721.14	0.07	36.42	1.92
59	1721.07	0.07	1720.94	0.13	0.00	1720.94	0.00	1720.94	0.00	36.42	0.00
61	1720.96	-0.02	1720.82	0.14	0.00	1720.82	0.00	1720.82	0.00	36.42	0.00
64	1720.77	0.05	1720.68	0.09	0.00	1720.68	0.00	1720.68	0.00	36.42	0.00
65	1720.61	0.07	1720.53	0.08	0.00	1720.53	0.00	1720.53	0.00	36.42	0.00

153

Cell UA2 (unit: g)

Days	W	Evp	Af mea W.	Mea. LS	WA	Mea. New W	Actual WA	Af mea W. 2	Mea. LS. 2	Res. Water	Water into soil
1	1761.63	0.00	1761.52	0.11	0.00	1761.52	0.00	1761.52	0.00	20.00	0.00
2	1761.52	0.00	1761.47	0.05	0.00	1761.47	0.00	1761.47	0.00	20.00	0.00
3	1761.44	0.03	1761.40	0.04	2.00	1763.39	1.99	1763.36	0.03	21.99	1.99
4	1763.35	0.01	1763.28	0.07	0.00	1763.28	0.00	1763.28	0.00	21.99	0.00
6	1763.24	0.04	1763.16	0.08	0.00	1763.16	0.00	1763.16	0.00	21.99	0.00
7	1763.13	0.03	1762.98	0.15	0.00	1762.98	0.00	1762.98	0.00	21.99	0.00
8	1762.99	-0.01	1762.91	0.08	0.00	1762.91	0.00	1762.91	0.00	21.99	0.00
9	1762.91	0.00	1762.82	0.09	0.00	1762.82	0.00	1762.82	0.00	21.99	0.00
10	1762.82	0.00	1762.67	0.15	0.00	1762.67	0.00	1762.67	0.00	21.99	0.00
11	1762.68	-0.01	1762.55	0.13	0.00	1762.55	0.00	1762.55	0.00	21.99	0.00
13	1762.54	0.01	1762.41	0.13	0.00	1762.41	0.00	1762.41	0.00	21.99	0.00
14	1762.40	0.01	1762.30	0.10	0.00	1762.30	0.00	1762.30	0.00	21.99	0.00
15	1762.26	0.04	1762.15	0.11	0.00	1762.15	0.00	1762.15	0.00	21.99	0.00
16	1762.14	0.01	1762.03	0.11	0.00	1762.03	0.00	1762.03	0.00	21.99	0.00
17	1762.03	0.00	1761.80	0.23	0.00	1761.80	0.00	1761.80	0.00	21.99	0.00
18	1761.79	0.01	1761.66	0.13	0.00	1761.66	0.00	1761.66	0.00	21.99	0.00
20	1761.67	-0.01	1761.56	0.11	4.00	1765.56	4.00	1765.46	0.10	25.99	4.00
21	1765.48	-0.02	1765.28	0.20	0.00	1765.28	0.00	1765.28	0.00	25.99	0.00
22	1765.28	0.00	1765.17	0.11	0.00	1765.17	0.00	1765.17	0.00	25.99	0.00
23	1765.15	0.02	1764.96	0.19	0.00	1764.96	0.00	1764.96	0.00	25.99	0.00
24	1764.93	0.03	1764.82	0.11	0.00	1764.82	0.00	1764.82	0.00	25.99	0.00
25	1764.86	-0.04	1764.68	0.18	0.00	1764.68	0.00	1764.68	0.00	25.99	0.00
26	1764.67	0.01	1764.56	0.11	0.00	1764.56	0.00	1764.56	0.00	25.99	0.00
27	1764.56	0.00	1764.44	0.12	0.00	1764.44	0.00	1764.44	0.00	25.99	0.00
28	1764.46	-0.02	1764.34	0.12	0.00	1764.34	0.00	1764.34	0.00	25.99	0.00
29	1764.33	0.01	1764.20	0.13	0.00	1764.20	0.00	1764.20	0.00	25.99	0.00
30	1764.23	-0.03	1764.06	0.17	0.00	1764.06	0.00	1764.06	0.00	25.99	0.00
31	1764.06	0.00	1763.92	0.14	0.00	1763.92	0.00	1763.92	0.00	25.99	0.00
32	1763.92	0.00	1763.79	0.13	0.00	1763.79	0.00	1763.79	0.00	25.99	0.00
36	1763.75	0.04	1763.55	0.20	2.50	1766.08	2.53	1765.96	0.12	28.52	2.53
37	1765.98	-0.02	1765.83	0.15	0.00	1765.83	0.00	1765.83	0.00	28.52	0.00
38	1765.83	0.00	1765.72	0.11	0.00	1765.72	0.00	1765.72	0.00	28.52	0.00
40	1765.71	0.01	1765.56	0.15	0.00	1765.56	0.00	1765.56	0.00	28.52	0.00
42	1765.58	-0.02	1765.40	0.18	0.00	1765.40	0.00	1765.40	0.00	28.52	0.00
43	1765.40	0.00	1765.11	0.29	0.00	1765.11	0.00	1765.11	0.00	28.52	0.00
44	1765.08	0.03	1764.88	0.20	0.00	1764.88	0.00	1764.88	0.00	28.52	0.00
46	1764.89	-0.01	1764.67	0.22	0.00	1764.67	0.00	1764.67	0.00	28.52	0.00
49	1764.66	0.01	1764.57	0.09	0.00	1764.57	0.00	1764.57	0.00	28.52	0.00
51	1764.50	0.07	1764.31	0.19	0.00	1764.31	0.00	1764.31	0.00	28.52	0.00
54	1764.27	0.04	1764.02	0.25	0.00	1764.02	0.00	1764.02	0.00	28.52	0.00
55	1764.08	-0.06	1763.93	0.15	0.00	1763.93	0.00	1763.93	0.00	28.52	0.00
57	1763.93	0.00	1763.71	0.22	4.00	1767.65	3.94	1767.56	0.09	32.46	3.94
59	1767.45	0.11	1767.40	0.05	0.00	1767.40	0.00	1767.40	0.00	32.46	0.00
61	1767.40	0.00	1767.02	0.38	0.00	1767.02	0.00	1767.02	0.00	32.46	0.00
64	1766.96	0.06	1766.86	0.10	0.00	1766.86	0.00	1766.86	0.00	32.46	0.00
65	1766.82	0.04	1766.75	0.07	0.00	1766.75	0.00	1766.75	0.00	32.46	0.00

154

Cell UA3 (unit: g)

Days	W	Evp	Af mea W.	Mea. LS	WA	Mea. New W	Actual WA	Af mea W. 2	Mea. LS. 2	Res. Water	Water into soil
1	1637.23	0	1637.12	0.11	0	1637.12	0	1637.12	0	20	0
2	1637.13	-0.01	1637.06	0.07	7	1644.02	6.96	1643.95	0.07	26.96	6.96
3	1643.94	0.01	1643.83	0.11	0	1643.83	0	1643.83	0	26.96	0
4	1643.85	-0.02	1643.78	0.07	5	1648.8	5.02	1648.77	0.03	31.98	5.02
6	1648.74	0.03	1648.62	0.12	0	1648.62	0	1648.62	0	31.98	0
7	1648.63	-0.01	1648.51	0.12	0	1648.51	0	1648.51	0	31.98	0
8	1648.52	-0.01	1648.4	0.12	0	1648.4	0	1648.4	0	31.98	0
9	1648.43	-0.03	1648.3	0.13	0	1648.3	0	1648.3	0	31.98	0
10	1648.27	0.03	1648.12	0.15	0	1648.12	0	1648.12	0	31.98	0
11	1648.13	-0.01	1648.02	0.11	0	1648.02	0	1648.02	0	31.98	0
13	1648.02	0	1647.93	0.09	0	1647.93	0	1647.93	0	31.98	0
14	1647.92	0.01	1647.83	0.09	0	1647.83	0	1647.83	0	31.98	0
15	1647.8	0.03	1647.68	0.12	0	1647.68	0	1647.68	0	31.98	0
16	1647.7	-0.02	1647.57	0.13	0	1647.57	0	1647.57	0	31.98	0
17	1647.56	0.01	1647.43	0.13	0	1647.43	0	1647.43	0	31.98	0
18	1647.43	0	1647.29	0.14	0	1647.29	0	1647.29	0	31.98	0
20	1647.31	-0.02	1647.17	0.14	5	1652.19	5.02	1652.1	0.09	37	5.02
21	1652.1	0	1651.93	0.17	0	1651.93	0	1651.93	0	37	0
22	1651.93	0	1651.75	0.18	0	1651.75	0	1651.75	0	37	0
23	1651.77	-0.02	1651.65	0.12	0	1651.65	0	1651.65	0	37	0
24	1651.62	0.03	1651.49	0.13	0	1651.49	0	1651.49	0	37	0
25	1651.45	0.04	1651.33	0.12	0	1651.33	0	1651.33	0	37	0
26	1651.33	0	1651.2	0.13	0	1651.2	0	1651.2	0	37	0
27	1651.2	0	1651.04	0.16	0	1651.04	0	1651.04	0	37	0
28	1651.04	0	1650.9	0.14	0	1650.9	0	1650.9	0	37	0
29	1650.88	0.02	1650.73	0.15	0	1650.73	0	1650.73	0	37	0
30	1650.72	0.01	1650.6	0.12	0	1650.6	0	1650.6	0	37	0
31	1650.63	-0.03	1650.52	0.11	0	1650.52	0	1650.52	0	37	0
32	1650.53	-0.01	1650.35	0.18	0	1650.35	0	1650.35	0	37	0
36	1650.35	0	1650.24	0.11	3	1653.24	3	1653.08	0.16	40	3
37	1653.09	-0.01	1652.95	0.14	0	1652.95	0	1652.95	0	40	0
38	1652.96	-0.01	1652.85	0.11	0	1652.85	0	1652.85	0	40	0
40	1652.65	0.2	1652.69	-0.04	0	1652.69	0	1652.69	0	40	0
42	1652.67	0.02	1652.51	0.16	0	1652.51	0	1652.51	0	40	0
43	1652.53	-0.02	1652.33	0.2	0	1652.33	0	1652.33	0	40	0
44	1652.28	0.05	1651.98	0.3	0	1651.98	0	1651.98	0	40	0
46	1652.02	-0.04	1651.79	0.23	0	1651.79	0	1651.79	0	40	0
49	1651.77	0.02	1651.69	0.08	0	1651.69	0	1651.69	0	40	0
51	1651.62	0.07	1651.31	0.31	0	1651.31	0	1651.31	0	40	0
54	1651.3	0.01	1651.1	0.2	0	1651.1	0	1651.1	0	40	0
55	1651.15	-0.05	1650.87	0.28	0	1650.87	0	1650.87	0	40	0
57	1650.84	0.03	1650.76	0.08	4	1654.59	3.83	1654.45	0.14	43.83	3.83
59	1654.35	0.1	1654.23	0.12	0	1654.23	0	1654.23	0	43.83	0
61	1654.19	0.04	1654	0.19	0	1654	0	1654	0	43.83	0
64	1653.95	0.05	1653.85	0.1	0	1653.85	0	1653.85	0	43.83	0
65	1653.8	0.05	1653.74	0.06	0	1653.74	0	1653.74	0	43.83	0

155

Cell UA4 (unit: g)

Days	W	Evp	Af mea W.	Mea. LS	WA	Mea. New W	Actual WA	Af mea W. 2	Mea. LS. 2	Res. Water	Water into soil
1	1637.93	0.00	1637.87	0.06	0.00	1637.87	0.00	1637.87	0.00	20.00	0.00
2	1637.86	0.01	1637.80	0.06	0.00	1637.80	0.00	1637.80	0.00	20.00	0.00
3	1637.78	0.02	1637.69	0.09	0.00	1637.69	0.00	1637.69	0.00	20.00	0.00
4	1637.69	0.00	1637.64	0.05	3.00	1640.66	3.02	1640.60	0.06	23.02	3.02
6	1640.58	0.02	1640.41	0.17	0.00	1640.41	0.00	1640.41	0.00	23.02	0.00
7	1640.43	-0.02	1640.31	0.12	0.00	1640.31	0.00	1640.31	0.00	23.02	0.00
8	1640.32	-0.01	1640.17	0.15	0.00	1640.17	0.00	1640.17	0.00	23.02	0.00
9	1640.18	-0.01	1640.11	0.07	0.00	1640.11	0.00	1640.11	0.00	23.02	0.00
10	1640.09	0.02	1640.00	0.09	0.00	1640.00	0.00	1640.00	0.00	23.02	0.00
11	1640.04	-0.04	1639.92	0.12	0.00	1639.92	0.00	1639.92	0.00	23.02	0.00
13	1639.93	-0.01	1639.84	0.09	0.00	1639.84	0.00	1639.84	0.00	23.02	0.00
14	1639.84	0.00	1639.71	0.13	7.00	1646.71	7.00	1646.63	0.08	30.02	7.00
15	1646.60	0.03	1646.46	0.14	0.00	1646.46	0.00	1646.46	0.00	30.02	0.00
16	1646.46	0.00	1646.33	0.13	0.00	1646.33	0.00	1646.33	0.00	30.02	0.00
17	1646.34	-0.01	1646.20	0.14	0.00	1646.20	0.00	1646.20	0.00	30.02	0.00
18	1646.20	0.00	1646.05	0.15	0.00	1646.05	0.00	1646.05	0.00	30.02	0.00
20	1646.03	0.02	1645.88	0.15	0.00	1645.88	0.00	1645.88	0.00	30.02	0.00
21	1645.87	0.01	1645.75	0.12	0.00	1645.75	0.00	1645.75	0.00	30.02	0.00
22	1645.72	0.03	1645.60	0.12	0.00	1645.60	0.00	1645.60	0.00	30.02	0.00
23	1645.60	0.00	1645.47	0.13	0.00	1645.47	0.00	1645.47	0.00	30.02	0.00
24	1645.48	-0.01	1645.34	0.14	0.00	1645.34	0.00	1645.34	0.00	30.02	0.00
25	1645.36	-0.02	1645.26	0.10	0.00	1645.26	0.00	1645.26	0.00	30.02	0.00
26	1645.28	-0.02	1645.16	0.12	0.00	1645.16	0.00	1645.16	0.00	30.02	0.00
27	1645.16	0.00	1645.06	0.10	5.00	1649.97	4.91	1649.87	0.10	34.93	4.91
28	1649.92	-0.05	1649.73	0.19	0.00	1649.73	0.00	1649.73	0.00	34.93	0.00
29	1649.74	-0.01	1649.62	0.12	0.00	1649.62	0.00	1649.62	0.00	34.93	0.00
30	1649.61	0.01	1649.48	0.13	0.00	1649.48	0.00	1649.48	0.00	34.93	0.00
31	1649.51	-0.03	1649.31	0.20	0.00	1649.31	0.00	1649.31	0.00	34.93	0.00
32	1649.33	-0.02	1649.15	0.18	0.00	1649.15	0.00	1649.15	0.00	34.93	0.00
36	1649.16	-0.01	1649.03	0.13	2.00	1651.00	1.97	1650.90	0.10	36.90	1.97
37	1650.89	0.01	1650.77	0.12	0.00	1650.77	0.00	1650.77	0.00	36.90	0.00
38	1650.78	-0.01	1650.67	0.11	0.00	1650.67	0.00	1650.67	0.00	36.90	0.00
40	1650.65	0.02	1650.54	0.11	0.00	1650.54	0.00	1650.54	0.00	36.90	0.00
42	1650.51	0.03	1650.37	0.14	0.00	1650.37	0.00	1650.37	0.00	36.90	0.00
43	1650.39	-0.02	1650.22	0.17	0.00	1650.22	0.00	1650.22	0.00	36.90	0.00
44	1650.20	0.02	1649.99	0.21	0.00	1649.99	0.00	1649.99	0.00	36.90	0.00
46	1650.00	-0.01	1649.77	0.23	0.00	1649.77	0.00	1649.77	0.00	36.90	0.00
49	1649.75	0.02	1649.66	0.09	0.00	1649.66	0.00	1649.66	0.00	36.90	0.00
51	1649.63	0.03	1649.44	0.19	0.00	1649.44	0.00	1649.44	0.00	36.90	0.00
54	1649.42	0.02	1649.23	0.19	0.00	1649.23	0.00	1649.23	0.00	36.90	0.00
55	1649.28	-0.05	1649.10	0.18	0.00	1649.10	0.00	1649.10	0.00	36.90	0.00
57	1649.09	0.01	1648.92	0.17	4.00	1652.79	3.87	1652.68	0.11	40.77	3.87
59	1652.58	0.10	1652.56	0.02	0.00	1652.56	0.00	1652.56	0.00	40.77	0.00
61	1652.52	0.04	1652.34	0.18	0.00	1652.34	0.00	1652.34	0.00	40.77	0.00
64	1652.32	0.02	1652.24	0.08	0.00	1652.24	0.00	1652.24	0.00	40.77	0.00
65	1652.24	0.00	1652.15	0.09	0.00	1652.15	0.00	1652.15	0.00	40.77	0.00

156

Cell UA5 (Unit: g)

Days	W	Evp	Af mea W.	Mea. LS	WA	Mea. New W	Actual WA	Af mea W. 2	Mea. LS. 2	Res. Water	Water into soil
1	1693.43	0.00	1693.37	0.06	0.00	1693.37	0.00	1693.37	0.00	20.00	0.00
2	1693.39	-0.02	1693.34	0.05	0.00	1693.34	0.00	1693.34	0.00	20.00	0.00
3	1693.33	0.01	1693.27	0.06	0.00	1693.27	0.00	1693.27	0.00	20.00	0.00
4	1693.30	-0.03	1693.22	0.08	0.00	1693.22	0.00	1693.22	0.00	20.00	0.00
6	1693.22	0.00	1693.08	0.14	0.00	1693.08	0.00	1693.08	0.00	20.00	0.00
7	1693.08	0.00	1692.94	0.14	0.00	1692.94	0.00	1692.94	0.00	20.00	0.00
8	1692.86	0.08	1692.84	0.02	0.00	1692.84	0.00	1692.84	0.00	20.00	0.00
9	1692.83	0.01	1692.74	0.09	0.00	1692.74	0.00	1692.74	0.00	20.00	0.00
10	1692.72	0.02	1692.64	0.08	0.00	1692.64	0.00	1692.64	0.00	20.00	0.00
11	1692.69	-0.05	1692.56	0.13	0.00	1692.56	0.00	1692.56	0.00	20.00	0.00
13	1692.58	-0.02	1692.44	0.14	0.00	1692.44	0.00	1692.44	0.00	20.00	0.00
14	1692.44	0.00	1692.34	0.10	0.00	1692.34	0.00	1692.34	0.00	20.00	0.00
15	1692.32	0.02	1692.23	0.09	0.00	1692.23	0.00	1692.23	0.00	20.00	0.00
16	1692.24	-0.01	1692.19	0.05	0.00	1692.19	0.00	1692.19	0.00	20.00	0.00
17	1692.16	0.03	1692.02	0.14	0.00	1692.02	0.00	1692.02	0.00	20.00	0.00
18	1692.03	-0.01	1691.90	0.13	0.00	1691.90	0.00	1691.90	0.00	20.00	0.00
20	1691.89	0.01	1691.80	0.09	8.00	1699.87	8.07	1699.75	0.12	28.07	8.07
21	1699.78	-0.03	1699.60	0.18	0.00	1699.60	0.00	1699.60	0.00	28.07	0.00
22	1699.59	0.01	1699.45	0.14	0.00	1699.45	0.00	1699.45	0.00	28.07	0.00
23	1699.45	0.00	1699.11	0.34	0.00	1699.11	0.00	1699.11	0.00	28.07	0.00
24	1699.12	-0.01	1698.97	0.15	0.00	1698.97	0.00	1698.97	0.00	28.07	0.00
25	1698.98	-0.01	1698.87	0.11	0.00	1698.87	0.00	1698.87	0.00	28.07	0.00
26	1698.86	0.01	1698.73	0.13	0.00	1698.73	0.00	1698.73	0.00	28.07	0.00
27	1698.75	-0.02	1698.63	0.12	0.00	1698.63	0.00	1698.63	0.00	28.07	0.00
28	1698.62	0.01	1698.47	0.15	0.00	1698.47	0.00	1698.47	0.00	28.07	0.00
29	1698.47	0.00	1698.32	0.15	0.00	1698.32	0.00	1698.32	0.00	28.07	0.00
30	1698.33	-0.01	1698.21	0.12	0.00	1698.21	0.00	1698.21	0.00	28.07	0.00
31	1698.24	-0.03	1698.01	0.23	0.00	1698.01	0.00	1698.01	0.00	28.07	0.00
32	1698.05	-0.04	1697.88	0.17	0.00	1697.88	0.00	1697.88	0.00	28.07	0.00
36	1697.86	0.02	1697.68	0.18	7.50	1705.14	7.46	1705.00	0.14	35.53	7.46
37	1704.98	0.02	1704.87	0.11	0.00	1704.87	0.00	1704.87	0.00	35.53	0.00
38	1704.86	0.01	1704.72	0.14	0.00	1704.72	0.00	1704.72	0.00	35.53	0.00
40	1704.75	-0.03	1704.54	0.21	0.00	1704.54	0.00	1704.54	0.00	35.53	0.00
42	1704.55	-0.01	1704.38	0.17	0.00	1704.38	0.00	1704.38	0.00	35.53	0.00
43	1704.41	-0.03	1704.29	0.12	0.00	1704.29	0.00	1704.29	0.00	35.53	0.00
44	1704.24	0.05	1703.96	0.28	0.00	1703.96	0.00	1703.96	0.00	35.53	0.00
46	1703.99	-0.03	1703.76	0.23	0.00	1703.76	0.00	1703.76	0.00	35.53	0.00
49	1703.75	0.01	1703.66	0.09	0.00	1703.66	0.00	1703.66	0.00	35.53	0.00
51	1703.63	0.03	1703.46	0.17	0.00	1703.46	0.00	1703.46	0.00	35.53	0.00
54	1703.43	0.03	1703.30	0.13	0.00	1703.30	0.00	1703.30	0.00	35.53	0.00
55	1703.32	-0.02	1703.10	0.22	0.00	1703.10	0.00	1703.10	0.00	35.53	0.00
57	1703.12	-0.02	1702.97	0.15	7.00	1709.74	6.77	1709.52	0.22	42.30	6.77
59	1709.37	0.15	1709.27	0.10	0.00	1709.27	0.00	1709.27	0.00	42.30	0.00
61	1709.23	0.04	1709.86	-0.63	0.00	1709.86	0.00	1709.86	0.00	42.30	0.00
64	1708.80	1.06	1708.68	0.12	0.00	1708.68	0.00	1708.68	0.00	42.30	0.00
65	1708.65	0.03	1708.58	0.07	0.00	1708.58	0.00	1708.58	0.00	42.30	0.00

157

A-2 Mass balance calculation (Units: concentration: mg/L, Volume: L, Mass: g)

		Diffusive equilibrium			1st injection			sampling @ 10 days				cumulative mass
		meas.conc.	pore vol.	mass in soils	Injec. conc.	Injec. vol.	Injec.mass	meas. conc.	meas. vol.	mass in reser.	mass in soils	10 days
NH_4^+	Cell UA1	1.00	0.13	0.13	5241.51	0.02	106.70	2423.33	0.02	49.98	56.72	56.84
	Cell UA2	1.00	0.13	0.13	5241.51	0.02	105.54	2417.31	0.02	50.08	55.47	55.59
	Cell UA3	1.00	0.17	0.17	5241.51	0.02	106.02	1767.41	0.02	35.16	70.85	71.03
	Cell UA4	1.00	0.17	0.17	5241.51	0.02	105.02	0.00	0.00	0.00	0.00	0.17
	Cell UA5	1.00	0.15	0.15	5241.51	0.02	102.96	1093.49	0.02	21.14	81.82	81.97
K^+	Cell UA1	10	0.13	1.26	1710.00	0.02	34.81	1260.00	0.02	25.99	8.82	10.08
	Cell UA2	10	0.13	1.26	1710.00	0.02	34.43	1340.00	0.02	27.76	6.67	7.93
	Cell UA3	6	0.17	1.02	1710.00	0.02	34.59	1260.00	0.02	25.07	9.52	10.54
	Cell UA4	6	0.17	1.01	1710.00	0.02	34.26	0.00	0.00	0.00	0.00	1.01
	Cell UA5	4	0.15	0.61	1710.00	0.02	33.59	1120.00	0.02	21.65	11.94	12.54
Na^+	Cell UA1	28.00	0.13	3.53	611.00	0.02	12.44	530.00	0.02	10.93	1.51	5.04
	Cell UA2	20.00	0.13	2.51	611.00	0.02	12.30	540.00	0.02	11.19	1.12	3.63
	Cell UA3	20.00	0.17	3.40	611.00	0.02	12.36	1520.00	0.02	30.24	-17.88	-14.48
	Cell UA4	21	0.17	3.53	611.00	0.02	12.24	0.00	0.00	0.00	0.00	3.53
	Cell UA5	20.00	0.15	3.04	611.00	0.02	12.00	510.00	0.02	9.86	2.14	5.18
Ca^{2+}	Cell UA1	16	0.13	2.02	199.00	0.02	4.05	190.00	0.02	3.92	0.13	2.15
	Cell UA2	10.00	0.13	1.26	199.00	0.02	4.01	150.00	0.02	3.11	0.90	2.16
	Cell UA3	13	0.17	2.21	199.00	0.02	4.02	180.00	0.02	3.58	0.44	2.66
	Cell UA4	13	0.17	2.19	199.00	0.02	3.99	0.00	0.00	0.00	0.00	2.19
	Cell UA5	10.00	0.15	1.52	199.00	0.02	3.91	250.00	0.02	4.83	-0.92	0.59
Mg^{2+}	Cell UA1	6	0.13	0.76	6.40	0.02	0.13	15.00	0.02	0.31	-0.18	0.58
	Cell UA2	2.00	0.13	0.25	6.40	0.02	0.13	8.00	0.02	0.17	-0.04	0.21
	Cell UA3	3	0.17	0.51	6.40	0.02	0.13	14.00	0.02	0.28	-0.15	0.36
	Cell UA4	3	0.17	0.50	6.40	0.02	0.13	0.00	0.00	0.00	0.00	0.50
	Cell UA5	2.00	0.15	0.30	6.40	0.02	0.13	28.00	0.02	0.54	-0.42	-0.11

		Diffusive equilibrium			1st injection			sampling @ 10 days				cumulative mass
		meas conc	pore vol	mass in soils	Injec conc	Injec vol	Injec mass	meas conc	meas vol	mass in reser	mass in soils	10 days
Cl	Cell UA1	20	0.13	2.52	1380.00	0.02	28.09	1110.00	0.02	22.89	5.20	7.72
	Cell UA2	20.00	0.13	2.51	1380.00	0.02	27.79	1150.00	0.02	23.82	3.96	6.48
	Cell UA3	20.00	0.17	3.40	1380.00	0.02	27.91	1120.00	0.02	22.28	5.63	9.03
	Cell UA4	20.00	0.17	3.37	1380.00	0.02	27.65	0.00	0.00	0.00	0.00	3.37
	Cell UA5	20.00	0.15	3.04	1380.00	0.02	27.11	1040.00	0.02	20.11	7.00	10.04
PO$_4^{\cdot}$	Cell UA1	1.00	0.13	0.13	1270.00	0.02	25.85	312.75	0.02	6.45	19.40	19.53
	Cell UA2	1.00	0.13	0.13	1270.00	0.02	25.57	282.09	0.02	5.84	19.73	19.85
	Cell UA3	1.00	0.17	0.17	1270.00	0.02	25.69	297.42	0.02	5.92	19.77	19.94
	Cell UA4	1.00	0.17	0.17	1270.00	0.02	25.44	0.00	0.00	0.00	0.00	0.17
	Cell UA5	1.00	0.15	0.15	1270.00	0.02	24.95	144.11	0.02	2.79	22.16	22.31
HCO$_3$	Cell UA1	200	0.13	25.22	14300.00	0.02	291.10	6670.00	0.02	137.57	153.53	178.75
	Cell UA2	200	0.13	25.11	14300.00	0.02	287.94	8920.00	0.02	184.78	103.16	128.27
	Cell UA3	200	0.17	34.03	14300.00	0.02	289.23	6570.00	0.02	130.70	158.53	192.56
	Cell UA4	200	0.17	33.66	14300.00	0.02	286.50	0.00	0.00	0.00	0.00	33.66
	Cell UA5	100	0.15	15.18	14300.00	0.02	280.90	5810.00	0.02	112.32	168.58	183.76
SO$_4^{2\cdot}$	Cell UA1	24	0.13	3.03	9.00	0.02	0.18	3.00	0.02	0.06	0.12	3.15
	Cell UA2	6	0.13	0.75	9.00	0.02	0.18	3.00	0.02	0.06	0.12	0.87
	Cell UA3	16	0.17	2.72	9.00	0.02	0.18	3.00	0.02	0.06	0.12	2.84
	Cell UA4	16	0.17	2.69	9.00	0.02	0.18	0.00	0.00	0.00	0.00	2.69
	Cell UA5	6	0.15	0.91	9.00	0.02	0.18	3.00	0.02	0.06	0.12	1.03

159

A.3 Speciation calculation for pore fluid using PHREEQC

1. INPUT CODE FOR PHREEQC

Table A-4.1 Input data for Cell UA1

INPUT code			G.F.W (g)	Calculated M (mol/L)	PHREEQC M (mol/L)	Validation
SOLUTION #CELL UA1			G.F.W (g)	M (mol/L)	M (mol/L)	
temp	22.87					
pH	7.03					
pe	4.00					
redox	pe					
units	mg/l					
density	1.00					
Cl	20.00		35.4527	5.641E-04	5.644E-04	-0.02%
Ca	16.00		40.0780	3.992E-04	3.994E-04	-0.02%
K	10.00		39.0983	2.558E-04	2.559E-04	-0.03%
Mg	6.00		24.3050	2.469E-04	2.469E-04	-0.01%
Na	28.00		22.9898	1.218E-03	1.219E-03	-0.04%
N(5)	0.60		14.0067	4.284E-05	4.286E-05	-0.03%
S(6)	24.00		96.0636	2.498E-04	2.500E-04	-0.03%
C	200.00	as HCO3	61.0171	3.278E-03	3.279E-03	-0.02%
Alkalinity	200.00	as Ca(CO3)	100.0872	1.998E-03	1.999E-03	-0.02%
water	0.01736	# kg				

Table A-4.2 Input data for Cell UA2

INPUT code			G.F.W (g)	Calculated M (mol/L)	PHREEQC M (mol/L)	Validation
SOLUTION #CELL UA2			G.F.W (g)	M (mol/L)	M (mol/L)	
temp	22.78					
PH	6.86					
Pe	4					
Redox	pe					
units	mg/L					
Density	1.00					
Cl	20		35.4527	5.641E-04	5.643E-04	-0.01%
Ca	10		40.0780	2.495E-04	2.496E-04	-0.02%
K	10		39.0983	2.558E-04	2.558E-04	-0.01%
Mg	2		24.3050	8.229E-05	8.229E-05	0.00%
Na	20		22.9898	8.700E-04	8.703E-04	-0.02%
N(5)	0		14.0067	0.000E+00	0.000E+00	-
S(6)	6		96.0636	6.246E-05	6.248E-05	-0.02%
C	200	as HCO3	61.0171	3.278E-03	3.279E-03	-0.02%
Alkalinity	100	as Ca(CO3)	100.0872	9.991E-04	9.995E-04	-0.02%
Water	0.01742	# kg				

160

Table A-4.3 Input data for Cell UA3

INPUT code				Calculated	PHREEQC	Validation
SOLUTION #CELL UA3			G.F.W (g)	M (mol/L)	M (mol/L)	
temp	22.77					
PH	7.04					
Pe	4					
Redox	pe					
units	mg/L					
Density	1.00					
Cl	20		35.4527	5.641E-04	5.643E-04	-0.01%
Ca	13		40.0780	3.244E-04	3.245E-04	-0.02%
K	6		39.0983	1.535E-04	1.535E-04	-0.01%
Mg	3		24.3050	1.234E-04	1.234E-04	0.01%
Na	20		22.9898	8.700E-04	8.703E-04	-0.02%
N(5)	0		14.0067	0.000E+00	0.000E+00	-
S(6)	16		96.0636	1.666E-04	1.666E-04	-0.01%
C	200	as HCO3	61.0171	3.278E-03	3.279E-03	-0.02%
Alkalinity	100	as Ca(CO3)	100.0872	9.991E-04	9.995E-04	-0.02%
Water	0.01769	# kg				

Table A-4.4 Input data for Cell UA4

INPUT code				Calculated	PHREEQC	Validation
SOLUTION #CELL UA4			G.F.W (g)	M (mol/L)	M (mol/L)	
temp	22.75					
PH	7.06					
Pe	4					
Redox	pe					
units	mg/L					
Density	1.00					
Cl	20		35.4527	5.641E-04	5.643E-04	-0.01%
Ca	13		40.0780	3.244E-04	3.245E-04	-0.02%
K	6		39.0983	1.535E-04	1.535E-04	-0.01%
Mg	3		24.3050	1.234E-04	1.234E-04	0.01%
Na	21		22.9898	9.134E-04	9.138E-04	-0.02%
N(5)	0		14.0067	0.000E+00	0.000E+00	-
S(6)	16		96.0636	1.666E-04	1.666E-04	-0.01%
C	200	as HCO3	61.0171	3.278E-03	3.279E-03	-0.02%
Alkalinity	100	as Ca(CO3)	100.0872	9.991E-04	9.995E-04	-0.02%
Water	0.01432	# kg				

161

Table A-4.5 Input data for Cell UA5

INPUT code				Calculated	PHREEQC	Validation
SOLUTION #CELL UA5			G.F.W (g)	M (mol/L)	M (mol/L)	
temp	22.77					
PH	7.07					
Pe	4					
Redox	pe					
units	mg/L					
Density	1.00					
Cl	20		35.4527	5.641E-04	5.643E-04	-0.01%
Ca	10		40.0780	2.495E-04	2.496E-04	-0.02%
K	4		39.0983	1.023E-04	1.023E-04	0.00%
Mg	2		24.3050	8.229E-05	8.229E-05	0.00%
Na	20		22.9898	8.700E-04	8.702E-04	-0.01%
N(3)	0.05		14.0067	3.570E-06	3.571E-06	-
S(6)	6		96.0636	6.246E-05	6.247E-05	-0.01%
C	100	as HCO3	61.0171	1.639E-03	1.639E-03	0.00%
Alkalinity	100	as Ca(CO3)	100.0872	9.991E-04	9.995E-04	-0.02%
Water	0.01506	# kg				

2. RESULTS

□ Cell UA 1 □ Cell UA 2 □ Cell UA 3 □ Cell UA 4 □ Cell UA 5
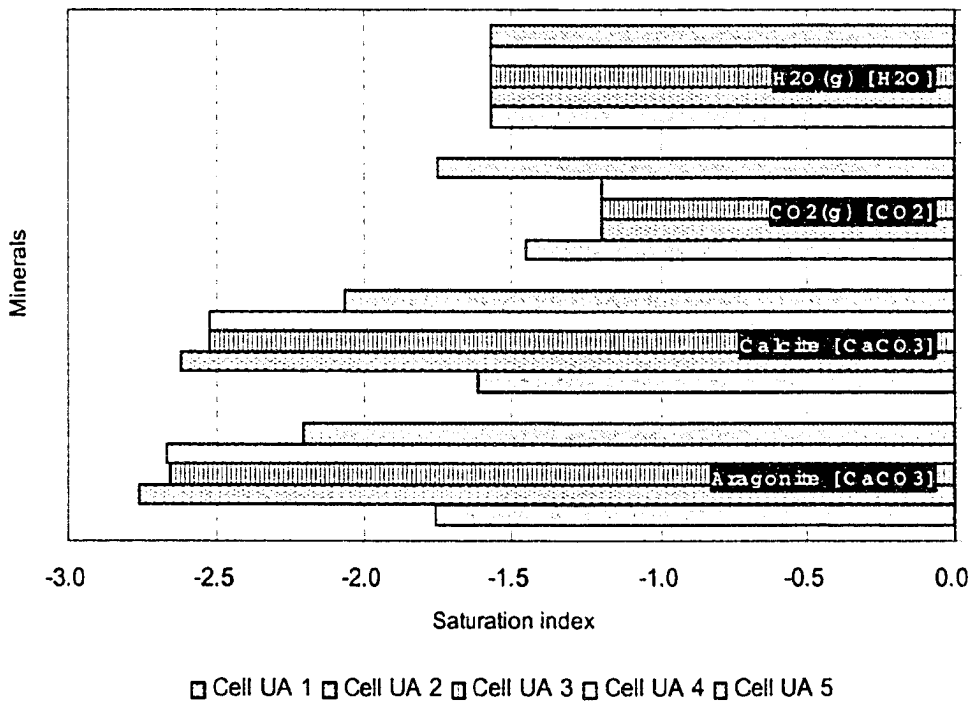
Figure A-4.1 Calculated saturation index of the samples

162

Table A-4.6 Summary of speciation calculation for initial pore fluid

	Cell UA 1	Cell UA 2	Cell UA 3	Cell UA 4	Cell UA 5
Ionic strength	3.736E-03	2.117E-03	2.478E-03	2.499E-03	2.041E-03
Mass of water (kg)	1.74E-02	1.74E-02	1.77E-02	1.43E-02	1.51E-02
Charge balance % error	-5.88	2.92	0.6	1.73	-1.69
SI [Saturation Index]					
Anhydrite CaSO4	-2.93	-3.66	-3.14	-3.14	-3.65
Aragonite CaCO3	-1.76	-2.76	-2.66	-2.67	-2.21
Calcite CaCO3	-1.61	-2.62	-2.52	-2.52	-2.07
CH4(g) CH4	-59.58	-54.98	-54.96	-54.96	-59.94
CO2(g) CO2	-1.45	-1.2	-1.2	-1.2	-1.75
Dolomite CaMg(CO3)2	-3.33	-5.61	-5.36	-5.36	-4.51
Gypsum CaSO4:2H2O	-2.70	-3.43	-2.91	-2.91	-3.43
H2(g) H2	-21.05	-19.97	-19.96	-19.96	-21.07
H2O(g) H2O	-1.57	-1.57	-1.57	-1.57	-1.57
Halite NaCl	-7.80	-7.93	-7.93	-7.91	-7.93
O2(g) O2	-41.74	-43.94	-43.95	-43.96	-41.73
SI < 5					
Aragonite [CaCO3]	-1.76	-2.76	-2.66	-2.67	-2.21
Calcite [CaCO3]	-1.61	-2.62	-2.52	-2.52	-2.07
CO2(g) [CO2]	-1.45	-1.2	-1.2	-1.2	-1.75
H2O(g) [H2O]	-1.57	-1.57	-1.57	-1.57	-1.57

Database: phreeqc.dat

163

A-4 Speciation calculation for the liquid hog manure using PHREEQC

1. INPUT CODE FOR PHREEQC

Table A-5.1 Input data for liquid hog manure

INPUT code			G.F.W (g)	Calculated M (mol/L)	PHREEQC M (mol/L)	Validation
SOLUTION 1 # Initial LHM						
temp	24.00					
pH	7.88					
pe	4.00					
redox	pe					
units	mg/l					
density	1.00					
Cl	1380		35.4527	3.893E-02	4.035E-02	-1.80%
Ca	199		40.0780	4.965E-03	5.147E-03	-1.80%
K	1710		39.0983	4.374E-02	4.533E-02	-1.79%
Mg	6.4		24.3050	2.633E-04	2.729E-04	-1.79%
Na	611		22.9898	2.658E-02	2.755E-02	-1.80%
N(5)	1		14.0067	7.139E-05	7.400E-05	-1.79%
S(6)	9		96.0636	9.369E-05	9.711E-05	-1.79%
C	14300	as HCO3	61.0171	2.344E-01	2.429E-01	-1.79%
Alkalinity	11700	as Ca(CO3)	100.0872	1.169E-01	1.212E-01	-1.81%
N(-3)	4070		14.0067	2.906E-01	3.012E-01	-1.80%
P	1270	as PO4	94.9714	1.337E-02	1.386E-02	-1.79%
water	0.02	# kg				

164

2. RESULTS

Table A-5.2 Summary of speciation calculation for liquid hog manure

		Initial LHM
Ionic strength		2.83E-01
Mass of water (kg)		2.00E-02
Redox couple[N(-3)/N(5)]		
pe		6.7949
Eh (volts)		0.4006
SI [Saturation Index]		
Anhydrite	$CaSO_4$	-3.58
Aragonite	$CaCO_3$	0.05
Calcite	$CaCO_3$	0.20
CH4(g)	CH_4	-54.76
CO2(g)	CO_2	0.58
Dolomite	$CaMg(CO_3)_2$	-0.75
Gypsum	$CaSO_4:2H_2O$	-3.36
H2(g)	H_2	-20.32
H2O(g)	H_2O	-1.54
Halite	$NaCl$	-4.85
Hydroxyapatite	$Ca_5(PO_4)_3OH$	3.29
NH3(g)		-5.62
O2(g)		-42.83
SI < 1		
Aragonite [CaCO3]		0.05
Calcite [CaCO3]		0.20
CO2(g) [CO2]		0.58
Dolomite		-0.75
H2O(g)		-1.54

165
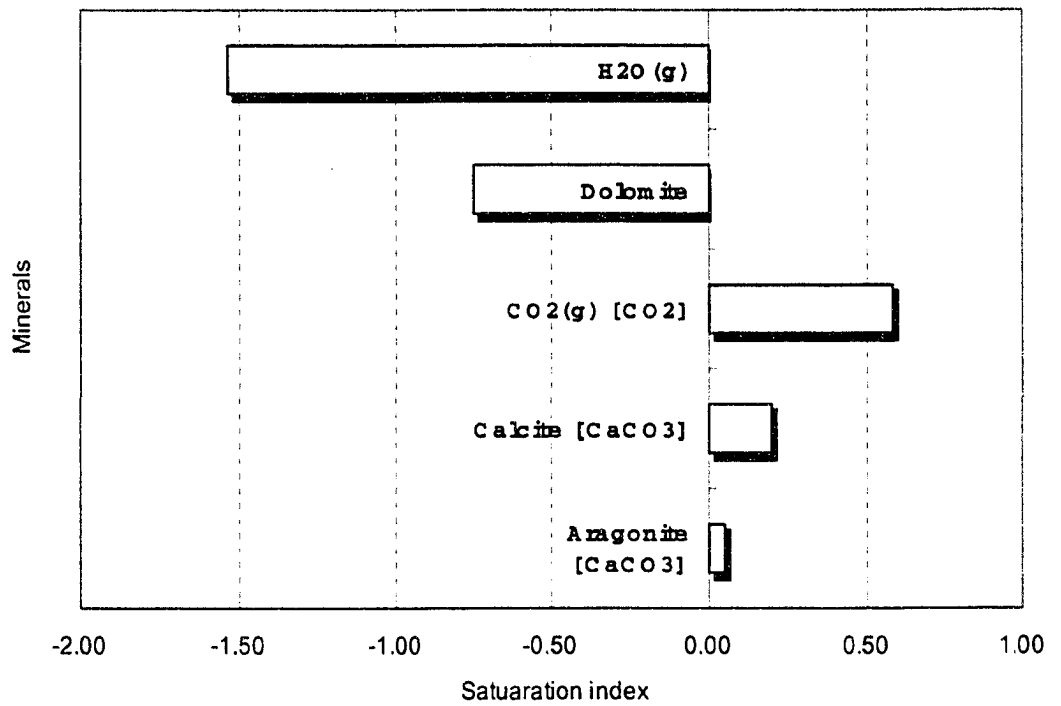
Figure A-5.1 Calculated saturation index of the samples

166

A-5 Geometry and weight of radial diffusion cells
Example Cell UA1

167

CELL UA 1-Example

Geometry of diffusion cell

Trials		1.00	2.00	3.00	4.00	5.00	6.00	7.00	Total	Average	
Diameter of cell Inner (mm)		72.07	72.15	72.18	72.09	72.09	72.09	72.11	504.78	72.11	
	Thickness (mm)	9.73	9.77	9.70	9.70	9.70	9.71		58.31	9.72	
	Outer (mm)									81.83	
	Height (mm)	89.00	88.90	88.95	88.90	88.94			444.69	88.94	
Area	Area of surface									4084.12	mm^2
										40.84	cm^2
										0.0040841	m^2
Volume	Volume of inner cell									363233.12	mm^3
										363.2331182	cm^3
										0.000363233	m^3
Weight	Cell (g)	306.80									
	Cap (g)	9.00									
	Upper plate (g)	269.70									
	Lower plate (g)	393.30									
	Total (g)	978.80									
	Total+nuts-cap	988.10	measured								
	Total+nuts+cap	997.10	measured								
		997.10	calculated								

Polyethylene (PE) POROUS LINERS FOR CELL UA1-Example

Geometry of casing

Trials		1.00	2.00	3.00	Total	Average (mm)	Average (cm)	Average (m)	Average (L)	Average (mL_
	Height (mm)	70.98	70.80	70.99	212.77	70.92	7.09	0.07		
	Inner diameter (mm)	23.66	23.40	23.64	70.70	23.57	2.36	0.02		
	Outer diameter (mm)	27.33	27.00	26.95	81.28	27.09	2.71	0.03		
	Thickness (mm)	3.67	3.60	3.31	10.58	3.53	0.35	0.00		
	Inner radius (mm)	11.83	11.70	11.82	35.35	11.78	1.18	0.01		
	Outer radius (mm)	13.67	13.50	13.48	40.64	13.55	1.35	0.01		
Area	Inner (mm^2)	439.66	430.05	438.92	1308.63	436.21	4.36	0.00		
	Outer (mm^2)	586.64	572.56	570.44	1729.63	576.54	5.77	0.00		
Surface area	plane (mm^2)	6094.32	6005.47	6010.43	18110.23	6036.74	60.37	0.01		
	plane+end circle (mm^2)	8440.87	8295.69	8292.18	25028.74	8342.91	83.43	0.01		
Volume	Inner (mm^3)	31207.24	30447.73	31158.89	92813.86	30937.95	30.94	0.00	0.03	30.938
	Outer (mm^3)	41639.46	40536.91	40495.30	122671.68	40890.56	40.89	0.00	0.04	40.891
Weight (No saturation)	Casing (g)	11.28	11.28		22.56	11.28				

A-6 Distribution coefficient, K_d

K_d (L/Cell)	0.197	0.197	0.197	0.197	0.197	* slope of lower limit	
Soils in each cell (g)	678.710	703.100	605.320	589.330	632.090		
Soils in each cell (kg)	0.679	0.703	0.605	0.589	0.632		
K_d (L/kg)	**0.290**	**0.280**	**0.325**	**0.334**	**0.312**		
DETERMINATION OF R							
Bulk dansity (g/cm³=g/mL)	1.748	1.718	1.463	1.461	1.611		
Volumetric water content	0.319	0.331	0.422	0.423	0.375		
Kd (L/kg)	0.310	0.316	0.371	0.371	0.337		
Retardation factor, R	**2.697**	**2.639**	**2.285**	**2.281**	**2.446**	12.348	2.470
Dry soils (g)	634.884	623.284	531.150	530.638	584.444		
Dry soils (kg)	0.635	0.623	0.531	0.531	0.584		
Kd (L/kg)	0.310	0.316	0.371	0.371	0.337	1.705	0.341
		Kd	R				
	Min	0.310	2.300				
	Max	0.370	2.700				
	Aver.	0.341	2.500				

$y = 0.1969x - 0.1075$
$R^2 = 0.9993$

Sorbed NH4 (mmol/Cell) vs. Equilibrium activity in soil phase (mmol/L)

170
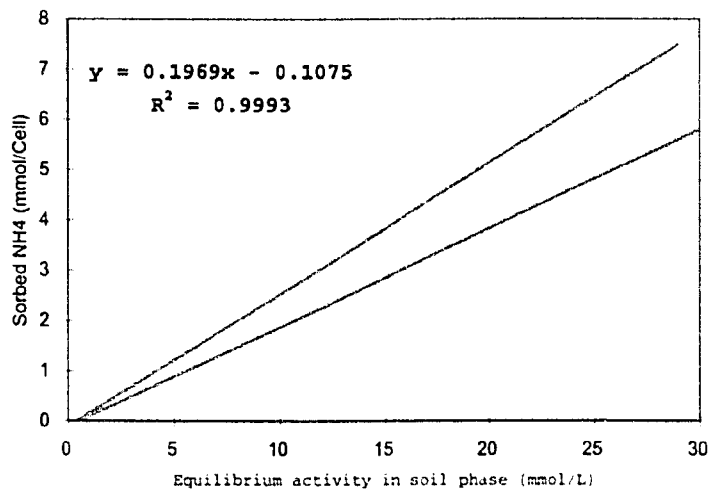
APPENDIX B. Numerical Modeling Codes

171

B-1 Radial diffusion domain

Table B-1.Nomenclature for a radial diffusion domain calculation

No.	Item	Nomenclature	Unit	Input value	
1	Number of cells	N	Unitless	5	
2	Cell I.D. Number	n	Unitless		
3	Solution No. in PHREEQC	S_n	Unitless	6	Including "0"
4	Length of cell (m)	l_c	m	0.005	
5	Radius from origin	r_n	m		
6	Area of each cell	A_n	m^2		
7	Volume of each cell	V_n	mL		
8	Volume of pore volume	nV_n	mL		
9	Volume of effective pore volume	n_eV_n	mL		
10	Pore volume ratio	nVR	Unitless		
11	Effective radial diffusion length	ECL	m		
12	Background concentration of solute	C_0	mg/L		
13	Mass of background solute in cell	M_0	mg		
14	Total mass of water for PHREEQC	MW	Kg		

Creating Radial Diffusion Cells

n	0	1	2	3	4	5	End of Cell
Sn	0	1	2	3	4	5	End of Cell
lc	0.01	0.005	0.005	0.005	0.005	0.005	
rn	0.01	0.015	0.02	0.025	0.03	0.035	
An	2.618E-05	3.272E-05	4.581E-05	5.890E-05	7.199E-05	8.508E-05	
Vn	2.618E-01	3.272E-01	4.581E-01	5.890E-01	7.199E-01	8.508E-01	
nVn	2.618E-01	1.044E-01	1.461E-01	1.879E-01	2.297E-01	2.714E-01	
MW	2.618E-04	1.044E-04	1.461E-04	1.879E-04	2.297E-04	2.714E-04	
nVR	2.508	1.000	1.400	1.800	2.200	2.600	
ECL	0.01066	0.00425	0.00595	0.01071	0.02356	0.06126	

Figure B-1.1 Calculated geometry of a radial diffusion domain

173

Concentrations in Solutions (mg/L)

		0	1	2	3	4	5	
	n	0	1	2	3	4	5	End of Cell
	Sn	0	1	2	3	4	5	End of Cell
1	Chloride	1380	20	20	20	20	20	End of Cell
2	Ammonium	4160	0	0	0	0	0	End of Cell
3	Nitrate	1	0.6	0.6	0.6	0.6	0.6	End of Cell
4	Nitrite	0	0.6	0.6	0.6	0.6	0.6	End of Cell
5	bicarbonate	14300	200	200	200	200	200	End of Cell
6	Sulphate	9	24	24	24	24	24	End of Cell
7	Calcium	199	16	16	16	16	16	End of Cell
8	Potasium	1710	10	10	10	10	10	End of Cell
9	Magnesium	6.4	6	6	6	6	6	End of Cell
10	Sodium	611	28	28	28	28	28	End of Cell
11	phosphate	1270	0	0	0	0	0	End of Cell
12	Specie 12	0	0	0	0	0	0	End of Cell
13	Specie 13	0	0	0	0	0	0	End of Cell
14	Specie 14	0	0	0	0	0	0	End of Cell
15	Specie 15	0	0	0	0	0	0	End of Cell

Figure B-1.2 Calculated pore fluid chemistry in a radial diffusion domain [1]

Mass of Solute in Solutions (mg)

	n	0	1	2	3	4	5	End of Cell
	Sn	0	1	2	3	4	5	End of Cell
1	Chloride	3.613E-01	2.088E-03	2.923E-03	3.758E-03	4.593E-03	5.428E-03	#VALUE!
2	Ammonium	1.089E+00	0.000E+00	0.000E+00	0.000E+00	0.000E+00	0.000E+00	#VALUE!
3	Nitrate	2.618E-04	6.264E-05	8.769E-05	1.127E-04	1.378E-04	1.629E-04	#VALUE!
4	Nitrite	0.000E+00	6.264E-05	8.769E-05	1.127E-04	1.378E-04	1.629E-04	#VALUE!
5	bicarbonate	3.744E+00	2.088E-02	2.923E-02	3.758E-02	4.593E-02	5.428E-02	#VALUE!
6	Sulphate	2.356E-03	2.505E-03	3.508E-03	4.510E-03	5.512E-03	6.514E-03	#VALUE!
7	Calcium	5.210E-02	1.670E-03	2.338E-03	3.007E-03	3.675E-03	4.343E-03	#VALUE!
8	Potasium	4.477E-01	1.044E-03	1.461E-03	1.879E-03	2.297E-03	2.714E-03	#VALUE!
9	Magnesium	1.676E-03	6.264E-04	8.769E-04	1.127E-03	1.378E-03	1.629E-03	#VALUE!
10	Sodium	1.600E-01	2.923E-03	4.092E-03	5.261E-03	6.431E-03	7.600E-03	#VALUE!
11	phosphate	3.325E-01	0.000E+00	0.000E+00	0.000E+00	0.000E+00	0.000E+00	#VALUE!
12	Specie 12	0.000E+00	0.000E+00	0.000E+00	0.000E+00	0.000E+00	0.000E+00	#VALUE!
13	Specie 13	0.000E+00	0.000E+00	0.000E+00	0.000E+00	0.000E+00	0.000E+00	#VALUE!
14	Specie 14	0.000E+00	0.000E+00	0.000E+00	0.000E+00	0.000E+00	0.000E+00	#VALUE!
15	Specie 15	0.000E+00	0.000E+00	0.000E+00	0.000E+00	0.000E+00	0.000E+00	#VALUE!

Figure B-1.3 Calculated pore fluid chemistry in a radial diffusion domain [2]

176
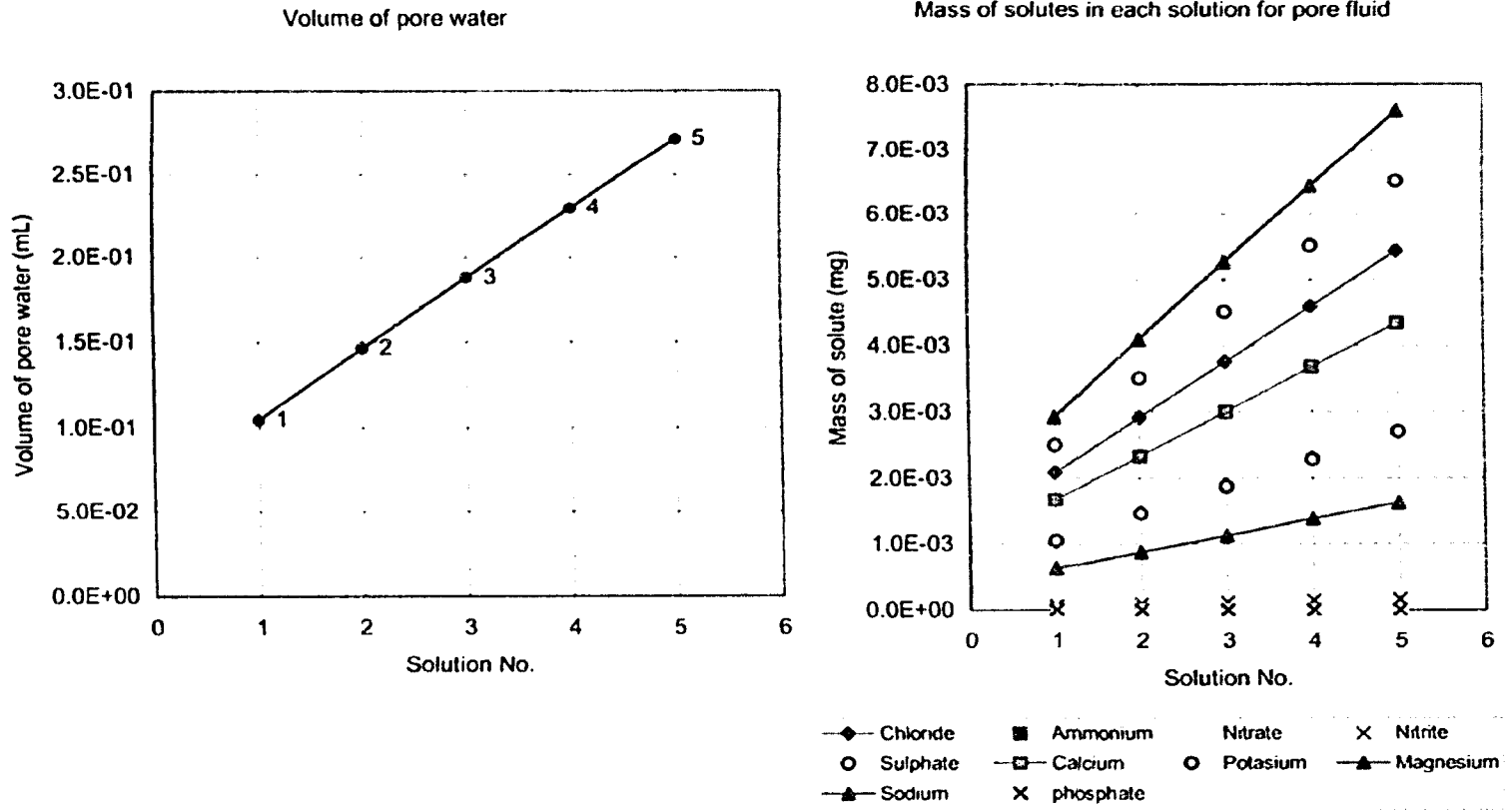
Figure B-1.4 Calculated volume of pore fluid and mass of solutes in a radial diffusion domain

B-2 SIMPLE MIX MODEL code

```
#TITLE: SIMPLE MIX
        # Equilibrated initial pore fluid + 20mL Liquid hog manure
        # Programmed by Won Jae Chang, GeoEnvironmental Engineering,
University of Alberta, Canada.
#############################################################################

SOLUTION 1                      #CELL UA1: Pore Fluid After Diffusive
Equilibrium
temp    22.87
pH      7.03
pe      4.00
redox   pe
units   mg/l
density         1.00
Cl      20.00
Ca      16.00
K       10.00
Mg      6.00
Na      28.00
N(5)    0.6
S(6)    24.00
C       200.00          as HCO3
Alkalinity   200.00          as Ca(CO3)
water  1 # kg                   # Solution compositon was verified by
comparing PHREEQC results and calculation
SAVE SOLUTION 1
END
SOLUTION 2                      # CELL UA2: Pore Fluid After Diffusive
Equilibrium
temp    22.78
pH      6.86
pe      4
redox   pe
units   mg/L
density         1.00
Cl      20
Ca      10
K       10
Mg      2
Na      20
N(5)    0
S(6)    6
C       200     as HCO3
Alkalinity   100    as Ca(CO3)
water  1 # kg                   # Solution compositon was verified by
comparing PHREEQC results and calculation
SAVE SOLUTION 2
END
SOLUTION 3                      # CELL UA3: Pore Fluid After Diffusive
Equilibrium
temp    22.77
pH      7.04
```

177

```
pe      4
redox   pe
units   mg/L
density         1.00
Cl      20
Ca      13
K       6
Mg      3
Na      20
N(5)    0
S(6)    16
C       200     as HCO3
Alkalinity      100     as Ca(CO3)
water   1 # kg                          # Solution compositon was verified by
comparing PHREEQC results and calculation
SAVE SOLUTION 3
END
SOLUTION 4                      # CELL UA4: Pore Fluid After Diffusive
Equilibrium
temp    22.75
pH      7.06
pe      4
redox   pe
units   mg/L
density         1.00
Cl      20
Ca      13
K       6
Mg      3
Na      21
N(5)    0
S(6)    16
C       200     as HCO3
Alkalinity      100     as Ca(CO3)
water   1 # kg                          # Solution compositon was verified by
comparing PHREEQC results and calculation
SAVE SOLUTION 4
END
SOLUTION 5                      # CELL UA5: Pore Fluid After Diffusive
Equilibrium
temp    22.77
pH      7.07
pe      4
redox   pe
units   mg/L
density         1.00
Cl      20
Ca      10
K       4
Mg      2
Na      20
N(3)    0.05
S(6)    6
C       100     as HCO3
Alkalinity      100     as Ca(CO3)
water   1 # kg                          # Solution compositon was verified by
```

178

```
comparing PHREEQC results and calculation
SAVE SOLUTION 5
END
SOLUTION 6                    # Initial liquid hog manure for injection to
diffusionc cells
    temp    24
    pH      7.88
    pe      4
    redox   pe
    units   mg/l
    density 1
    Cl      1380
    Ca      199
    K       1710
    Mg      6.4
    Na      611
    N(5)    1
    S(6)    9
    C       14300 as HCO3
    Alkalinity 11700 as Ca(CO3)
    N(-3)   4070
    P       1270 as PO4
    -water  1 # kg
SAVE SOLUTION 6
END
MIX 1
      1      0.867
      6      0.133
SAVE SOLUTION 7
SELECTED_OUTPUT
    -file            C:\Program Files\USGS\Phreeqc Interactive
2.6\Msc_FINALS\LAST\SIMPLE MIX\Simple_NH4.out.sel
    -reset           false
    -molalities      NH4+
END
MIX 2
      2      0.87
      6      0.13
SAVE SOLUTION 8
END
MIX 3
      3      0.90
      6      0.10
SAVE SOLUTION 9
END
MIX 4
      4      0.90
      6      0.10
SAVE SOLUTION 10
END
MIX 5
      5      0.89
      6      0.11
SAVE SOLUTION 11
END
```

179

B-3 MIX MODEL code

```
# TITLE: MAXIMUM CAPACITY OF AMMONIUM IN RADAIL DIFFUSION CELLS
# Programmed by Won Jae Chang, GeoEnvironmental Engineering, University
of Alberta, Canada
###################################################################
# Cell No. : Cell UA1
SOLUTION 1                      #CELL UA1: Pore Fluid After Diffusive
Equilibrium
temp   22.87
pH     7.03
pe     4.00
redox  pe
units  mg/l
density        1.00
Cl     20.00
Ca     16.00
K      10.00
Mg     6.00
Na     28.00
N(5)   0.6
S(6)   24.00
C      200.00          as HCO3
Alkalinity   200.00        as Ca(CO3)
water  1 * kg                  # Solution compositon was verified by
comparing PHREEQC results and calculation
SAVE SOLUTION 1
END
SOLUTION 2                      # Initial liquid hog manure for injection to
diffusionc cells
   temp    24
   pH      7.88
   pe      4
   redox    pe
   units    mg/l
   density  1
   Cl       1380
   Ca       199
   K        1710
   Mg       6.4
   Na       611
   N(5)     1
   S(6)     9
   C        14300 as HCO3
   Alkalinity 11700 as Ca(CO3)
   N(-3)    4070
   P        1270 as PO4
   -water   1 # kg
SAVE SOLUTION 2
END
MIX 1
      1      0.867
      2      0.133
SAVE SOLUTION 3

SELECTED_OUTPUT
```

180

B-4 Reactive radial diffusion (radial diffusion + exchange reactions + competition) code

```
#TITLE: RADIAL DIFFUSION + ADSORPTION + CATION EXCHANGE OF LIQUID HOG
MANURE THROUGH CLAYEY SOILS
# Programmed by Won Jae Chang, GeoEnvironmental Engineering, University
of Alberta
##############################################################################
##################

SOLUTION 0                          Initial LHM as a contaminant
    temp    24
    pH      7.88
    pe      4
    redox   pe
    units   mg/l
    density 1
    Cl      270
    Ca      9
    K       450
    Mg      4.2
    Na      70
    N(5)    1
    S(6)    9
    C       14300 as HCO3
    Alkalinity 11700 as Ca(CO3)
    N(-3)   1000
    P       1270 as PO4
    -water  0.0002618 # kg
SOLUTION 1                          Slice 1 Solution For Cell UA1 Pore
fluid based on Radial Diffusion
temp  22.87
pH    7.03
pe    4.00
redox pe
units mg/l
density     1.00
Cl    20.00
Ca    199
K     10.00
Mg    6.00
Na    28.00
N(5)  0.6
S(6)  24.00
C     200.00        as HCO3
Alkalinity    200.00        as Ca(CO3)
    -water  0.0001044 # kg
SOLUTION 2                          Slice 2 Solution For Cell UA1 Pore
fluid based on Radial Diffusion
temp  22.87
pH    7.03
```

181

```
pe      4.00
redox   pe
units   mg/l
density         1.00
Cl      20.00
Ca      199
K       10.00
Mg      6.00
Na      28.00
N(5)    0.6
S(6)    24.00
C       200.00          as HCO3
Alkalinity      200.00          as Ca(CO3)
    -water      0.0001461 # kg
SOLUTION 3                       Slice 3 Solution For Cell UA1 Pore
fluid based on Radial Diffusion
temp    22.87
pH      7.03
pe      4.00
redox   pe
units   mg/l
density         1.00
Cl      20.00
Ca      199
K       10.00
Mg      6.00
Na      28.00
N(5)    0.6
S(6)    24.00
C       200.00          as HCO3
Alkalinity      200.00          as Ca(CO3)
    -water      0.0001879 # kg
SOLUTION 4                       Slice 4 Solution For Cell UA1 Pore
fluid based on Radial Diffusion
temp    22.87
pH      7.03
pe      4.00
redox   pe
units   mg/l
density         1.00
Cl      20.00
Ca      199
K       10.00
Mg      6.00
Na      28.00
N(5)    0.6
S(6)    24.00
C       200.00          as HCO3
Alkalinity      200.00          as Ca(CO3)
    -water      0.0002297 # kg
SOLUTION 5                       Slice 5 Solution For Cell UA1 Pore
fluid based on Radial Diffusion
temp    22.87
pH      7.03
pe      4.00
redox   pe
```

```
units  mg/l
density        1.00
Cl     20.00
Ca     199
K      10.00
Mg     6.00
Na     28.00
N(5)   0.6
S(6)   24.00
C      200.00        as HCO3
Alkalinity  200.00        as Ca(CO3)
   -water   0.0002714 # kg
EXCHANGE 1-5
   NH4X   0.002534
   KX     0.0002256
   CaX2   3.295e-006
   NaX    6.552e-005
   MgX2   7.369e-006
 TRANSPORT
   -cells              5
   -shifts             100
   -time_step          86400 # seconds
   -flow_direction     diffusion_only
   -boundary_conditions  constant closed
   -lengths            0.00425 0.00595 0.00765 0.00935 0.01105
   -diffusion_coefficient 1.1250E-10
   -print_cells        1
   -punch_cells        1
   -warnings           true
KNOBS
   -iterations         500
   -convergence_tolerance 1e-008
   -tolerance          1e-015
   -step_size          100
   -pe_step_size       5
   -diagonal_scale     false
   -debug_model        false
   -debug_prep         false
   -debug_set          false
   -debug_inverse      false
   -logfile            false
   -debug_diffuse_layer  false
   -delay_mass_water     false
SELECTED_OUTPUT
   -file            C:\Program Files\USGS\Phreeqc Interactive
2.6\Msc_FINALS\pH.sel
   -selected_out       true
   -user_punch         false
   -high_precision     false
   -reset              false
   -time               true
   -step               true
   -ph                 true
   -inverse_modeling   false
END
```

B-5 Reactive radial diffusion for ammonium saturation code

```
#Diffusion + Ammonium Exchange Model for Cell UA 1
SOLUTION 0 HOG MANURE AS A CONTAMINANT
##################################################################
###
Programmed by Won Jae Chang, GeoEnvironmental Engineering, University
of Alberta
##################################################################
###


      temp      24
      pH        7.88
      pe        4
      redox     pe
      units     mg/L
      density   1
Cl        7303
N(5)      16
N(3)      22
S(6)      162
Ca        103
K         27103
Mg        65
Na        4734
P         34352  as PO4
N(-3)  110090
C 386801 as HCO3
      -water    0.0002618 # kg
SOLUTION 1 Slice 1 Solution For Cell UA1 Pore fluid based on Radial
Diffusion
      temp      22.9
      pH        6.7
      pe        4
      redox     pe
      units     mg/l
      density   1
      Cl        20
      N(-3)     0
      N(5)      0.6
      N(3)      0.6
      S(6)      24
      Ca        16
      K         10
      Mg        6
      Na        63.36                       # Original 28 for all others
      P         0
      -water    0.0001044 # kg
SOLUTION 2 Slice 2 Solution For Cell UA1 Pore fluid based on Radial
Diffusion
      temp      22.9
      pH        6.7
      pe        4
      redox     pe
      units     mg/l
```

184

```
density  1
Cl       20
N(-3)    0
N(5)     0.6
N(3)     0.6
S(6)     24
Ca       16
K        10
Mg       6
Na       63.36
P        0
-water   0.0001461 # kg
SOLUTION 3 Slice 3 Solution For Cell UA1 Pore fluid based on Radial
Diffusion
temp     22.9
pH       6.7
pe       4
redox    pe
units    mg/l
density  1
Cl       20
N(-3)    0
N(5)     0.6
N(3)     0.6
S(6)     24
Ca       16
K        10
Mg       6
Na       63.36
P        0
-water   0.0001879 # kg
SOLUTION 4 Slice 4 Solution For Cell UA1 Pore fluid based on Radial
Diffusion
temp     22.9
pH       6.7
pe       4
redox    pe
units    mg/l
density  1
Cl       20
N(-3)    0
N(5)     0.6
N(3)     0.6
S(6)     24
Ca       16
K        10
Mg       6
Na       63.36
P        0
-water   0.0002297 # kg
SOLUTION 5 Slice 5 Solution For Cell UA1 Pore fluid based on Radial
Diffusion
temp     22.9
pH       6.7
pe       4
redox    pe
```

```
    units    mg/l
    density  1
    Cl       20
    N(-3)    0
    N(5)     0.6
    N(3)     0.6
    S(6)     24
    Ca       16
    K        10
    Mg       6
    Na       63.36
    P        0
    -water   0.0002714 # kg
EXCHANGE 1-5
    NH4X     0.002534
    KX       0.0002256
    CaX2     2.272e-005
    NaX      9.095e-006
    MgX2     8.369e-005
TRANSPORT
    -cells               5
    -shifts              185
    -time_step           86400 # seconds
    -flow_direction      diffusion_only
    -boundary_conditions constant closed
    -lengths             0.00425 0.00595 0.00765 0.00935 0.01105
    -diffusion_coefficient 2.29167e-010
    -print_cells         5
    -punch_cells         5
    -warnings            true
KNOBS
    -iterations          500
    -convergence_tolerance 1e-008
    -tolerance           1e-015
    -step_size           100
    -pe_step_size        5
    -diagonal_scale      false
    -debug_model         false
    -debug_prep          false
    -debug_set           false
    -debug_inverse       false
    -logfile             false
    -debug_diffuse_layer false
    -delay_mass_water    false
SELECTED_OUTPUT
    -file                C:\Documents and Settings\□□□\My
Documents\MSc_research\Phreeqc\Radial diffusion1\Sat_NH4\Sandy\S-MCEC
lower\sandy-mcec-lower.sel
    -selected_out        true
    -user_punch          true
    -reset               false
    -time                true
    -step                true
    -totals              N(-3)
SELECTED_OUTPUT
    -file                C:\Documents and Settings\□□□\My
```

186

```
Documents\MSc_research\Phreeqc\Radial diffusion1\Sat_NH4\Sandy\S-MCEC
lower\geochem-S-1.out.sel
    -reset              false
    -step               true
    -ph                 true
    -pe                 true
    -alkalinity         true
    -ionic_strength     true
    -totals             N(3) N(5) S(-2) S(6)
    -saturation_indices Anhydrite N2(g) Sulfur CH4(g)
                        CO2(g)
END
#Diffusion + Ammonium Exchange Model for Cell UA 1
SOLUTION 0 HOG MANURE AS A CONTAMINANT
##################################################################
Programmed by Won Jae Chang, GeoEnvironmental Engineering, University
of Alberta
##################################################################


    temp    24
    pH      7.88
    pe      4
    redox   pe
    units   mg/l
    density 1
Cl      11026
N(5)    25
N(3)    33
S(6)    245
Ca      155
K       40919
Mg      98
Na      7146
P       51863
N(-3)   166206
C   58396  as HCO3
    -water    0.0002618 # kg
SOLUTION 1 Slice 1 Solution For Cell UA1 Pore fluid based on Radial
Diffusion
    temp    22.9
    pH      6.7
    pe      4
    redox   pe
    units   mg/l
    density 1
    Cl      20
    N(-3)   0
    N(5)    0.6
    N(3)    0.6
    S(6)    24
    Ca      16
    K       10
    Mg      6
    Na      63.36                       # Original 28 for all others
    P       0
```

```
     -water    0.0001044 # kg
SOLUTION 2 Slice 2 Solution For Cell UA1 Pore fluid based on Radial
Diffusion
     temp     22.9
     pH       6.7
     pe       4
     redox    pe
     units    mg/l
     density  1
     Cl       20
     N(-3)    0
     N(5)     0.6
     N(3)     0.6
     S(6)     24
     Ca       16
     K        10
     Mg       6
     Na       63.36
     P        0
     -water    0.0001461 # kg
SOLUTION 3 Slice 3 Solution For Cell UA1 Pore fluid based on Radial
Diffusion
     temp     22.9
     pH       6.7
     pe       4
     redox    pe
     units    mg/l
     density  1
     Cl       20
     N(-3)    0
     N(5)     0.6
     N(3)     0.6
     S(6)     24
     Ca       16
     K        10
     Mg       6
     Na       63.36
     P        0
     -water    0.0001879 # kg
SOLUTION 4 Slice 4 Solution For Cell UA1 Pore fluid based on Radial
Diffusion
     temp     22.9
     pH       6.7
     pe       4
     redox    pe
     units    mg/l
     density  1
     Cl       20
     N(-3)    0
     N(5)     0.6
     N(3)     0.6
     S(6)     24
     Ca       16
     K        10
     Mg       6
     Na       63.36
```

188

```
        P       0
        -water   0.0002297 # kg
SOLUTION 5 Slice 5 Solution For Cell UA1 Pore fluid based on Radial
Diffusion
        temp     22.9
        pH       6.7
        pe       4
        redox    pe
        units    mg/l
        density  1
        Cl       20
        N(-3)    0
        N(5)     0.6
        N(3)     0.6
        S(6)     24
        Ca       16
        K        10
        Mg       6
        Na       63.36
        P        0
        -water   0.0002714 # kg
EXCHANGE 1-5
        NH4X     0.002534
        KX       0.0002256
        CaX2     2.272e-005
        NaX      9.095e-006
        MgX2     8.369e-005
TRANSPORT
        -cells              5
        -shifts             185
        -time_step          86400 # seconds
        -flow_direction       diffusion_only
        -boundary_conditions  constant closed
        -lengths            0.00425 0.00595 0.00765 0.00935 0.01105
        -diffusion_coefficient 1.125e-010
        -print_cells        5
        -punch_cells        5
        -warnings           true
KNOBS
        -iterations         500
        -convergence_tolerance 1e-008
        -tolerance          1e-015
        -step_size          100
        -pe_step_size       5
        -diagonal_scale     false
        -debug_model        false
        -debug_prep         false
        -debug_set          false
        -debug_inverse      false
        -logfile            false
        -debug_diffuse_layer  false
        -delay_mass_water     false
SELECTED_OUTPUT
        -file               C:\Documents and Settings\    \My
Documents\MSc_research\Phreeqc\Radial diffusion1\Sat_NH4\Clayey\MCEC
lower\clay-mcec-lower.sel
```

189

```
    -selected_out        true
    -user_punch          true
    -reset               false
    -time                true
    -step                true
    -totals              N(-3)

SELECTED_OUTPUT
    -file                C:\Documents and Settings\□□□\My
Documents\MSc_research\Phreeqc\Radial diffusion1\Sat_NH4\Clayey\MCEC
lower\geochem1.out.sel
    -reset               false
    -step                true
    -ph                  true
    -pe                  true
    -alkalinity          true
    -ionic_strength      true
    -totals              N(3)  N(5)  S(-2)  S(6)
    -saturation_indices  Anhydrite  N2(g)  Sulfur  CH4(g)
                         CO2(g)
END
```

190